

**DOKUZ EYLÜL UNIVERSITY**  
**GRADUATE SCHOOL OF NATURAL AND APPLIED SCIENCES**

**LITTLE HIGGS BOSON MODELS RESEARCH  
VIA NEUTRINO-ELECTRON ELASTIC  
SCATTERING CHANNEL AT LOW ENERGY**

by  
**Ahmad AJJAQ**

**June, 2018**

**İZMİR**

**LITTLE HIGGS BOSON MODELS RESEARCH  
VIA NEUTRINO-ELECTRON ELASTIC  
SCATTERING CHANNEL AT LOW ENERGY**

**A Thesis Submitted to the  
Graduate School of Natural and Applied Sciences of Dokuz Eylül University  
In Partial Fulfillment of the Requirements for the Degree of  
Master of Science in Physics**

**by  
Ahmad AJJAQ**

**June, 2018**

**İZMİR**

**M.Sc THESIS EXAMINATION RESULT FORM**

We have read the thesis entitled “**LITTLE HIGGS BOSON MODELS RESEARCH VIA NEUTRINO-ELECTRON ELASTIC SCATTERING CHANNEL AT LOW ENERGY**” completed by **AHMAD AJJAQ** under supervision of **PROF. DR. MUHAMMED DENİZ** and **ASST. PROF. DR. MEHMET DEMİRCİ** and we certify that in our opinion it is fully adequate, in scope and in quality, as a thesis for the degree of Master of Science.



Prof. Dr. Muhammed DENİZ

Supervisor



(Jury Member)



(Jury Member)



Prof. Dr. Latif SALUM

Director

Graduate School of Natural and Applied Sciences

## ACKNOWLEDGMENTS

It had been a long road with all the ups and downs, smiles and frowns, encouragements and discouragements before finally concluding to this thesis work. This was made true by the help of many people who I consider to be my second family in Turkey.

I would like first to express my deep gratitude to my dear supervisor Prof. Dr. Muhammed DENİZ for introducing me to such an important newly born topic which is currently being examined extensively in the literature. I do also thank him for sharing his own deep experience in the field and for the fruitful discussions, comments and engagement through the learning process of this master thesis. He was like a father in every sense of that word who assisted me academically, personally, financially and many more.

And absolutely I would like also to thank Asst. Prof. Dr. Mehmet DEMİRCİ as my secondary supervisor from Karadeniz Technical University in Trabzon with whom I luckily got the chance to meet once in Izmir. He had willingly shared his precious time in following up with the theoretical calculations I had done in the scope of my research work in addition to carefully reading and editing the contents of my thesis, all from afar. He was not only my academic supervisor but also a close real friend who had always thought of my own goodness.

Not to forget, I do also thank the DEU academic staff in the physics department with no exception but with a very special and warm thanks to Prof. Dr. Saime KERMAN and Prof. Dr. Hamza POLAT who did their best in every kind of support to help me along the way. I do also thank the Taiwan experiment on neutrino (TEXONO) collaboration -in which we are an active member- for the useful experimental data we got using their reactor apparatus. And I surely thank the scientific and technological research council of Turkey (TÜBİTAK) which had partially supported my work in this thesis via a project titled "Beyond the Standard Model New Physics Researches using

Antineutrino-Electron Scattering at Low Energy: Tensorial Non-standard Interactions of Neutrino, Unparticle Physics, Extra Z-prime Boson Models and Little Higgs Boson Models" under grant number 114F374.

With no doubt, I thank my precious real family in general and my dear father Jalal, my sweetheart mother Siham and my lovely brother Isa and sisters Rasmia and Racha in specific who had supported me from abroad throughout the entire process and who was always there for me in my good as well as bad days. I dedicate all my work and success to them!

Without your supports, it would have been almost impossible to withstand all the troubles I have come across on the way. I will literally be grateful for all of you forever for bearing the weight with me.

Ahmad AJJAQ

**LITTLE HIGGS BOSON MODELS RESEARCH VIA  
NEUTRINO-ELECTRON ELASTIC SCATTERING CHANNEL AT LOW  
ENERGY**

**ABSTRACT**

The standard model (SM) of particle physics had aptly achieved a remarkable success in describing the interactions of the subatomic world. Some serious problems, however, put the SM in a critical situation, doubted its ability to be the whole story of nature and motivated physicists to look for physics beyond the SM (BSM). The hierarchy problem, which is one of the focal points in this thesis work, is a major problem within the SM by which the Higgs mass is unwillingly large. In this work, the origin of the Higgs by the famous Higgs mechanism is first examined and then, as a solution to the hierarchy problem, a model-dependent BSM theory dubbed little Higgs models (LHMs) is extensively studied. In the scope of LHMs, two different classes known as  $SU(5)$  littlest Higgs model (LTHM) with no T-parity and  $SU(3)$  simple little Higgs model (SLHM) are theoretically and analytically examined using (anti)neutrino-electron scattering channel at low energies. Theoretically, taking into consideration the flavor conserving (FC) and flavor violating (FV) processes, the corrections of both of these models to the SM  $\nu_e (\bar{\nu}_e) - e$  scattering cross section are calculated. Experimentally, then, 90% C.L. ( $\approx 2 \sigma$  equivalence) bounds on the relevant free parameters of both models are obtained utilizing TEXONO ( $\bar{\nu}_e e$ ) and LSND ( $\nu_e e$ ) experiments.

**Keywords:** Standard model, beyond the standard model, hierarchy problem, Higgs, Higgs mechanism, little Higgs models, flavor conserving, flavor violating, neutrino-electron scattering, TEXONO, LSND

# NÖTRİNO-ELEKTRON ELASTİK SAÇILIM KANALINDAN DÜŞÜK ENERJİLERDE LITTLE HIGGS MODEL ARAŞTIRMALARI

## ÖZ

Parçacık fiziğinin standart modeli (SM), atomaltı dünyasının etkileşimlerini tarif etmede dikkate değer bir başarı sağlamıştır. Bununla birlikte, bazı ciddi sorunlar SM'yi doğanın tam bir öyküsü olabilme konusunda kritik duruma düşürerek, fizikçileri SM ötesini araştırmaya motive etmiştir. SM'de Higgs kütesine gelen kuantum düzeltmelerin oldukça büyük olmasından dolayı ortaya çıkan hiyerarşi problemi, bu tezin odak noktalarından biridir. Bu çalışmada Higgs mekanizması ile Higgs'in kökeni incelenmiş ve daha sonra hiyerarşi probleminin bir çözümü olarak SM ötesi model bağımlı little Higgs modelleri (LHM'ler) kapsamlı bir şekilde çalışılmıştır. LHM'ler kapsamında, T-parite olmayan  $SU(5)$  littlest Higgs model (LTHM) ve  $SU(3)$  simple little Higgs model (SLHM) olarak bilinen iki farklı sınıf, düşük enerjili nötrino-elektron saçılım kanalı kullanılarak teorik ve analitik olarak incelenmiştir. Teorik olarak, flavor conserving (FC) ve flavor violating (FV) göz önüne alınarak, bu modellerin her ikisinin de  $\nu_e (\bar{\nu}_e) - e$  saçılma süreci için SM'ye gelen düzeltmeler hesaplanmıştır. Daha sonra da, deneysel olarak, bu modellerin serbest parametrelerinin üzerindeki 90% C.L. ( $\approx 2 \sigma$ 'a denk gelen) sınırlamalar TEXONO ( $\bar{\nu}_e e$ ) ve LSND ( $\nu_e e$ ) deneyleri kullanılarak elde edilmiştir.

**Anahtar Kelimeler:** Standart model, standart model ötesi, Hiyerarşi problemi, Higgs, Higgs mekanizması, little Higgs modelleri, flavor conserving, flavor violating, nötrino-elektron saçılması, TEXONO, LSND

## CONTENTS

	<b>Page</b>
M.Sc THESIS EXAMINATION RESULT FORM.....	ii
ACKNOWLEDGMENTS .....	iii
ABSTRACT.....	v
ÖZ .....	vi
LIST OF FIGURES.....	ix
LIST OF TABLES .....	xii
<b>CHAPTER ONE – INTRODUCTION AND MOTIVATION .....</b>	<b>1</b>
<b>CHAPTER TWO – THE STANDARD MODEL .....</b>	<b>3</b>
2.1 Review of the Standard Model .....	3
2.2 Higgs Mechanism and Spontaneous Symmetry Breaking .....	8
2.2.1 In U(1) Abelian Theory.....	11
2.2.2 In SU(2) Non-abelian Theory.....	16
2.2.2.1 SU(2) with a Higgs Doublet .....	16
2.2.2.2 SU(2) with a Higgs Triplet .....	19
2.2.3 In the Glashow–Weinberg–Salam Theory of the Electroweak Interaction.....	22
2.3 Neutrinos .....	29
2.3.1 History and Discovery.....	30
2.3.2 Sources and Significance.....	31
2.3.3 Properties.....	34
2.4 Neutrino Interactions in the Standard Model .....	35
2.4.1 Antineutrino-Electron Elastic Scattering .....	36
2.4.2 Neutrino-Electron Elastic Scattering .....	39
<b>CHAPTER THREE – WHY TO GO BEYOND THE STANDARD MODEL ...</b>	<b>42</b>
3.1 Standard Model as an Effective Theory .....	42

3.2 Shortcomings of the Standard Model.....	43
3.3 Scalar, Pseudoscalar and Tensorial Non-standard Interaction of Neutrinos....	50
<b>CHAPTER FOUR – LITTLE HIGGS MODELS.....</b>	<b>54</b>
4.1 The SU(5) Littlest Higgs Model .....	54
4.1.1 Antineutrino-Electron Scattering.....	57
4.1.1.1 $\bar{\nu}_e + e \rightarrow \bar{\nu}_e + e$ (FC) .....	57
4.1.1.2 $\bar{\nu}_e + e \rightarrow \bar{\nu}_{\alpha \neq e} + e$ (FV).....	67
4.1.2 Neutrino-Electron Scattering.....	73
4.1.2.1 $\nu_e + e \rightarrow \nu_e + e$ (FC) .....	73
4.1.2.2 $\nu_e + e \rightarrow \nu_{\alpha \neq e} + e$ (FV).....	80
4.2 The SU(3) Simple Little Higgs Model.....	85
<b>CHAPTER FIVE – ANALYSIS AND DISCUSSION .....</b>	<b>95</b>
5.1 NSI Analysis Results .....	100
5.2 SU(5) LTHM Analysis Results.....	102
5.3 SU(3) SLHM Analysis Results.....	105
<b>CHAPTER SIX – CONCLUSION AND PROSPECTS .....</b>	<b>108</b>
<b>REFERENCES.....</b>	<b>113</b>
<b>APPENDICES .....</b>	<b>119</b>
Appendix A : Differential Scattering Cross Section.....	119
Appendix B : Kinematic Terms.....	126

## LIST OF FIGURES

	<b>Page</b>
Figure 2.1 A schematic diagram of the standard model of particle physics .....	3
Figure 2.2 A schematic diagram of the core idea of the Higgs mechanism.....	25
Figure 2.3 Projection in the plane $\phi^\dagger = 0$ of the potential $V(\phi)$ in the cases $\mu^2 > 0$ ( <i>left</i> ) and "Mexican hat" $\mu^2 < 0$ ( <i>right</i> ) .....	29
Figure 2.4 The beta decay spectrum of tritium ( ${}^3_1H \rightarrow {}^3_2He$ ) .....	31
Figure 2.5 Neutrino sources versus decades of energy with the cross section of $\bar{\nu}_e e$ elastic scattering versus neutrino energy (for massless neutrinos) superimposed for comparison .....	32
Figure 2.6 A schematic representation of the right-handedness and left-handedness of a particle .....	34
Figure 2.7 Feynman diagrams of (a) $Z$ -mediated and (b) $W$ -mediated antineutrino-electron scattering in the SM.....	36
Figure 2.8 Feynman diagrams of neutrino-electron scattering via the exchange of a (a) $Z$ -boson (NC) and (b) $W$ -boson (CC) in the SM.....	39
Figure 3.1 Feynman diagrams of the Higgs interaction with the SM top quark ( <i>left</i> ), gauge bosons ( <i>center</i> ) and Higgs boson ( <i>right</i> ).....	46
Figure 3.2 Higher order Feynman diagrams of the Higgs interaction with the SM particles .....	46
Figure 3.3 The fine-tuning required ( <i>red histogram</i> ) to obtain an acceptable Higgs mass in the SM with cut-offs $\Lambda \approx 10^{16} TeV$ , $\Lambda = 10 TeV$ and $\Lambda = 1 TeV$ .....	49
Figure 3.4 Lepton flavor violating processes .....	51
Figure 3.5 NSIs of neutrinos described as four-Fermi interaction with new couplings.....	52

Figure 4.1	Feynman diagrams of (a) $Z$ -mediated and (b) $W$ -mediated antineutrino-electron FC scattering in the $SU(5)$ LTHM along with the corresponding vertex and propagator factors .....	58
Figure 4.2	Feynman diagrams of (a) $Z_H$ -mediated, (b) $A_H$ -mediated and (c) $W_H$ -mediated antineutrino-electron FC scattering in the $SU(5)$ LTHM together with the convenient vertex and propagator factors .....	63
Figure 4.3	Feynman diagram of antineutrino-electron FV scattering via the exchange of a $Z$ boson (NC) in the $SU(5)$ LTHM with the relevant vertex and propagator factors are also shown.....	68
Figure 4.4	Feynman diagrams of antineutrino-electron FV scattering via the exchange of (a) $Z_H$ and (b) $A_H$ bosons in the $SU(5)$ LTHM where the necessary vertex and propagator factors have been also given.....	70
Figure 4.5	Feynman diagrams of (a) $Z$ -mediated and (b) $W$ -mediated FC scattering of neutrino with electron in the $SU(5)$ LTHM with the appropriate vertex and propagator factors are also shown.....	73
Figure 4.6	Feynman diagrams of the FC neutrino-electron scattering process transmitted by (a) $Z_H$ , (b) $A_H$ and (c) $W_H$ bosons of the $SU(5)$ LTHM in addition to the suitable vertex and propagator factors.....	76
Figure 4.7	Feynman diagram of $Z$ -mediated neutrino-electron FV scattering in the $SU(5)$ LTHM.....	80
Figure 4.8	Feynman diagrams of (a) $Z_H$ -mediated and (b) $A_H$ -mediated neutrino-electron FV scattering in the $SU(5)$ LTHM where the corresponding vertex and propagator factors are also shown .....	82
Figure 5.1	The best fit result of (a) TEXONO and (b) LSND experimental measured values to the theoretical ones.....	97
Figure 5.2	The 90% C.L. allowed region put by TEXONO and LSND experiments on the $(g_V, g_A)$ space and $\sin^2\theta_W$ .....	98

Figure 5.3	Differential cross section as a function of the recoil energy $T$ with typical reactor $\bar{\nu}_e$ spectra for scalar, pseudoscalar and tensorial NSIs .....	100
Figure 5.4	(a) $\Delta\chi^2$ of one-parameter-at-a-time analysis for $g_{S,P}^{e,e}$ , $(g_{S=P}^{e,e})^2$ and $(g_T^{e,e})^2$ , the 90% C.L. allowed regions from TEXONO and LSND data sets in the parameter spaces of (b) $g_S^{e,e} - g_P^{e,e}$ and (c) $g_S^{e,e} (g_P^{e,e}) - (g_T^{e,e})^2$ , and (d) the 90% C.L. upper limits of $g_T^{e,e}$ as a function of $g_S^{e,e}$ and $g_P^{e,e}$ .....	101
Figure 5.5	Exclusion limits at 95% C.L. (light blue) and 99% C.L. (dark blue) from EWPD and Higgs data combined as a function of the $SU(5)$ LTHM scale $f$ with the thick black lines represent contours of required fine-tuning.	103
Figure 5.6	Differential cross section as a function of the recoil energy $T$ with typical reactor $\bar{\nu}_e$ spectra for $SU(5)$ LTHM.....	103
Figure 5.7	The 90% C.L. allowed regions in the $(c^2, c'^2)$ parameter space for FC $SU(5)$ LTHM at (a) $f = 500 \text{ GeV}$ and (c) $f = 2 \text{ TeV}$ with their corresponding upper and lower bounds in the $(c, c')$ parameter space given by (b) and (f) respectively from TEXONO and LSND data sets .....	104
Figure 5.8	Exclusion limits at 95% C.L. (light blue) and 99% C.L. (dark blue) from EWPD and Higgs data combined as a function of the $SU(3)$ SLHM scale $f$ with the thick black lines represent contours of required fine-tuning.	106
Figure 5.9	The upper and lower limits at 90% C.L. on $t_\beta$ versus $f$ from TEXONO and LSND experimental measured values, respectively .....	107

## LIST OF TABLES

	Page
Table 2.1 The fields multiplets in the SM and their quantum numbers .....	4
Table 2.2 Coefficients in the expression of the SM $(\bar{\nu}_e)e$ scattering cross section given by Equation 2.98 .....	41
Table 4.1 Couplings of the SM $Z$ and $W$ gauge bosons and the new heavy $Z_H, A_H$ and $W_H$ gauge bosons with leptons in the $SU(5)$ LTHM .....	57
Table 4.2 Couplings of the SM $Z$ and $W$ gauge bosons and the new heavy $Z', Y$ and $X$ gauge bosons with leptons in the $SU(3)$ SLHM .....	86
Table 5.1 A summary of the published measurements of cross section and weak mixing angle by some $\nu_e - e$ and $\bar{\nu}_e - e$ experiments .....	95
Table 5.2 $\Delta\chi^2$ as a function of confidence level and number of degrees of freedom	99
Table 5.3 Bounds on NSI parameters from a one-dimensional analysis using TEXONO and LSND data sets.....	102
Table 5.4 Global bounds from TEXONO and LSND experimental data on $c$ and $c'$ as a function of $f$ ranges at 90% C.L. via a one-dimensional statistical analysis .....	105
Table 5.5 Global bounds from TEXONO and LSND experimental data on $t_\beta$ as a function of $f$ ranges at 90% C.L. via a one-dimensional statistical analysis .	106
Table 6.1 Coefficients in the expression of the FC and FV $SU(5)$ LTHM differential cross section of $(\bar{\nu}_e)e$ scattering given by Equation 6.1.....	110
Table 6.2 Coefficients in the expression of the FC and FV $SU(3)$ SLHM differential cross section of $\nu_e(\bar{\nu}_e)e$ scattering given by Equation 6.1.....	111

# CHAPTER ONE

## INTRODUCTION AND MOTIVATION

Known as “the theory of almost everything”, the standard model (SM) of particle physics is an elegant weakly coupled quantum field theory used to describe, to a very good extent, the behavior of all discovered fundamental particles. It is the whole story of our everyday life but surely not that of the universe.

Despite its precise agreement with the results of almost all experiments carried out at relatively low energies, there are still some good reasons for the crucial need of new physics beyond the SM (BSM) at relatively high energies. As far as this thesis work is concerned, the so-called “hierarchy problem” of the SM was one of the many reasons that motivated particle physicists to look eagerly for new theories BSM. Indeed, at very high energies, the mass of the SM Higgs boson suffers from quadratically divergent radiative corrections mainly due to the SM electroweak gauge bosons, top quark and the Higgs boson itself. That is, the SM can have the chance to survive at very high energies if and only if its parameters are hugely fined-tuned in such a way to get an accepted Higgs boson mass of at most a few hundred  $GeV$ . Actually, the SM breaks down much earlier, at the  $TeV$  energy scale, due to its insufficient elucidation of electroweak symmetry breaking (EWSB) by the Higgs mechanism.

In this regard and in an aim of solving the SM hierarchy problem without fine-tuning its parameters, many BSM physics theories have been explored; the most recent of which dubbed little Higgs (LH) theories will be the central theme of this thesis.

To better understand the presented problem and the expected solution, this thesis work is designed as follows: Chapter 2 will be a precise introduction to what is known as the SM of particle physics and its formulation with an emphasis on the neutrino and the Higgs sectors. Chapter 3 will provide a comprehensive description of some of the shortcomings of the SM with an emphasis on the hierarchy problem of the Higgs boson mass hinting to the crucial need of BSM physics, in addition to an example

of a model-independent BSM theory known as scalar, pseudoscalar and tensorial non-standard interaction (NSI) of neutrinons. As the main theme of this work, chapter 4 will display a great deal of theoretical calculations done for two different little Higgs models (LHMs), suggested recently as a solution to the SM hierarchy problem. Chapter 5 will contain all the analysis done in the scope of NSI of neutrinos and LHMs using different low and high energy experimental data sets; TEXONO, LSND, LEP and EWP. Last but not least, chapter 6 will contain a brief summary of theoretical and analytic results and will shed the light on some of our future works regarding this topic.

At the end of the day and after doing all the long and tremendous theoretical calculations of LHMs suggested to solve the hierarchy problem of the SM, our main motivation is to constraint some of their different free parameters at the low energy region. Having done so, we can then compare our constraints with the corresponding ones put by other collaborations at high energy regions. This would allow us to decide whether it is advantageous to have a costly high energy experiment in the scope of LHMs or otherwise low energy experiments can do the exact same job with less energy and less money.

## CHAPTER TWO

### THE STANDARD MODEL

#### 2.1 Review of the Standard Model

The standard model (SM) of particle physics is a gauge field theory that describes the fundamental weak, electromagnetic and strong interactions between elementary particles with the renormalizable quantum field theory, which is locally invariant under an inner symmetry group  $SU(3)_C \times SU(2)_L \times U(1)_Y$  and globally invariant under the space-time transformations of the Poincaré group (Demirci, 2015).

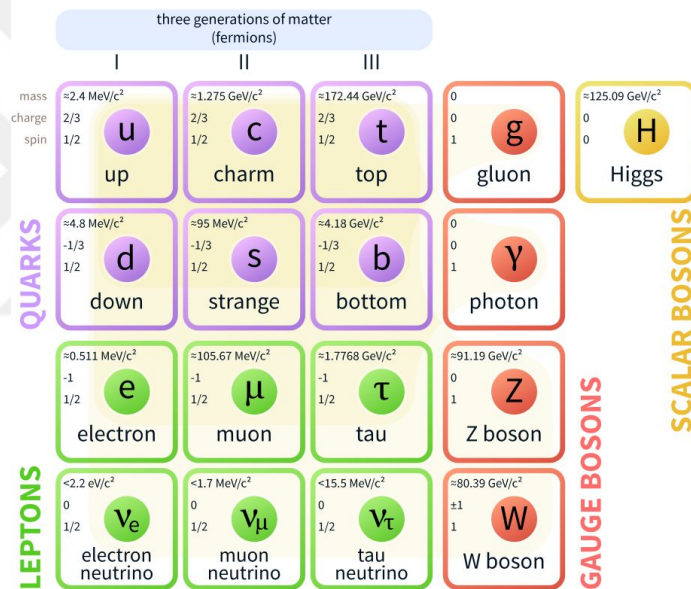


Figure 2.1 A schematic diagram of the standard model of particle physics (Fehling, 2008)

As is schematically presented in Figure 2.1, it is made up of a total of 17 fundamental particles, categorized basically into two main groups of 12 fermions known as the basic building blocks of matter and 5 bosons known as the force carriers. The fermions are divided into 6 quarks, 3 charged leptons and 3 neutral leptons accompanied in three generations. Excluding the dark matter and dark energy which form about 96% of the known universe, all other ordinary matter around us is made up mainly of these fermions with an emphasis on the first generation ones being the lightest and most

stable ones. The bosons, however, are divided into 4 vector gauge bosons and 1 scalar boson. The vector bosons are the corresponding mediators of the strong, electromagnetic and weak forces that act on the matter particles via the exchange of force-carrier particles. Particles of matter transfer discrete amounts of energy by exchanging bosons with each other. Each fundamental force has its own corresponding boson – the electromagnetic force is carried by the “photon”, the weak force is carried by the “W and Z bosons” and the “gluon” is responsible for the strong force. In addition to the scalar boson which is the mediator of the Higgs field.

The particles of the SM are often displayed in groupings known as multiplets. A particle multiplet is a combination of particles that transform into each other under a symmetry transformation. The different field multiplets of the SM along with their quantum numbers corresponding to each symmetry group are summarized in Table 2.1.

Table 2.1 The fields multiplets in the SM and their quantum numbers

Multiplets	$SU(3)_C \times SU(2)_L \times U(1)_Y$	I	II	III
Quarks ( $s = \frac{1}{2}$ )	$(\mathbf{3}, \mathbf{2}, -\frac{1}{6})$	$\begin{pmatrix} u \\ d \end{pmatrix}_L$	$\begin{pmatrix} c \\ s \end{pmatrix}_L$	$\begin{pmatrix} t \\ b \end{pmatrix}_L$
	$(\mathbf{3}, \mathbf{1}, \frac{2}{3})$	$u_R$	$c_R$	$t_R$
	$(\mathbf{3}, \mathbf{1}, -\frac{1}{3})$	$d_R$	$s_R$	$b_R$
Leptons ( $s = \frac{1}{2}$ )	$(\mathbf{1}, \mathbf{2}, -\frac{1}{2})$	$\begin{pmatrix} \nu_e \\ e \end{pmatrix}_L$	$\begin{pmatrix} \nu_\mu \\ \mu \end{pmatrix}_L$	$\begin{pmatrix} \nu_\tau \\ \tau \end{pmatrix}_L$
	$(\mathbf{1}, \mathbf{1}, -1)$	$e_R$	$\mu_R$	$\tau_R$
Higgs ( $s = 0$ )	$(\mathbf{1}, \mathbf{2}, \frac{1}{2})$	$H = \begin{pmatrix} h^+ \\ h^0 \end{pmatrix}$		

Based on the  $SU(3) \times SU(2) \times U(1)$  symmetry group, the SM Lagrangian, which describes the principle interactions between fermions, gauge bosons and Higgs bosons,

can be written as (Cottingham, 2007)

$$\begin{aligned}
\mathcal{L}_{SM} = & -\frac{1}{4}B_{\mu\nu}B^{\mu\nu} - \frac{1}{8}Tr(\mathbf{W}_{\mu\nu}\mathbf{W}^{\mu\nu}) - \frac{1}{2}Tr(\mathbf{G}_{\mu\nu}\mathbf{G}^{\mu\nu}) \\
& + (\bar{\nu}_L, \bar{e}_L) \tilde{\sigma}^\mu iD_\mu \begin{pmatrix} \nu_L \\ e_L \end{pmatrix} + \bar{e}_R \sigma^\mu iD_\mu e_R + \bar{\nu}_R \sigma^\mu iD_\mu \nu_R + (\text{h.c.}) \\
& - \frac{\sqrt{2}}{v} \left[ (\bar{\nu}_L, \bar{e}_L) \phi M^e e_R + \bar{e}_R \bar{M}^e \bar{\phi} \begin{pmatrix} \nu_L \\ e_L \end{pmatrix} \right] \\
& - \frac{\sqrt{2}}{v} \left[ (-\bar{e}_L, \bar{\nu}_L) \phi^* M^e \nu_R + \bar{\nu}_R \bar{M}^e \phi^T \begin{pmatrix} -e_L \\ \nu_L \end{pmatrix} \right] \\
& + (\bar{u}_L, \bar{d}_L) \tilde{\sigma}^\mu iD_\mu \begin{pmatrix} u_L \\ d_L \end{pmatrix} + \bar{u}_R \sigma^\mu iD_\mu u_R + \bar{d}_R \sigma^\mu iD_\mu d_R + (\text{h.c.}) \\
& - \frac{\sqrt{2}}{v} \left[ (\bar{u}_L, \bar{d}_L) \phi M^d d_R + \bar{d}_R \bar{M}^d \bar{\phi} \begin{pmatrix} u_L \\ d_L \end{pmatrix} \right] \\
& - \frac{\sqrt{2}}{v} \left[ (-\bar{d}_L, \bar{u}_L) \phi^* M^d u_R + \bar{u}_R \bar{M}^d \phi^T \begin{pmatrix} -d_L \\ u_L \end{pmatrix} \right] \\
& + (\overline{D_\mu \phi}) D^\mu \phi - \frac{m_h^2}{2v^2} \left( \bar{\phi} \phi - \frac{v^2}{2} \right)^2,
\end{aligned} \tag{2.1}$$

where the first line corresponds to  $U(1)$ ,  $SU(2)$  and  $SU(3)$  gauge terms, the second to lepton dynamical term, the third to electron, muon and tau mass term, the fourth to neutrino mass term, the fifth to quark dynamical term, the sixth to down, strange and bottom mass term, the seventh to up, charm and top mass term, and the last to Higgs dynamical and mass term.

In the above Lagrangian,

- $B_\mu$ ,  $\mathbf{W}_\mu$  and  $\mathbf{G}_\mu$  are the gauge boson vector potentials with their respective field

tensors given as

$$\begin{aligned}
B_{\mu\nu} &= \partial_\mu B_\nu - \partial_\nu B_\mu, \\
\mathbf{W}_{\mu\nu} &= \partial_\mu \mathbf{W}_\nu - \partial_\nu \mathbf{W}_\mu + \frac{ig_2}{2} (\mathbf{W}_\mu \mathbf{W}_\nu - \mathbf{W}_\nu \mathbf{W}_\mu), \\
\mathbf{G}_{\mu\nu} &= \partial_\mu \mathbf{G}_\nu - \partial_\nu \mathbf{G}_\mu + ig_3 (\mathbf{G}_\mu \mathbf{G}_\nu - \mathbf{G}_\nu \mathbf{G}_\mu).
\end{aligned} \tag{2.2}$$

- the derivative operators are

$$\begin{aligned}
D_\mu \begin{pmatrix} \nu_L \\ e_L \end{pmatrix} &= \left[ \partial_\mu - \frac{ig_1}{2} B_\mu + \frac{ig_2}{2} \mathbf{W}_\mu \right] \begin{pmatrix} \nu_L \\ e_L \end{pmatrix}, \\
D_\mu \begin{pmatrix} u_L \\ d_L \end{pmatrix} &= \left[ \partial_\mu + \frac{ig_1}{6} B_\mu + \frac{ig_2}{2} \mathbf{W}_\mu + ig_3 \mathbf{G}_\mu \right] \begin{pmatrix} u_L \\ d_L \end{pmatrix}, \\
D_\mu \nu_R &= [\partial_\mu] \nu_R, \\
D_\mu e_R &= [\partial_\mu - ig_1 B_\mu] e_R, \\
D_\mu u_R &= \left[ \partial_\mu + \frac{2ig_1}{3} B_\mu + ig_3 \mathbf{G}_\mu \right] u_R, \\
D_\mu d_R &= \left[ \partial_\mu - \frac{ig_1}{3} B_\mu + ig_3 \mathbf{G}_\mu \right] d_R, \\
D_\mu \phi &= \left[ \partial_\mu + \frac{ig_1}{2} B_\mu + \frac{ig_2}{2} \mathbf{W}_\mu \right] \phi.
\end{aligned} \tag{2.3}$$

- $\phi$  is a two-component complex Higgs field that can have the form

$$\phi^T = \frac{1}{\sqrt{2}} (0, v + h) \tag{2.4}$$

with a vacuum expectation value (VEV)

$$\langle \phi \rangle_0^T = \frac{1}{\sqrt{2}} (0, v) \tag{2.5}$$

under  $SU(2)$  gauge invariance. Here  $v$  is a real constant such that  $\mathcal{L}_\phi$  (the last line of Equation 2.1 with  $D_\mu \rightarrow \partial_\mu$ ) is minimized, and  $h$  is a residual Higgs field.

- h.c. infers the hermitian conjugation of previous terms; that is,  $\bar{\psi} = (\text{h.c.}) \psi = \psi^\dagger = \psi^{*T}$ .

- $L$  and  $R$  denote respectively a left-handed fermion doublet and a right-handed fermion singlet.

The SM of particle physics explains the interactions among elementary particles by three main forces: electromagnetic, weak and strong. The weak forces, however, are somehow strange compared to the other two fundamental forces as they get to conflict by four main items:

- The weak forces are inescapable in a way that all the particles feel them, far from the electromagnetic and strong interactions that are only sensitive to the charged leptons and quarks, respectively.
- The force mediators of the weak interactions are extremely massive, unlike those of the electromagnetic and strong interactions which are massless.
- In contrast to the electromagnetic and strong interactions, the weak interactions violate parity (P) and charge conjugation (C) as well as their combination (CP).
- As opposed to the electromagnetic and strong interactions through which flavor does not change, the weak interactions do change flavor and are therefore the only forces responsible for true decays.

Nowadays, the electroweak theory of the SM is known -and without any suspect- as the theory that incarnates the interactions of the elementary particles at the electroweak scale. However, we have many signs from fields that are even outside high energy physics that warn us to the fact that electroweak theory is an effective theory; a theory that is brilliantly successful at the electroweak scale but not much far beyond that.

The three fundamental interactions managed by the SM are based on  $SU(3) \times SU(2) \times U(1)$  gauge symmetry, where  $SU(3)$ ,  $SU(2)$  and  $U(1)$  reflect respectively the symmetry of the strong, weak and electromagnetic interactions at high energies. At

low energies, however, the weak interactions seem to represent a state of broken symmetry when combined with electromagnetic interactions, the reason they are treated as an electroweak gauge theory ( $SU(2)_L \times U(1)_Y \rightarrow U(1)_{EM}$ ).

## 2.2 Higgs Mechanism and Spontaneous Symmetry Breaking

In this section, the light will be shed on the principle of gauge symmetry in general and the mechanism through which the underlying symmetry of the SM electroweak interactions is broken, the so-known Higgs mechanism (Englert et al., 1964; Higgs, 1964).

The principle of gauge invariance is the core ingredient of the electroweak and strong theories of the SM of particle physics. It dates back to the 19<sup>th</sup> century when the electromagnetic theory was first put, in which the electromagnetic scalar and vector potentials were believed to be arbitrary and not restricted to have one absolute form. That is to say, different forms of the vector potential (differing for example in a gradient of some scalar function)

$$\vec{A} \rightarrow \vec{A}' = \vec{A} + \vec{\nabla}\chi \quad (2.6)$$

produce the same physical fields  $\vec{E}$  and  $\vec{B}$  given in terms of  $V$  and  $\vec{A}$  by

$$\begin{aligned} \vec{E} &= -\vec{\nabla}V - \frac{\partial\vec{A}}{\partial t}, \\ \vec{B} &= \vec{\nabla} \times \vec{A}, \end{aligned} \quad (2.7)$$

as long as the scalar potential transforms simultaneously in the form

$$V \rightarrow V' = V - \frac{\partial\chi}{\partial t} \quad (2.8)$$

to pay for the change in  $\vec{A}$ .

Later in 1926, Fock realized that the wave equation of a charged particle under the

effect of an external electromagnetic field is symmetric under some space-time  $U(1)$  phase transformation  $\phi \rightarrow e^{i\alpha(\vec{x},t)}\phi$ , provided that the corresponding gauge bosons in the theory transform in such a way as to compensate the change of phase.

Moreover, and around 1955, Yang and Mills announced the fact that the principle of gauge invariance is not confined to  $U(1)$  phase transformations but could also be extended to  $SU(2)$  isospin transformations. The main difference in the latter transformations and the reason it is more difficult to work with them is the incompatibility of the group generators with one another.

Nevertheless, gauge invariance was at first distrusted to be a principle on which all the modern interactions are built as it courageously demands all the gauge bosons involved in the theory to be massless. This would not fit, for example, in the electroweak theory because of its extremely massive gauge bosons. This problem can indeed be approached in two ways: either the gauge bosons can get a mass term through spontaneous symmetry breaking of the Higgs mechanism as it is realized in electroweak interactions or the bosons can not be seen due to confinement as it is realized in strong interactions. Being interested in electroweak interactions and the Higgs mechanism, the former will be our main topic in this section.

The Higgs mechanism -which is sort of assumed as part of the SM- is perhaps the simplest possible or the most economic way that introduces the least number of degrees of freedom to realize electroweak symmetry breaking (EWSB).

The key idea of the Higgs mechanism is the possibility of recognizing some symmetry of the theory at the level of the Lagrangian but not at the level of the ground state of the symmetry. It is, however, not only a matter of symmetry but also a matter of the intrinsic features of the spectrum of fields in the concerned theory that would modify abruptly once working out over the ground state level of the theory.

It is very often heard that the Higgs field gives mass to particles that interact with it and the bigness or smallness or maybe the full absence of the mass is usually related

to the strength of the coupling of the particle with the field. To see how the Higgs mechanism actually works, a very rough explanation is first needed followed by an explicit representation of the mechanism in a simple abelian and non-abelian model all the way towards the actual Higgs mechanism in Glashow-Weinberg-Salam (GWS) model of the SM.

Suppose that some particle field  $\psi$  and its corresponding antiparticle field  $\bar{\psi}$  couples to a Higgs field  $\phi$  with a coupling constant  $g$  as is roughly given by the interaction term

$$g\bar{\psi}\psi\phi. \tag{2.9}$$

By spontaneous symmetry breaking, the Higgs field breaks down into two components; the first one, denoted by  $v$ , is a constant (VEV) and the second one, denoted by  $H$ , is some new dynamic field and its quanta are the Higgs bosons as is given by

$$\phi = v + H. \tag{2.10}$$

Putting this into the interaction term of Equation 2.9 gives as a result

$$g\bar{\psi}\psi v + g\bar{\psi}\psi H. \tag{2.11}$$

The second term represents an interaction among  $H$ ,  $\psi$  and  $\bar{\psi}$  rather than  $\phi$ ,  $\psi$  and  $\bar{\psi}$  as in the original interaction term. The first term, however, is where the mass comes from. It is an interaction term between a particle and its antiparticle with no third field. The interaction term that used to describe the coupling of the Higgs field to other fields now describes the other fields coupling (quadratically) to themselves, which in quantum field theory is interpreted as giving mass to a field. By this term, the particles of the field  $\psi$  and the antiparticles of the field  $\bar{\psi}$  both have mass  $m = gv$  that did not have it before. But by the Higgs field's VEV, the massless fields managed to gain a mass term "out of nothing" which is roughly what is meant by expression that

the Higgs field gives mass to particles.

### 2.2.1 In $U(1)$ Abelian Theory

In general, a family of  $N$  real scalar fields

$$\vec{\phi}(x) : \{\phi_1(x), \phi_2(x), \dots, \phi_N(x)\}$$

in an interacting purely scalar theory obeying the following hypothetical "Klein-Gordon analogous" Lagrangian density

$$\mathcal{L}(\vec{\phi}) = \frac{1}{2}(\delta_\mu \vec{\phi})^2 - \frac{1}{2}\mu^2 \vec{\phi}^2 - \frac{1}{4}\lambda \vec{\phi}^4 \quad (2.12)$$

is symmetric under  $U(N)$  gauge theory at the Lagrangian level but not at the ground state level of the symmetry.

Working out the  $N = 1$  case is not the best decision as it is a simple, direct and straightforward replacement of  $\vec{\phi}$  by  $\phi$ , denoting only a one single real scalar field in the theory.

Consider instead a family of  $N = 2$  real scalar fields

$$\vec{\phi}(x) : \{\phi_1(x), \phi_2(x)\}$$

with charge  $-g$  in a purely interacting scalar gauge theory. Working out this theory in details is an advantage as all the methodology that is going to be developed here can be applied for the actual Higgs mechanism of GWS theory of the SM but at a more advanced level.

It is tremendously appropriate to switch to complex representation once dealing

with two fields

$$\Phi = \frac{1}{\sqrt{2}}(\phi_1 + i\phi_2). \quad (2.13)$$

The new defined complex scalar field  $\Phi$  obeys the analogous form of the Lagrangian of Equation 2.12 written in terms of the newly defined  $\Phi$  as

$$\mathcal{L}(\Phi, \Phi^*) = (\partial^\mu \Phi)^* \partial_\mu \Phi - \mu^2 \Phi^* \Phi - \lambda (\Phi^* \Phi)^2. \quad (2.14)$$

Compared to the free spin-0 Klein-Gordon Lagrangian with a real scalar field  $\phi$

$$\mathcal{L}(\phi) = \frac{1}{2} (\delta_\mu \phi)^2 + \frac{1}{2} m^2 \phi^2, \quad (2.15)$$

the hypothesized Lagrangian seems to have a "wrong sign" in the mass term which would consequently imply a tachyonic particle moving with  $v > c$ . This is, of course, unusual in particle physics but has a very congenial clarification in quantum field theory.

It is a straightforward mission to show that the hypothesized Lagrangian is globally invariant under the abelian  $U(1)$  symmetry with the global transformation  $\Phi \rightarrow e^{i\alpha} \Phi$ . However, such an invariance will clearly not be preserved under the local form transformation  $\Phi \rightarrow e^{i\alpha(x)} \Phi$ .

The local invariance can be normally repaired with a new derivative operator

$$\partial_\mu \rightarrow D_\mu \equiv \partial_\mu - igA_\mu \quad (2.16)$$

with the gauge fields transform under  $U(1)$  as

$$A_\mu(x) \rightarrow A_\mu(x) + \frac{1}{g} \partial_\mu \alpha(x), \quad (2.17)$$

in addition to a kinetic-like term from the Proca Lagrangian for the new vector gauge field  $A_\mu$  to allow it to propagate

$$-\frac{1}{4}F_{\mu\nu}F^{\mu\nu} \quad (2.18)$$

where the strength tensor for an abelian symmetry is simply

$$F_{\mu\nu} = \partial_\mu A_\nu - \partial_\nu A_\mu. \quad (2.19)$$

Note that adding a mass term for the gauge field  $A_\mu$  clearly violates the local gauge invariance. In other words, the  $U(1)$  gauge symmetry requires  $A_\mu$  to be massless.

Under these modifications, a locally  $U(1)$  symmetric Lagrangian of the complex scalar field  $\Phi$  can be reproduced from the original hypothesized Lagrangian as

$$\begin{aligned} \mathcal{L}(\Phi, \Phi^*, A_\mu, A^\mu) &= (D_\mu \Phi)^* (D^\mu \Phi) - \mu^2 \Phi^* \Phi - \lambda (\Phi^* \Phi)^2 - \frac{1}{4} F_{\mu\nu} F^{\mu\nu} \\ &= [(\delta_\mu + igA_\mu) \Phi^* (\delta^\mu - igA^\mu) \Phi] - \mu^2 \Phi^* \Phi \\ &\quad - \lambda (\Phi^* \Phi)^2 - \frac{1}{4} F_{\mu\nu} F^{\mu\nu}. \end{aligned} \quad (2.20)$$

This Lagrangian, besides from being locally invariant, has one more very interesting feature: the gauge fields  $A_\mu$  that look massless at the Lagrangian level are indeed massive at the ground state level. That is, when  $\Phi$  goes to some constant value at the minimum  $\Phi_o$ , the square-bracketed term of the Lagrangian of Equation 2.20 yields something that looks like

$$+igA_\mu \Phi_o (-igA^\mu \Phi_o) \quad (2.21)$$

which can be a real mass term for the  $A_\mu$  fields. Having roughly explained the origin of the gauge fields' mass term, we are going to elaborate on it in more details below.

Particle physicists usually treat fields as particle-like tiny localized fluctuations. The

fields  $\Phi(x^\mu)$  and  $A_\mu(x^\mu)$  can then be written as

$$\begin{aligned}\Phi(x^\mu) &= \Phi_0 + \delta\Phi(x^\mu), \\ A_\mu(x^\mu) &= A_{\mu_0} + \delta A_\mu(x^\mu),\end{aligned}\tag{2.22}$$

where the nod terms ( $\Phi_0 \equiv \langle \Phi \rangle$  and  $A_{\mu_0} \equiv \langle A_\mu \rangle$ ) are the background configurations or the so-called VEVs of the corresponding fields and the delta terms ( $\delta\phi = \frac{1}{\sqrt{2}}(\delta\phi_1 + i\delta\phi_2)$  and  $\delta A_\mu$ ) are the tiny fluctuations about the VEVs that can be treated quantum mechanically. Note that the VEVs are most often assumed to be zero during a calculation in particle physics.

Looking at a boring configuration of static solutions, externalizing the potential

$$V(|\Phi|^2) = \mu^2 \Phi^* \Phi + \lambda (\Phi^* \Phi)^2\tag{2.23}$$

with respect to  $\Phi^*$

$$\frac{\partial V}{\partial \Phi^*} = (\mu^2 + 2\lambda |\Phi|^2) \Phi = 0\tag{2.24}$$

is enough to get the corresponding equation of motion of  $\Phi$ .

The first trivial solution is

$$\begin{cases} \Phi = 0 \\ A_\mu = 0 \end{cases}\tag{2.25}$$

or in terms of fluctuations

$$\begin{cases} \Phi(x) = 0 + \delta\Phi(x) \\ A_\mu(x) = 0 + \delta A_\mu(x). \end{cases}\tag{2.26}$$

The Lagrangian governing fluctuations is then

$$\begin{aligned} \mathcal{L}(\delta\Phi, \delta\Phi^*, \delta A_\mu, \delta A^\mu) = & [(\partial_\mu + ig\delta A_\mu) \delta\Phi^* (\partial^\mu - ig\delta A^\mu) \delta\Phi] \\ & - \mu^2 \delta\Phi^* \delta\Phi - \lambda (\delta\Phi^* \delta\Phi)^2 - \frac{1}{4} F'_{\mu\nu} F'^{\mu\nu} \end{aligned} \quad (2.27)$$

where

$$F'_{\mu\nu} = \partial_\mu \delta A_\nu - \partial_\nu \delta A_\mu. \quad (2.28)$$

This Lagrangian also shares the local symmetry of the original Lagrangian  $\mathcal{L}(\Phi, \Phi^*, A_\mu, A^\mu)$  of Equation 2.20 under  $U(1)$  transformation.

The other non-trivial solution is

$$\begin{cases} \Phi = \Phi_o \text{ where } |\Phi_o|^2 = -\frac{\mu^2}{2\lambda} \\ A_\mu = 0 \end{cases} \quad (2.29)$$

A one particular solution in terms of fluctuations can be then

$$\begin{cases} \phi_1(x) = \sqrt{-\frac{\mu^2}{2\lambda}} + \delta\phi_1(x) \equiv \frac{v}{\sqrt{2}} + \eta(x) \\ \phi_2(x) = 0 + \delta\phi_2(x) \equiv \beta(x) \\ A_\mu(x) = 0 + \delta A_\mu(x) \equiv A_\mu(x) \end{cases} \quad (2.30)$$

where  $\eta(x)$  and  $\beta(x)$  are respectively the fluctuations of the real and imaginary parts of the complex scalar field  $\Phi$  and  $A_\mu(x)$  is the corresponding fluctuation of the vector gauge field  $A_\mu$ .

The Lagrangian in terms of this particular solution becomes

$$\begin{aligned}
\mathcal{L}(\eta, \beta, A_\mu) = & \left[ \frac{1}{2} (\partial_\mu \eta) (\partial^\mu \eta) + \mu^2 \eta^2 \right] + \left[ \frac{1}{2} (\partial_\mu \beta) (\partial^\mu \beta) \right] + \left[ \frac{1}{16\pi} F_{\mu\nu} F^{\mu\nu} \right] \\
& + \frac{1}{2} \left[ \left( \frac{q}{c} \right)^2 A_\mu A^\mu \right] + \left\{ \frac{q}{\hbar c} [\eta (\partial_\mu \beta) - \beta (\partial_\mu \eta)] A^\mu \right. \\
& + \frac{\mu}{\lambda} \left( \frac{q}{c} \right)^2 \eta A_\mu A^\mu + \frac{1}{2} \left( \frac{q}{c} \right)^2 (\beta^2 + \eta^2) A_\mu A^\mu \\
& \left. + \lambda \mu (\eta^3 + \eta \beta^2) + \frac{1}{4} \lambda^2 (\eta^4 + \eta^3 \beta^3 + \beta) \right\} + \left( \frac{q}{c} \right) (\partial_\mu \beta) A^\mu - \left( \frac{q}{c} \right)^2.
\end{aligned} \tag{2.31}$$

This miracle-like Lagrangian summarizes all the incredible outcomes of the brilliant Higgs mechanism in the simplest possible way as is realized in the simple  $U(1)$  abelian systems. The gauge bosons  $A_\mu$  that seemed massless at the Lagrangian level exhibited a mass term  $m_{A_\mu} = g^2$  at the VEV level. Furthermore, upon choosing the VEV in the direction of  $\phi_1$ ,  $\beta$  (the oscillations about  $\phi_2$ ) and consequently  $\phi_2$  became a massless boson (the so-called goldstone boson) which is later got "absorbed" by  $A_\mu$  to gain its missing longitudinal degree of freedom. This happened, however, at the expense of the symmetry of the theory. Although, the original theory is still symmetric, such symmetry is unseen at the level of VEV. We say that the symmetry has been broken or more accurately hidden by the chose of VEV.

## 2.2.2 In $SU(2)$ Non-abelian Theory

### 2.2.2.1 $SU(2)$ with a Higgs Doublet

To illustrate the non-abelian Higgs mechanism, consider the example of  $SU(2)$  gauge theory coupled to a doublet of complex scalar fields  $\Phi_i(x)$ . In terms of canonically normalized fields, the Lagrangian can be written as (Dawson, 1999)

$$\mathcal{L} = -\frac{1}{4} F_{\mu\nu}^a F^{a\mu\nu} + D_\mu \Phi^{*i} D^\mu \Phi_i - \frac{\lambda}{2} \left( \Phi^{*i} \Phi_i - \frac{v^2}{2} \right)^2, \tag{2.32}$$

where

$$\begin{aligned}
D_\mu \Phi_i &= \partial_\mu \Phi_i + \frac{i}{2} g A_\mu^a (\sigma^a)_i^j \Phi_j, \\
D_\mu \Phi^{*i} &= \partial_\mu \Phi^{*i} - \frac{i}{2} g A_\mu^a (\sigma^a)^i_j \Phi^{*j}, \\
F_{\mu\nu}^a &= \partial_\mu A_\nu^a - \partial_\nu A_\mu^a - g \varepsilon^{abc} A_\mu^b A_\nu^c.
\end{aligned} \tag{2.33}$$

For  $v^2 > 0$ , the scalar potential has a local maximum at  $\Phi_i = 0$  while the minima form a spherical shell  $\Phi^{*i} \Phi_i = \frac{v^2}{2}$  in the  $\mathbf{C}^2 = \mathbf{R}^4$  field space and are related by  $SU(2)$  symmetries to

$$\langle \Phi \rangle = \frac{v}{\sqrt{2}} \begin{pmatrix} 0 \\ 1 \end{pmatrix}. \tag{2.34}$$

Note that this VEV spontaneously breaks the  $SU(2)$  symmetry down to nothing; there is no subgroup of  $SU(2)$  which leaves this VEV invariant. Consequently, it is expected that all three vector fields  $A_\mu^a(x)$  to become massive.

In the process, three would-be Goldstone scalars should be eaten by the Higgs mechanism. Since the theory has two complex (or equivalently four real) scalars, only one real scalar should survive un-eaten. Ironically, it is this un-eaten scalar  $\sigma(x)$  which is called the physical Higgs field.

To see how this works, let us fix the unitary gauge where

$$\begin{aligned}
\text{Re } \Phi_1(x) &\equiv \text{Im } \Phi_1(x) \equiv \text{Im } \Phi_2(x) \equiv 0, \\
\Phi(x) &= \frac{1}{\sqrt{2}} \begin{pmatrix} 0 \\ \phi_r(x) \end{pmatrix} \text{ with } \phi_r(x) > 0,
\end{aligned} \tag{2.35}$$

and then shift the  $\phi_r$  field by the VEV

$$\phi_r(x) = v + \sigma(x). \tag{2.36}$$

For  $v = 0$ , such gauge fixing would be terribly singular but it is perfectly OK for  $v \neq 0$  and  $|\sigma(x)| < v$  which implies that  $\phi_r(x) \neq 0$ .

In the unitary gauge, the physical Higgs field  $\sigma(x)$  is the only scalar field while the rest are frozen by the gauge-fixing conditions of Equation 2.35. In terms of  $\sigma$ , the scalar potential becomes

$$\begin{aligned} V &= \frac{\lambda}{2} \left( \Phi^\dagger \Phi - \frac{v^2}{2} \right)^2 \\ &= \frac{\lambda}{8} (2v\sigma + \sigma^2)^2 = \frac{\lambda v^2}{2} \sigma^2 + \frac{\lambda v}{2} \sigma^3 + \frac{\lambda}{8} \sigma^4, \end{aligned} \quad (2.37)$$

where the first term is the mass term ( $m^2 = \lambda v^2$ ) while the remaining terms are self-interactions.

More interestingly, the covariant derivative of the Higgs doublet  $\Phi$  becomes

$$\begin{aligned} D_\mu \Phi &= \frac{1}{\sqrt{2}} \left[ \begin{pmatrix} 0 \\ \partial_\mu \sigma \end{pmatrix} + \frac{ig}{2} A_\mu^3 \begin{pmatrix} 1 & 0 \\ 0 & -1 \end{pmatrix} \begin{pmatrix} 0 \\ v + \sigma \end{pmatrix} \right. \\ &\quad \left. + \frac{ig}{2} A_\mu^1 \begin{pmatrix} 0 & 1 \\ 1 & 0 \end{pmatrix} \begin{pmatrix} 0 \\ v + \sigma \end{pmatrix} + \frac{ig}{2} A_\mu^2 \begin{pmatrix} 0 & -i \\ i & 0 \end{pmatrix} \begin{pmatrix} 0 \\ v + \sigma \end{pmatrix} \right] \\ &= \frac{1}{\sqrt{2}} \begin{pmatrix} \frac{i}{2} g (A_\mu^1 - iA_\mu^2) (v + \sigma) \\ \partial_\mu \sigma - \frac{i}{2} g A_\mu^3 (v + \sigma) \end{pmatrix}, \end{aligned} \quad (2.38)$$

hence

$$\begin{aligned} (D_\mu \Phi)^\dagger D^\mu \Phi &= \frac{1}{2} \left| \frac{i}{2} g (A_\mu^1 - iA_\mu^2) (v + \sigma) \right|^2 + \frac{1}{2} \left| \partial_\mu \sigma - \frac{i}{2} g A_\mu^3 (v + \sigma) \right|^2 \\ &= \frac{g^2 (v + \sigma)^2}{8} \left( (A_\mu^1)^2 + (A_\mu^2)^2 \right) + \frac{g^2 (v + \sigma)^2}{8} (A_\mu^3)^2 \\ &\quad + \frac{1}{2} (\partial_\mu \sigma)^2. \end{aligned} \quad (2.39)$$

The last term in the above equation is the kinetic term for the Higgs scalar  $\sigma(x)$  while the rest are mass terms for the vector fields and the interaction terms between

the vectors and the  $\sigma$ .

Indeed, all three vector fields  $A_\mu^a$  achieve the same mass and similar interactions

$$\begin{aligned}\mathcal{L} &\supset \frac{g^2(v+\sigma)^2}{8} A_\mu^a A^{a\mu} \\ &= \frac{M^2}{2} A_\mu^a A^{a\mu} + \frac{g^2 v}{4} \sigma A_\mu^a A^{a\mu} + \frac{g^2}{8} \sigma^2 A_\mu^a A^{a\mu},\end{aligned}\tag{2.40}$$

where

$$M^2 = \frac{g^2 v^2}{4}.\tag{2.41}$$

#### 2.2.2.2 $SU(2)$ with a Higgs Triplet

Now consider the example of a partially broken gauge symmetry,  $SU(2)$  Higgsed down to a  $U(1)$  subgroup, or equivalently  $SO(3) \rightarrow SO(2)$ . This time, the scalar fields  $\Phi^a(x)$  are real and form a triplet of the  $SU(2)$  rather than a doublet. Thus, the Lagrangian density is (Dawson, 1999)

$$\mathcal{L} = -\frac{1}{4} F_{\mu\nu}^a F^{a\mu\nu} + \frac{1}{2} D_\mu \Phi^a D^\mu \Phi^a - \frac{\lambda}{8} (\Phi^a \Phi^a - v^2)^2,\tag{2.42}$$

where

$$\begin{aligned}D_\mu \Phi^a &= \partial_\mu \Phi^a - g \varepsilon^{abc} A_\mu^b \Phi^c, \\ F_{\mu\nu}^a &= \partial_\mu A_\nu^a - \partial_\nu A_\mu^a - g \varepsilon^{abc} A_\mu^b A_\nu^c.\end{aligned}\tag{2.43}$$

Again, for  $v^2 > 0$  the scalar potential  $V(\Phi)$  has a degenerate family of minima which form a spherical shell  $\Phi^a \Phi^a = v^2$  in the scalar field space  $\mathbf{R}^3$ , and all such

minima are equivalent by  $SU(2) \cong SO(3)$  symmetries to

$$\langle \Phi \rangle = \begin{pmatrix} 0 \\ 0 \\ v \end{pmatrix}. \quad (2.44)$$

This time, this VEV is invariant under the  $SO(2)$  subgroup of  $SO(3)$ , or equivalently under the  $U(1)$  subgroup of  $SU(2)$ , generated by the  $T^3$  (the third component of the isospin  $\mathbf{T}$ ). Consequently, out of three vector fields  $A_\mu^a$ , it is expected that  $A_\mu^3$  remains massless while the other two fields  $A_\mu^{1,2}$  become massive.

In the process, the Higgs mechanism should eat two real scalar fields. Since we only have three real scalars to begin with, only one scalar should survive un-eaten, the physical Higgs field  $\sigma(x)$ .

To see how this works, we fix the unitary gauge

$$\Phi^1(x) \equiv \Phi^2(x) \equiv 0, \Phi^3(x) > 0. \quad (2.45)$$

As usual, this gauge is badly singular for  $\Phi = 0$  but it is OK for  $\Phi(x)$  being close to the VEV  $\langle \Phi \rangle \neq 0$ .

Shifting  $\Phi^3(x)$  by the VEV, we get

$$\Phi^3(x) = v + \sigma(x), \quad (2.46)$$

where  $\sigma(x)$  is the physical Higgs scalar, the only scalar remaining in the theory in the unitary gauge.

In terms of  $\sigma(x)$ , the scalar potential becomes

$$V(\sigma) = \frac{\lambda}{8} (2v\sigma + \sigma^2)^2 = \frac{\lambda v^2}{2} \sigma^2 + \frac{\lambda v}{2} \sigma^3 + \frac{\lambda}{8} \sigma^4, \quad (2.47)$$

where the first terms give the Higgs scalar mass-squared ( $m^2 = \lambda v^2$ ).

More interestingly, the covariant derivative of the scalar triplet  $\Phi^a(x)$  becomes

$$\begin{aligned} D_\mu \Phi^a &= \begin{pmatrix} 0 \\ 0 \\ \partial_\mu \sigma \end{pmatrix} - g \begin{pmatrix} A_\mu^1 \\ A_\mu^2 \\ A_\mu^3 \end{pmatrix} \times \begin{pmatrix} 0 \\ 0 \\ v + \sigma \end{pmatrix} \\ &= \begin{pmatrix} -gA_\mu^2 (v + \sigma) \\ gA_\mu^1 (v + \sigma) \\ \partial_\mu \sigma \end{pmatrix}, \end{aligned} \quad (2.48)$$

hence the covariant kinetic terms for the scalar become

$$\frac{1}{2} D_\mu \Phi^a D^\mu \Phi^a = \frac{1}{2} (\partial_\mu \sigma)^2 + \frac{g^2 (v + \sigma)^2}{2} \times \left( (A_\mu^1)^2 + (A_\mu^2)^2 \right). \quad (2.49)$$

As usual, the first term of Equation 2.49 is the kinetic term for the physical Higgs scalar  $\sigma$  while the second term contains mass terms

$$\frac{M^2}{2} \times \left( (A_\mu^1)^2 + (A_\mu^2)^2 \right), \quad \text{where } M^2 = g^2 v^2, \quad (2.50)$$

for the vector fields, but only for the  $A_\mu^1$  and  $A_\mu^2$ ; the third vector  $A_\mu^3$  remains massless.

The massless vector  $A_\mu^3(x)$  is the gauge field of the un-Higgsed  $SO(2) \cong U(1)$  subgroup of the  $SO(3) \cong SU(2)$ . Interpreting the generator  $Q = gT^3$  of this subgroup as electric charge, we find that the massive vector fields or rather their combinations

$$W_\mu^+ = \frac{1}{\sqrt{2}} (A_\mu^1 + iA_\mu^2) \quad \text{and} \quad W_\mu^- = \frac{1}{\sqrt{2}} (A_\mu^1 - iA_\mu^2) \quad (2.51)$$

have charges  $\pm g$  while the physical Higgs field  $\sigma$  is neutral.

For completeness sake, let us re-express the theory at hand (usually called Georgi-Glashow model) in terms of physical fields of definite charges. Using  $U(1)$ -covariant derivatives

$$\tilde{D}_\mu W_\nu^\pm \pm igA_\mu^3 W_\nu^\pm, \quad (2.52)$$

we have

$$W_{\mu\nu}^\pm = \frac{1}{\sqrt{2}} \left( F_{\mu\nu}^1 \pm iF_{\mu\nu}^2 \right) = \tilde{D}_\mu W_\nu^\pm - \tilde{D}_\nu W_\mu^\pm, \quad (2.53)$$

but

$$F_{\mu\nu}^3 = \partial_\mu A_\nu^3 - \partial_\nu A_\mu^3 + 2gIm \left( W_\mu^+ W_\nu^- \right). \quad (2.54)$$

Consequently, the Lagrangian of the whole model -the kinetic terms, the mass terms, and the interactions- can be expressed as

$$\begin{aligned} \mathcal{L} = & \frac{1}{2} (\partial_\mu \sigma)^2 - V(\sigma) - \frac{1}{4} \left( \partial_\mu A_\nu^3 - \partial_\nu A_\mu^3 + 2gIm \left( W_\mu^+ W_\nu^- \right) \right)^2 \\ & - \frac{1}{2} W_{\mu\nu}^+ W^{-\mu\nu} + (M + g\sigma)^2 \times W_\mu^+ W^{-\mu}. \end{aligned} \quad (2.55)$$

### 2.2.3 In the Glashow–Weinberg–Salam Theory of the Electroweak Interaction

Glashow-Weinberg-Salam theory (Glashow, 1961; Salam, 1968; Weinberg, 1967), also known as the SM electroweak theory, is -as its name implies- built upon the unification of the SM weak and electromagnetic interactions into a one united  $SU(2)_W \times U(1)_Y$  gauged theory of four gauge fields,  $W_\mu^a$  ( $a = 1, 2, 3$ ) and  $B_\mu$ . Its main feature is the spontaneous breaking of the underlying electroweak symmetry down to the  $U(1)_{EM}$  after which three gauge fields, out of the four, become massive and me-

mediate the weak interactions while one gauge field remains massless and mediates the electromagnetic interactions.

As is the case in the  $U(1)$  abelian theory, the reason behind this symmetry breaking is what is known as the Higgs field  $H$ . It is defined in the SM electroweak theory as a doublet of complex scalar fields,  $H_\alpha (\alpha = 1, 2)$ , rather than a singlet as it was in the previous theory, with a hypercharge quantum number  $Y = \frac{1}{2}$  as is manifested by Table 2.1 in Chapter 2. Accordingly,

$$D_\mu H_\alpha(x) = \partial_\mu H_\alpha + \frac{ig'}{2} \tau_{\alpha\beta}^a W_\mu^a(x) H_\beta(x) + \frac{ig}{2} B_\mu H_\alpha, \quad (2.56)$$

where  $g$  and  $g'$  are respectively the  $U(1)_Y$  and  $SU(2)_W$  gauge couplings.

The gauge fields ( $W_\mu^a$  and  $B_\mu$ ) and the Higgs fields ( $H_\alpha$ ) are the only bosonic fields of the GWS theory. Besides from the other twenty four fermionic fields describing the quarks and the leptons, the bosonic part of the theory's Lagrangian is (Dawson, 1999)

$$\mathcal{L} = -\frac{1}{4} W_{\mu\nu}^a W^{a\mu\nu} - \frac{1}{4} B_{\mu\nu} B^{\mu\nu} + D_\mu H^\dagger D^\mu H - \frac{\lambda}{2} \left( H^\dagger H - \frac{v^2}{2} \right)^2, \quad (2.57)$$

where

$$\begin{aligned} B_{\mu\nu} &= \partial_\mu B_\nu - \partial_\nu B_\mu, \\ W_{\mu\nu}^a &= \partial_\mu W_\nu^a - \partial_\nu W_\mu^a - g' \epsilon^{abc} W_\mu^b W_\nu^c, \\ H &= \begin{pmatrix} h^+ \\ h^0 \end{pmatrix} \quad \& \quad H^\dagger = (h^{+*}, h^{0*}), \end{aligned} \quad (2.58)$$

and  $D_\mu H / (D_\mu H)^\dagger$  is the column/row vector form of  $D_\mu H_a / (D_\mu H_a)^*$  of Equation 2.56.

The scalar potential of the Higgs field in our GWS theory

$$V = \frac{\lambda}{2} \left( H^\dagger H - \frac{v^2}{2} \right)^2 \quad (2.59)$$

has a local maximum rather than a minimum at  $H = 0$ , while its minima form a spher-

ical shell  $H^\dagger H = \frac{v^2}{2}$  in the scalar field space  $\mathbf{C}^2 = \mathbf{R}^4$ . All such minima are related to each other by the gauge symmetry, so we can safely assume without any loss of generality that the Higgs fields have a VEV of

$$\langle H \rangle_0 \equiv \langle 0|H|0 \rangle = \frac{1}{\sqrt{2}} \begin{pmatrix} 0 \\ v \end{pmatrix}. \quad (2.60)$$

It is literally this VEV of the Higgs field that breaks three of the four gauge symmetries of the theory leaving one combination of the  $U(1)_Y$  and  $U(1)$  subgroup of the  $SU(2)_2$  unbroken. Indeed, the  $U(1)_Y$  symmetry  $e^{i\Theta(x)\hat{Y}}$  acts on the Higgs fields as  $H(x) \rightarrow e^{iy\Theta(x)}H(x) = e^{\frac{i}{2}\Theta(x)}H(x)$  while the  $SU(2)_W$  symmetry  $e^{i\Theta(x)\hat{T}^3}$  acts on the  $SU(2)$  doublet  $H$  as  $H(x) \rightarrow e^{\frac{i}{2}\Theta(x)\tau^3}H(x)$ .

Merging both symmetries is the  $SU(2)_W \times U(1)_Y$  symmetry and it acts on  $H$  as

$$H(x) \rightarrow e^{\frac{i}{2}\Theta(x)} e^{\frac{i}{2}\Theta(x)\hat{\tau}^3} H(x) = \begin{pmatrix} e^{i\Theta(x)} & 0 \\ 0 & 1 \end{pmatrix} H(x), \quad (2.61)$$

which indeed leaves the VEV of Equation 2.60 invariant. Thus the  $U(1)$  subgroup of the electroweak  $SU(2)_W \times U(1)_Y$  generated by the operator

$$\hat{Q} = \hat{Y} + \hat{T}^3 \quad (2.62)$$

remains unbroken. Physically, this subgroup is the  $U(1)_Q$  gauge symmetry of electromagnetism and  $\hat{Q}$  is the electric charge operator (or rather electric charge in units of  $e$ ).

We shall see in a moment that one linear combination of the four  $SU(2)_W \times U(1)_Y$  gauge fields corresponding to the  $\hat{Q}$  generator remains massless while the other three combinations become massive via the Higgs mechanism. The same mechanism also "swallows" or eliminates three scalar fields, which become the longitudinal components of the three massive vector fields. Since the two complex Higgs fields are equiv-

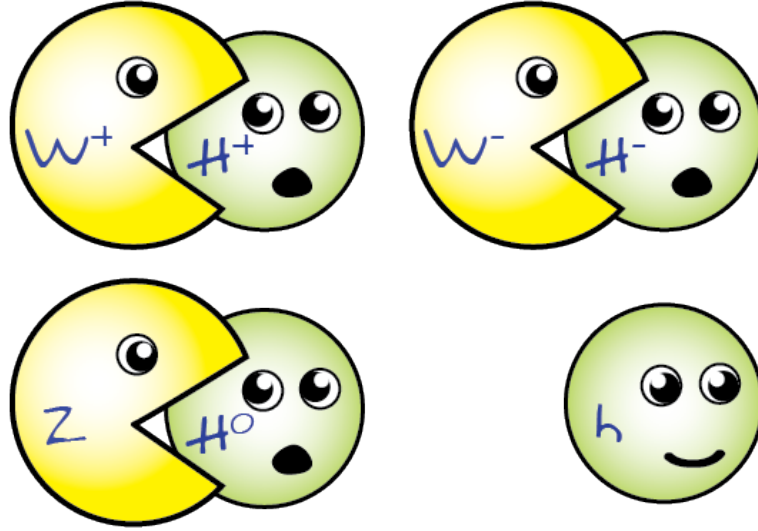


Figure 2.2 A schematic diagram of the core idea of the Higgs mechanism

alent to four real scalars, we end up with  $4 - 3 = 1$  physical scalar field  $h(x)$ , whose quanta are called the physical Higgs particles that were experimentally detected by the ATLAS and CMS experiments at the LHC in 2012. Figure 2.2 is a schematic illustration of the  $4 - 3 = 1$  equation.

The simplest way to see how this works is to fix the unitary gauge for the spontaneously broken symmetries. Note that any complex doublet  $H(x)$  can be  $SU(2)$ -rotated to

$$H'(x) = U(x)H(x) = \frac{1}{\sqrt{2}} \begin{pmatrix} 0 \\ \tilde{h}(x) \end{pmatrix} \text{ for a real } \tilde{h}(x) \geq 0. \quad (2.63)$$

This gauge transform would be singular for  $H(x) \approx 0$  but it is nice and smooth for  $H(x)$  in the vicinity of the VEV of Equation 2.60, so we may use it to fix the unitary gauge  $h^+(x) \equiv 0$  and  $h^0(x) \equiv 0$ . Once we fix this gauge, we are left with a single real scalar field  $\tilde{h}(x)$ , which we may now shift by its VEV,

$$\tilde{h}(x) = v + h(x). \quad (2.64)$$

In terms of this shifted field,

$$H^\dagger H - \frac{v^2}{2} = \frac{(v+h)^2}{2} - \frac{v^2}{2} = vh + \frac{1}{2}h^2, \quad (2.65)$$

and so the scalar potential becomes

$$V(h) = \frac{\lambda}{2} \left( H^\dagger H - \frac{v^2}{2} \right)^2 = \frac{\lambda}{2} \left( vh + \frac{1}{2}h^2 \right)^2 = \frac{\lambda v^2}{2} h^2 + \frac{\lambda v}{2} h^3 + \frac{\lambda}{8} h^4, \quad (2.66)$$

with  $m^2 = \lambda v^2 > 0$  for the physical Higgs field. Experimentally,  $v \approx 246 \text{ GeV}$  while the physical Higgs mass is near  $125 \text{ GeV}$ , implying that  $\lambda \approx 0.26$ .

On the other hand, the mass term of the vector fields emerge from the kinetic portion  $(D_\mu H)^\dagger D^\mu H$  of the Higgs doublets. Indeed, in the unitary gauge

$$\begin{aligned} D_\mu H &= \frac{1}{\sqrt{2}} \begin{pmatrix} \frac{i}{2} g' (W_\mu^1 - iW_\mu^2) \tilde{h} \\ \partial_\mu \tilde{h} + \frac{i}{2} (gB_\mu - g'W_\mu^3) \tilde{h} \end{pmatrix} \\ &= \frac{1}{\sqrt{2}} \begin{pmatrix} \frac{i}{2} g' (W_\mu^1 - iW_\mu^2) (v+h) \\ \partial_\mu h + \frac{i}{2} (gB_\mu - g'W_\mu^3) (v+h) \end{pmatrix}, \end{aligned} \quad (2.67)$$

and hence

$$\begin{aligned} (D_\mu H)^\dagger D^\mu H &= \frac{1}{2} |\partial_\mu h + \frac{i}{2} (gB_\mu - g'W_\mu^3) (v+h)|^2 + \frac{1}{2} |\frac{i}{2} g' (W_\mu^1 - iW_\mu^2) (v+h)|^2 \\ &= \frac{1}{2} (\partial_\mu h)^2 + \frac{(v+h)^2}{8} (gB_\mu - g'W_\mu^3)^2 + \frac{g'^2 (v+h)^2}{8} (W_\mu^{12} + W_\mu^{22}). \end{aligned} \quad (2.68)$$

The first term on the last line is clearly the kinetic term for the physical Higgs field while the rest is both the mass term for the vector fields as well as their interactions with the physical Higgs field  $h(x)$ . In particular, the vector mass terms can be obtained from truncating the  $(v+h(x))^2$  factors to simply  $v^2$ , thus

$$\mathcal{L}_{masses}^{vector} = \frac{g_2^2 v^2}{8} (W_\mu^{12} + W_\mu^{22}) + \frac{v^2}{8} (g_1 B_\mu - g_2 W_\mu^3)^2. \quad (2.69)$$

In particular, the  $W_\mu^1$  and  $W_\mu^2$  vector fields have masses

$$M_W^2 = \frac{g_2^2 v^2}{4} \implies M_W = \frac{g_2 v}{2}, \quad (2.70)$$

while the  $W_\mu^3$  and  $B_\mu$  vector fields have a  $2 \times 2$  mass matrix

$$M^2 = \frac{v^2}{4} \begin{pmatrix} g_2^2 & -g_2 g_1 \\ -g_2 g_1 & g_1^2 \end{pmatrix}, \quad (2.71)$$

with mass eigenvalues

$$M_Z^2 = \frac{(g_1^2 + g_2^2) v^2}{4} \quad \& \quad M_A^2 = 0 \quad (2.72)$$

and corresponding mass eigenstates

$$\begin{aligned} Z_\mu(x) &= W_\mu^3(x) \cos \theta - B_\mu(x) \sin \theta, \\ A_\mu(x) &= W_\mu^3(x) \sin \theta + B_\mu(x) \cos \theta, \end{aligned} \quad (2.73)$$

where

$$\theta = \tan^{-1} \left( \frac{g}{g'} \right) \quad (2.74)$$

is the weak mixing angle or the Weinberg angle; experimentally,  $\sin^2 \theta \approx 0.23$ .

Physically, the  $A_\mu(x)$  is the electromagnetic field whose quanta are massless photons, the  $Z_\mu(x)$  is the neutral weak field whose quanta are  $Z^0$  particles of mass  $M_Z \approx 91 \text{ GeV}$ , and the  $W_\mu^{1,2}(x)$  or rather their linear combinations

$$W_\mu^+(x) = \frac{W_\mu^1(x) + iW_\mu^2(x)}{\sqrt{2}} \quad \& \quad W_\mu^-(x) = \frac{W_\mu^1(x) - iW_\mu^2(x)}{\sqrt{2}} \quad (2.75)$$

are the charged weak fields (electric charges  $g = \pm 1$ ) whose quanta are  $W^+$  and  $W^-$  particles of mass  $M_W \approx 80 \text{ GeV}$ .

Note that the experimentally found mass ratio between the  $W^\pm$  and  $Z^0$  particles

gives us the value of the weak mixing angle as

$$\begin{aligned}\frac{M_W^2}{M_Z^2} &= \frac{g_2^2}{g_1^2 + g_2^2} = \frac{1}{1 + \tan^2 \theta} = \cos^2 \theta, \\ \implies \cos^2 \theta &\approx 0.77, \\ \implies \sin^2 \theta &\approx 0.23.\end{aligned}\tag{2.76}$$

In all the cases discussed above, symmetry breaking has taken place at the level of the ground state of the scalar field in question. More generally, the phenomenon of EWSB is recently one of the main concerns of particle physicists at the LHC and many other particle accelerators. In the SM, the symmetry between electromagnetic interactions and weak interactions is assumed to be broken by the popular Higgs mechanism which in turn gives mass to the electroweak gauge bosons  $W^\pm$  and  $Z^0$ .

As was explained before in this section, the Higgs mechanism generates the mass property for the particles but, in doing so, it breaks simultaneously the symmetry embedded in the theory.

A theory is said to be symmetric when a change of something in the Lagrangian gives rise to the same Lagrangian. The term "symmetry breaking" is somehow misleading as it only means that the symmetry that was at the level of the Lagrangian is now not seen (or hidden) at the level of the VEV of the field.

To see this very briefly, consider the following potential for a real scalar field

$$V(\phi) = \frac{1}{2}\mu^2\phi^2 + \frac{1}{4}\lambda\phi^4.\tag{2.77}$$

In the above potential,  $\lambda$  is always positive because otherwise  $V$  would be unbounded from below and would have no state of minimum energy. With the assumption  $\lambda > 0$ , there are only two possibilities of the theory

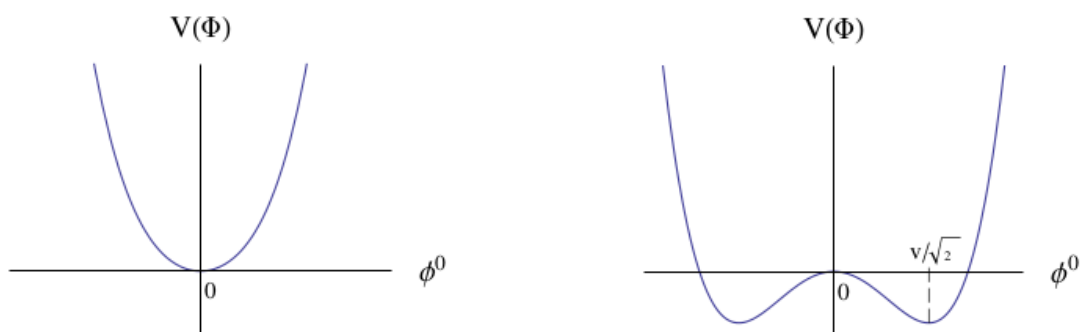


Figure 2.3 Projection in the plane  $\phi^\dagger = 0$  of the potential  $V(\phi)$  in the cases  $\mu^2 > 0$  (left) and "Mexican hat"  $\mu^2 < 0$  (right)

- If  $\mu^2 > 0$ , the potential has the shape in Figure 2.3 (left) and clearly preserves the symmetries of the Lagrangian. The state of lowest energy is that with  $\phi = 0$ , the vacuum state. The theory is simply quantum electrodynamics with a massless photon and a charged scalar field  $\phi$  with a real (positive or negative) mass  $\mu$ .
- More interestingly, if  $\mu^2 < 0$ , the potential has the "Mexican hat" shape shown in Figure 2.3 (right). In this case the minimum energy state is not at  $\phi = 0$  but rather at

$$\langle \phi \rangle = \sqrt{-\frac{\mu^2}{2\lambda}} \equiv \frac{v}{\sqrt{2}},$$

known as the VEV of  $\phi$  which clearly breaks the global  $U(1)$  symmetry of the original theory (potential or Lagrangian as a whole).

### 2.3 Neutrinos

The subatomic world is full of particles (like quarks, bosons..), each of which has its own independent personality and behavior. One of the particles, however, is particularly weird and full of secrets, the nowadays so-called neutrino. Neutrinos are sometimes known as the ghost of the subatomic world as they interact incredibly weak with matter and less than any of the other known particles. Even though we are constantly bombarded by them with indeed hundreds of trillions of neutrinos hitting us every second, it took around thirty years to prove that they exist at all.

### 2.3.1 History and Discovery

Neutrinos were first proposed by Pauli in 1930s as a solution to the energy conservation problem that arose from a study on a radioactive nuclear decay called beta decay. He first gave them the name "neutron" after which Fermi renamed them as "neutrino" being the small version of a neutron.

A beta decay is generally shown as



where  $Z$  is the atomic number (number of protons) and  $A$  is the atomic weight (number of nucleons) of the corresponding element.  $X$  can be any radioactive nucleus (known as the parent nucleus) that decays into a slightly lighter nucleus  $Y$  (known as the daughter nucleus) accompanied by the emission of an electron (known at that time as a beta particle, from which the name beta decay came out). The basic underlying process, however, is the decay of a neutron to a proton with the emission of an electron which is the reason why  $Y$  lies on the same row but one column ahead of  $X$  in the periodic table.

The problem was that the energy of the original nucleus did not balance the combined energy of the daughter nucleus and the electron, or simply  $E_X \neq E_Y + E_e$ , saying for the first glance that energy has been destroyed during the decay. More specifically, if  $X$  is at rest then from conservation of momentum

$$P_X^\mu = P_Y^\mu + P_e^\mu, \quad (2.79)$$

where  $P_X^\mu = (m_X, \vec{0})$ ,  $P_Y^\mu = (E_Y, \vec{p}_Y)$  and  $P_e^\mu = (E_e, \vec{p}_e)$  and the invariant quantity  $P^2 = P \cdot P = P^\mu P_\mu = m^2$ , the electron energy is theoretically found to be (Griffiths, 2008)

$$E_e = \frac{m_X^2 - m_Y^2 + m_e^2}{2m_X} = \text{constant}. \quad (2.80)$$

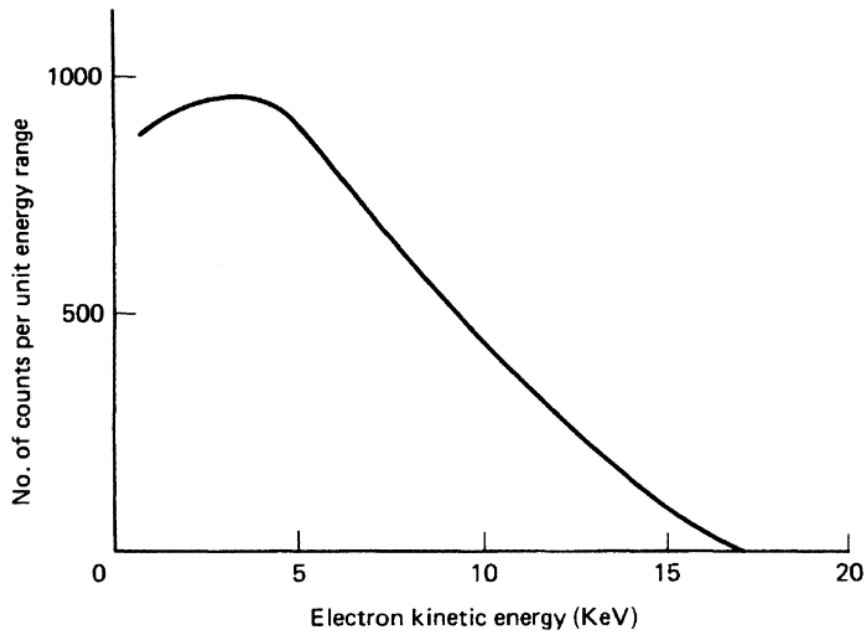


Figure 2.4 The beta decay spectrum of tritium ( ${}^3_1H \rightarrow {}^3_2He$ ) (Lewis, 1970)

It turned out, however, that this equation shows only the maximum energy that the emitted electron can have in the absence of any neutrinos. In contrast to Equation 2.80, experiments have found that the energy of the emitted electrons is not fixed but vary considerably as is clear in the beta decay spectrum of tritium given by Figure 2.4.

Only then, physicists came up with the idea that the reason of the non-steady electron energy (or in other words the missing energy) is the existence of an unobserved ghost-like particle emitted in beta decay. That day was the birthday of the neutrino or rather the antineutrino!

### 2.3.2 Sources and Significance

Although neutrinos do not leave any trace behind them, they are there and are indeed the most abundant particles in the universe. They were first come to existence by the big bang after which they continued to be produced naturally from natural sources and are even generated by human via artificial sources as is manifested in Figure 2.5. The most effective sources of neutrino productions are summarized as:

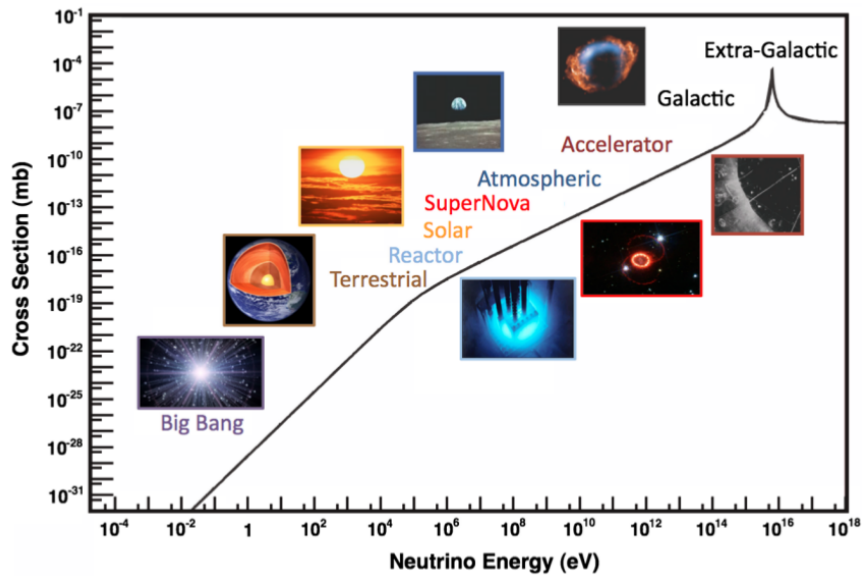


Figure 2.5 Neutrino sources versus decades of energy with the cross section of  $\bar{\nu}_e e$  elastic scattering versus neutrino energy (for massless neutrinos) superimposed for comparison (Formaggio et al., 2012)

- **Natural Sources**

- **Sun**

Neutrinos originate from nuclear interactions and the biggest nuclear reactor around us is the sun. Although it is about ninety million miles away from the earth, the sun emits hundreds of trillions of neutrinos every second from the thermal nuclear reactions of proton-proton fusions happening at its core;  $p + p \rightarrow {}^2_1H + e^+ + \nu$ . Such neutrinos are usually called solar neutrinos.

- **Atmosphere**

The primary cosmic rays (typically protons) coming from the universe collide with the nuclei in the atmosphere of the earth generating a shower of hadrons, like pions and kaons. These short-lived mesons eventually decay into neutrinos and other mesons that invade the earth intensively. Such neutrinos are usually called atmospheric neutrinos.

- **Supernova**

Neutrinos have been also suddenly detected in huge numbers from distant

supernova. When a massive star at the end of its life collapses to a neutron star by squashing protons and electrons, it radiates almost all of its binding energy in the form of neutrinos;  $p + e \rightarrow n + \nu$ . Such neutrinos are usually called supernova neutrinos.

– **Terrestrial**

Due to the remarkable abundance of radioactive elements within the earth, neutrinos get emitted from these elements in decay processes. Such neutrinos are usually called terrestrial neutrinos.

• **Artificial Sources**

– **Particle Accelerators**

Particle accelerators are a good source of high energy muon-type neutrinos/antineutrinos. As their name may imply, they accelerate protons from hydrogen gas close to the speed of light and then get them smashed into a thick nuclear target (usually made up of graphite or beryllium) to produce a bunch of charged mesons (like pions and kaons) as well as protons and neutrons. Then by means of some magnetic field, a selection of the positively/negatively charged pions occur. These short-lived pions are then magnetically focused into a long tunnel where they spontaneously decay into antimuons/muons and muon-type neutrinos/antineutrinos while in flight. Then a block of aluminum, concrete and steel is used to filter the muons/antimuons while leaving the neutrinos to pass through yielding eventually a high-energetic pure beam of neutrino. Such neutrinos are usually called accelerator neutrinos. Some famous examples of particle accelerators are the large hadron collider (LHC), Japan proton accelerator research complex (J-PARC), Fermi national accelerator laboratory (Fermilab) and liquid scintillator neutrino detector (LSND).

– **Nuclear Reactors**

Nuclear reactors are a very intense source of electron-type antineutrinos from the beta decays of the neutron-rich fission products. Such neutrinos are usually called reactor neutrinos. One well-known nuclear reactor is

the Taiwan experiment on neutrino (TEXONO) in which we are actively engaging.

Having mentioned this, understanding neutrinos is an important step in understanding the fundamental processes by which neutrinos can be produced. Many low energy and high energy neutrino experiments have been launched worldwide for this aim.

### 2.3.3 Properties

Neutrinos are neutral leptons that belong to the fermion family with a spin angular momentum quantum number  $s = \frac{1}{2}$ . They do not feel the electromagnetic and strong forces because they neither carry an electric charge nor a color charge. And due to the fact that gravitational forces are absent from the SM, neutrinos can only interact via weak nuclear forces of the SM.

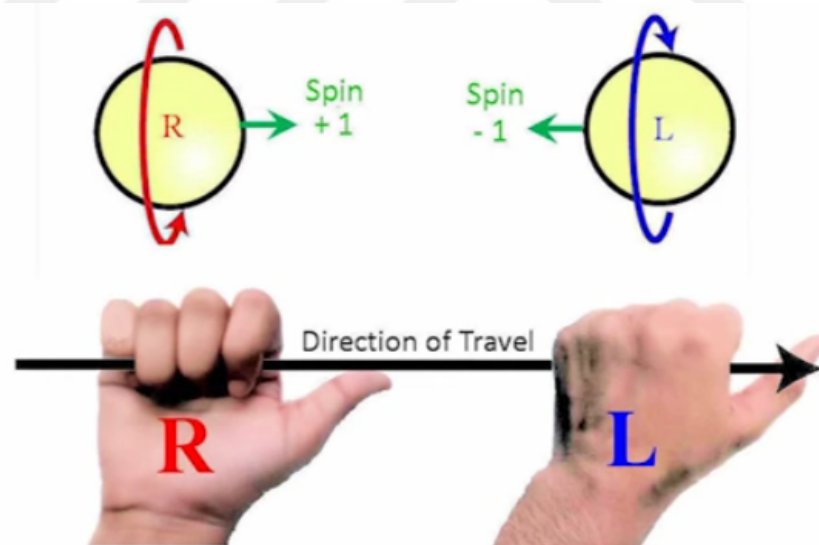


Figure 2.6 A schematic representation of the right-handedness and left-handedness of a particle

In the scope of the SM, neutrinos are massless and so they always travel at the speed of light and it is impossible to reverse their direction of motion by getting into a faster-moving reference system. Experimentally, neutrinos/antineutrinos have an intrinsic left-handed/right-handed chirality (or equivalently helicity as long as  $m_\nu = 0$ ) defined

by

$$\mathcal{H} = \frac{\vec{P} \cdot \vec{S}}{|\vec{P} \cdot \vec{S}|} = \begin{cases} +1 & \text{for right-handed antineutrinos} \\ -1 & \text{for left-handed neutrinos} \end{cases} \quad (2.81)$$

and shown by Figure 2.6.

There are three kinds or flavors of neutrinos; one kind is associated with electrons and is known as electron-type neutrino and two others similarly associated with muons and taus. The way scientists discovered that there are three different kinds of neutrinos is that neutrinos seem to remember their origins. If, for instance, a neutrino created from muons is made to collide with an atomic nucleus only muons will be generated in the collision never electrons nor taus hinting to the fact that neutrinos do remember how they have been made.

Although neutrinos were long believed to be massless, it is now known that there are also three discrete neutrino masses, but they do not correspond uniquely to the three flavors. This what makes neutrinos unique in the subatomic world as they can actually change their identity by oscillating back and forth between their different flavors. More on this will be given in the next chapter in the scope of non-standard interactions (NSIs) of neutrinos.

## 2.4 Neutrino Interactions in the Standard Model

Neutrino-electron scattering is a purely leptonic process where a neutrino scatters off an electron by the exchange of a virtual vector boson. The SM readily gives a prescription to define neutrino-electron interactions via the leptonic neutral current (NC) and charged current (CC) in the weak interaction Lagrangian.

In the SM, the scattering process  $\nu_e(\bar{\nu}_e) + e \rightarrow \nu_e(\bar{\nu}_e) + e$  proceeds via NC  $t$ -channel  $Z$  boson exchange and CC  $t(s)$ -channel  $W$  boson exchange and therefore there interference which is destructive does also contribute to the cross section. On the other hand,

the scattering process  $\nu_\alpha (\bar{\nu}_\alpha) + e \rightarrow \nu_\alpha (\bar{\nu}_\alpha) + e$  (where  $\alpha \neq e$ ) proceeds only via NC  $t$ -channel  $Z$  boson exchange.

### 2.4.1 Antineutrino-Electron Elastic Scattering

There are two possible tree-level Feynman diagrams that contribute to the SM  $\bar{\nu}_e e$  elastic scattering process.

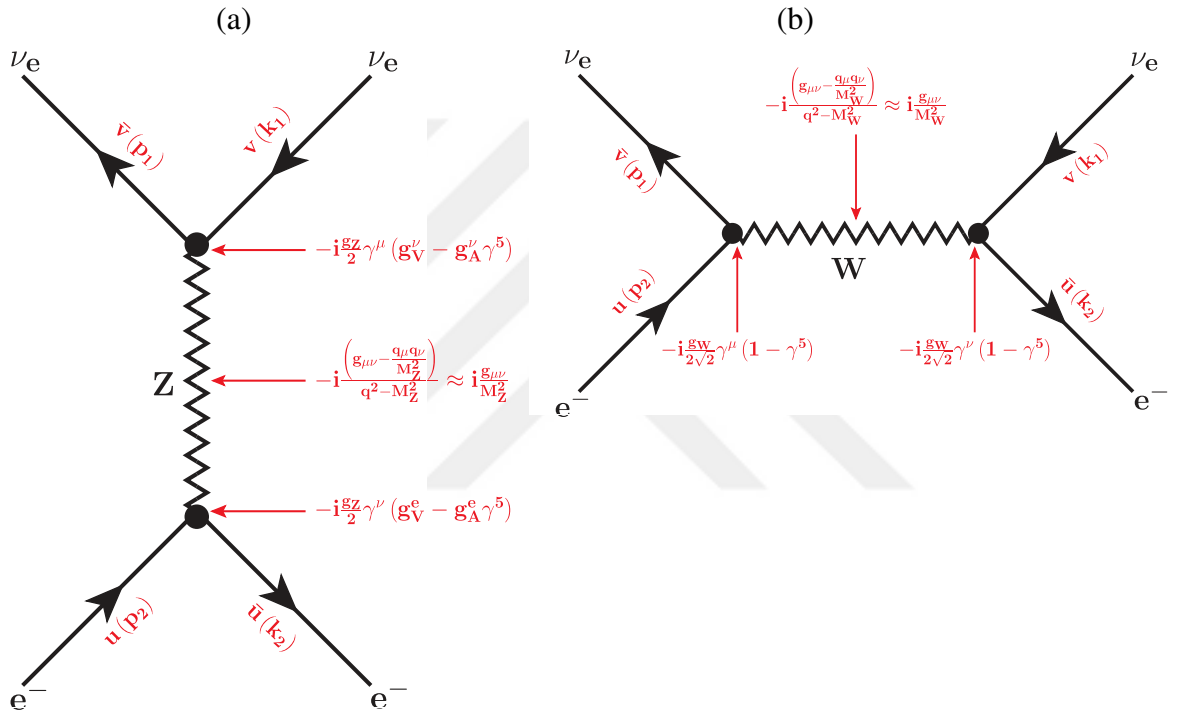


Figure 2.7 Feynman diagrams of (a)  $Z$ -mediated and (b)  $W$ -mediated antineutrino-electron scattering in the SM

- One is mediated by  $Z^0$  through a neutral weak process and is manifested by the Feynman diagram in Figure 2.7 (a) with the corresponding amplitude given by

$$\mathcal{M}_Z = \frac{G_F}{\sqrt{2}} \left[ \bar{\nu}(p_1) \gamma^\mu (1 - \gamma^5) \nu(k_1) \right] \left[ \bar{u}(k_2) \gamma_\mu (g_V^e - g_A^e \gamma^5) u(p_2) \right]. \quad (2.82)$$

- The other is mediated by  $W^\pm$  through a charged weak process and is manifested

by the Feynman diagram in Figure 2.7 (b) with the corresponding amplitude given using Fierz transformation by

$$\mathcal{M}_W = \frac{G_F}{\sqrt{2}} \left[ \bar{v}(p_1) \gamma^\mu (1 - \gamma^5) v(k_1) \right] \left[ \bar{u}(k_2) \gamma_\mu (1 - \gamma^5) u(p_2) \right]. \quad (2.83)$$

Then the total amplitude can be simply written as

$$\begin{aligned} \mathcal{M}_t &= \mathcal{M}_Z + \mathcal{M}_W \\ &= \frac{G_F}{\sqrt{2}} \left[ \bar{v}(p_1) \gamma^\mu (1 - \gamma^5) v(k_1) \right] \\ &\quad \times \left[ \bar{u}(k_2) \gamma_\mu \left\{ (g_V^e + 1) - (g_A^e + 1) \gamma^5 \right\} u(p_2) \right], \end{aligned} \quad (2.84)$$

and then together with its hermitian conjugate  $\mathcal{M}_t^\dagger$ , the spin-averaged amplitude square is

$$\begin{aligned} \langle |\mathcal{M}_t|^2 \rangle &= \frac{1}{2} \sum_{\text{spins}} |\mathcal{M}_t|^2 \\ &= \frac{G_F^2}{4} \sum_{\text{spins}} \left[ \bar{v}(p_1) \gamma^\mu (1 - \gamma^5) v(k_1) \right] \left[ \bar{v}(p_1) \gamma^\nu (1 - \gamma^5) v(k_1) \right]^\dagger \\ &\quad \times \sum_{\text{spins}} \left[ \bar{u}(k_2) \gamma_\mu \left\{ (g_V^e + 1) - (g_A^e + 1) \gamma^5 \right\} u(p_2) \right] \\ &\quad \times \left[ \bar{u}(k_2) \gamma_\nu \left\{ (g_V^e + 1) - (g_A^e + 1) \gamma^5 \right\} u(p_2) \right]^\dagger, \end{aligned} \quad (2.85)$$

where using Casimir's trick (Griffiths, 2008) yields

$$\begin{aligned} &= \frac{G_F^2}{4} \text{Tr} \left[ \gamma^\mu (1 - \gamma^5) (\not{k}_1 - m_\nu) \gamma^\nu (1 - \gamma^5) (\not{p}_1 - m_\nu) \right] \\ &\quad \times \text{Tr} \left[ \gamma_\mu \left\{ (g_V^e + 1) - (g_A^e + 1) \gamma^5 \right\} (\not{p}_2 + m_e) \right] \\ &\quad \times \gamma_\nu \left\{ (g_V^e + 1) - (g_A^e + 1) \gamma^5 \right\} (\not{k}_2 + m_e) \right], \end{aligned} \quad (2.86)$$

and then calculating the resulted traces yields

$$\begin{aligned} \langle |\mathcal{M}_t|^2 \rangle &= 16G_F^2 \left[ (g_V - g_A)^2 (k_1 \cdot k_2) (p_1 \cdot p_2) + (g_V + g_A + 2)^2 (k_1 \cdot p_2) (k_2 \cdot p_1) \right. \\ &\quad \left. - m_e^2 (g_V - g_A) (g_V + g_A + 2) (k_1 \cdot p_1) \right]. \end{aligned} \quad (2.87)$$

Note that in all what follows, our manual calculations of traces have been also checked out by "FeynCalc" (Mertig et al., 1991; Shtabovenko et al., 2016).

Plugging the necessary kinematic terms given in Equations B.3, B.4 and B.5 followed by inserting  $\langle |\mathcal{M}_t|^2 \rangle$  into  $\frac{d\sigma}{dT}$  found in Appendix A

$$\frac{d\sigma}{dT} = \frac{\langle |\mathcal{M}|^2 \rangle}{32\pi m_2 |\vec{p}_1|^2},$$

where  $m_2 \equiv m_e$  and  $|\vec{p}_1|^2 \equiv |\vec{p}_\nu|^2 = E_\nu^2 - m_\nu^2 = E_\nu^2$  gives as a final result

$$\left[ \frac{d\sigma}{dT} (\bar{\nu}_e e) \right]_{SM} = \frac{G_F^2 m_e}{2\pi} \left[ (g_V - g_A)^2 + (g_V + g_A + 2)^2 \left( 1 - \frac{T}{E_\nu} \right)^2 - (g_V - g_A)(g_V + g_A + 2) \frac{m_e T}{E_\nu^2} \right] \quad (2.88)$$

in terms of the weak couplings  $g_V$  and  $g_A$ .

This can also be written easily in terms of the weak mixing angle  $\sin^2 \theta_W$  using the fact that

$$\begin{aligned} g_V &= -\frac{1}{2} + 2s_w^2, \\ g_A &= -\frac{1}{2}, \end{aligned} \quad (2.89)$$

or in terms of the right and left handed chiral coupling constants  $g_L$  and  $g_R$  using the fact that

$$\begin{aligned} g_L &= \frac{1}{2} (g_V - g_A) = 2 \sin^2 \theta_W, \\ g_R &= \frac{1}{2} (g_V + g_A) = 2 \sin^2 \theta_W - 1, \end{aligned} \quad (2.90)$$

and thus verifying the table given in Chapter 2.

## 2.4.2 Neutrino-Electron Elastic Scattering

There are two possible tree-level Feynman diagrams that contribute to the SM process of  $\nu_e e$  elastic scattering.

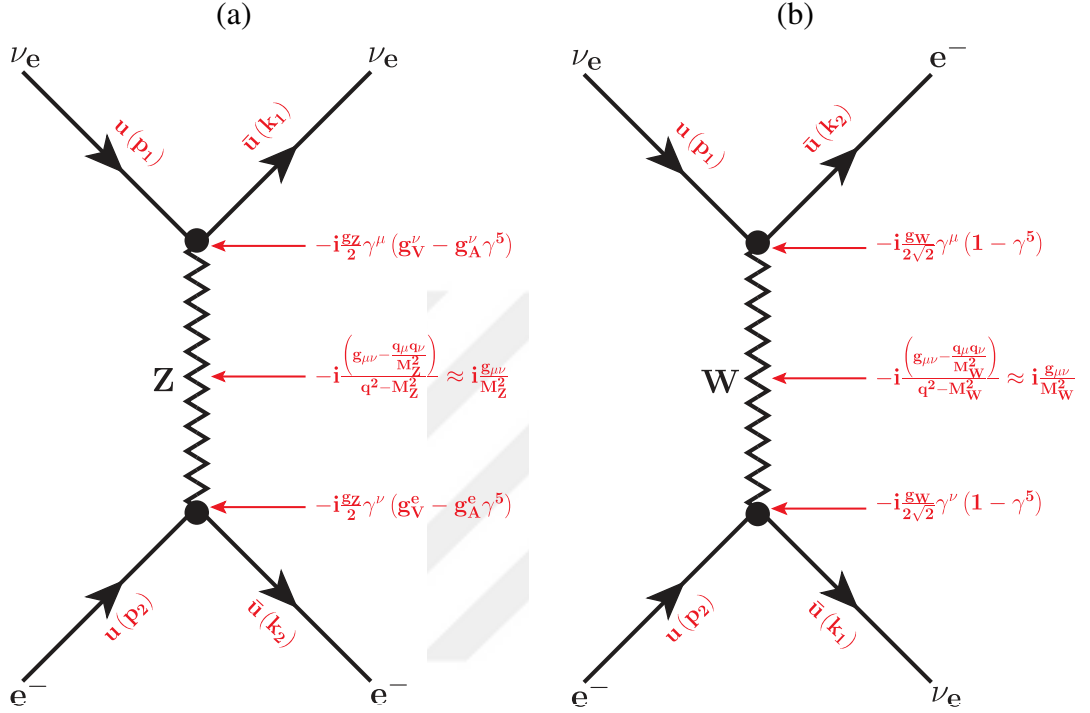


Figure 2.8 Feynman diagrams of neutrino-electron scattering via the exchange of a (a) Z-boson (NC) and (b) W-boson (CC) in the SM

- One is mediated by  $Z^0$  through a neutral weak process and is manifested by the Feynman diagram in Figure 2.8 (a) with the corresponding amplitude given by

$$\mathcal{M}_Z = \frac{G_F}{\sqrt{2}} \left[ \bar{u}(k_1) \gamma^\mu (1 - \gamma^5) u(p_1) \right] \left[ \bar{u}(k_2) \gamma_\mu (g_V^e - g_A^e \gamma^5) u(p_2) \right]. \quad (2.91)$$

- Another is mediated by  $W^\pm$  through a charged weak process and is manifested by the Feynman diagram in Figure 2.8 (b) with the corresponding amplitude

given using Fierz transformation by

$$\mathcal{M}_W = \frac{G_F}{\sqrt{2}} \left[ \bar{u}(k_1) \gamma^\mu (1 - \gamma^5) u(p_1) \right] \left[ \bar{u}(k_2) \gamma_\mu (1 - \gamma^5) u(p_2) \right]. \quad (2.92)$$

Then the total amplitude can be simply written as

$$\begin{aligned} \mathcal{M}_t &= \mathcal{M}_Z + \mathcal{M}_W \\ &= \frac{G_F}{\sqrt{2}} \left[ \bar{u}(k_1) \gamma^\mu (1 - \gamma^5) u(p_1) \right] \\ &\quad \times \left[ \bar{u}(k_2) \gamma_\mu \left\{ (g_V^e + 1) - (g_A^e + 1) \gamma^5 \right\} u(p_2) \right], \end{aligned} \quad (2.93)$$

and then together with its hermitian conjugate  $\mathcal{M}_t^\dagger$ , the spin-averaged amplitude square is

$$\begin{aligned} \langle |\mathcal{M}_t|^2 \rangle &= \frac{1}{2} \sum_{\text{spins}} |\mathcal{M}_t|^2 \\ &= \frac{G_F^2}{4} \sum_{\text{spins}} \left[ \bar{u}(k_1) \gamma^\mu (1 - \gamma^5) u(p_1) \right] \left[ \bar{u}(k_1) \gamma^\nu (1 - \gamma^5) u(p_1) \right]^\dagger \\ &\quad \times \sum_{\text{spins}} \left[ \bar{u}(k_2) \gamma_\mu \left\{ (g_V^e + 1) - (g_A^e + 1) \gamma^5 \right\} u(p_2) \right] \\ &\quad \times \left[ \bar{u}(k_2) \gamma_\nu \left\{ (g_V^e + 1) - (g_A^e + 1) \gamma^5 \right\} u(p_2) \right]^\dagger, \end{aligned} \quad (2.94)$$

where using Casimir's trick yields

$$\begin{aligned} &= \frac{G_F^2}{4} \text{Tr} \left[ \gamma^\mu (1 - \gamma^5) (\not{p}_1 + m_\nu) \gamma^\nu (1 - \gamma^5) (\not{k}_1 + m_\nu) \right] \\ &\quad \times \text{Tr} \left[ \gamma_\mu \left\{ (g_V^e + 1) - (g_A^e + 1) \gamma^5 \right\} (\not{p}_2 + m_e) \right. \\ &\quad \left. \times \gamma_\nu \left\{ (g_V^e + 1) - (g_A^e + 1) \gamma^5 \right\} (\not{k}_2 + m_e) \right], \end{aligned} \quad (2.95)$$

and then evaluating the traces yields

$$\begin{aligned} \langle |\mathcal{M}_t|^2 \rangle &= 16G_F^2 \left[ (g_V + g_A + 2)^2 (k_1 \cdot k_2) (p_1 \cdot p_2) + (g_V - g_A)^2 (k_1 \cdot p_2) (k_2 \cdot p_1) \right. \\ &\quad \left. - m_e^2 (g_V - g_A) (g_V + g_A + 2) (k_1 \cdot p_1) \right]. \end{aligned} \quad (2.96)$$

Plugging the necessary kinematic terms and inserting  $\langle |\mathcal{M}_i|^2 \rangle$  into  $\frac{d\sigma}{dT}$  gives

$$\left[ \frac{d\sigma}{dT}(\nu_e e) \right]_{SM} = \frac{G_F^2 m_e}{2\pi} \left[ (g_V + g_A + 2)^2 + (g_V - g_A)^2 \left( 1 - \frac{T}{E_\nu} \right)^2 - (g_V - g_A)(g_V + g_A + 2) \frac{m_e T}{E_\nu^2} \right] \quad (2.97)$$

in terms of the weak couplings ( $g_V$  and  $g_A$ ) which can also be easily written in terms of Weinberg angle and chiral couplings using Equations 2.89 and 2.90, respectively.

In general, the tree-level SM differential cross section for the process  $\nu_e(\bar{\nu}_e) + e \rightarrow \nu_e(\bar{\nu}_e) + e$  is well known and can be expressed in the laboratory frame as (Bilmiş et al., 2012, 1; Chen et al., 2014; Deniz et al., 2010, 1; Kayser et al., 1979)

$$\left[ \frac{d\sigma}{dT}(\bar{\nu}_e e) \right]_{SM} = \frac{2G_F^2 m_e}{\pi} \left[ a^2 + b^2 \left( 1 - \frac{T}{E_\nu} \right)^2 - ab \frac{m_e T}{E_\nu^2} \right], \quad (2.98)$$

where  $G_F = \frac{\sqrt{2}}{8} \left( \frac{g_w}{M_W} \right)^2$  is the Fermi coupling constant,  $m_e$  is the electron mass,  $T$  is the electron recoil kinetic energy,  $E_\nu$  is the incoming neutrino energy, and the coefficients  $a$  and  $b$  are given in Table 2.2 in terms of vector and axial vector coupling constants ( $g_V = -\frac{1}{2} + 2s_W^2$  and  $g_A = -\frac{1}{2}$  as predicted by the GWS model), electroweak mixing angle ( $\sin^2\theta_W \equiv s_W^2$ ), and chiral coupling constants ( $g_L$  and  $g_R$ ).

Table 2.2 Coefficients in the expression of the SM  $(\bar{\nu}_e e)$  scattering cross section given by Equation 2.98

Process	$a$	$b$
	$\frac{1}{2}(g_V - g_A)$	$\frac{1}{2}(g_V + g_A + 2)$
$\bar{\nu}_e + e \rightarrow \bar{\nu}_e + e$	$s_W^2$	$s_W^2 + \frac{1}{2}$
	$g_R$	$g_L + 1$
	$\frac{1}{2}(g_V + g_A + 2)$	$\frac{1}{2}(g_V - g_A)$
$\nu_e + e \rightarrow \nu_e + e$	$\frac{s_W^2 + \frac{1}{2}}{g_L + 1}$	$\frac{s_W^2}{g_R}$

## CHAPTER THREE

### WHY TO GO BEYOND THE STANDARD MODEL

In an aim to test the SM and/or find an answer to some of its critical problems, theoretical particle physicists have come up with a wide range of new physics scenarios intended to look for physics BSM using different interaction channels. Until now, there is no experimental evidence that neutrinos have some non-standard properties beyond masses and mixing or some extra new interactions, different from the weak interaction, not explained by the SM. Such interactions are often called non-standard interactions (NSIs) of neutrinos. These interactions are interesting from a phenomenological point of view, because they directly point out the presence of some new physics BSM. NSIs of neutrinos is one concrete example of a model-independent BSM research. On the other hand, unparticle physics (UP), extra  $Z'$  gauge boson model, new light spin-1 boson (NLS1B) model, charged Higgs boson (CHB) model and little Higgs models (LHMs) are some famous examples of model-dependent BSM researches.

#### 3.1 Standard Model as an Effective Theory

Known as "the theory of almost everything", the SM of particle physics is a theory whose predictions verify to a very good extent the data of almost all particle physics experiments implemented at currently reachable energies.

Nevertheless, it is dubbed an effective theory that is valid only up to a certain energy scale  $\Lambda$  beyond which it gives up and dies. Clearly, the SM, which describes interactions only through electromagnetic, weak and strong forces and which fails to include the gravitational force, must cease to work at the Planck energy scale at which the gravitational forces become comparable in strength to other forces. Indeed, the SM breaks down much earlier, at the  $TeV$  energy scale, due to its insufficient elucidation of electroweak symmetry breaking (EWSB) by the Higgs mechanism.

## 3.2 Shortcomings of the Standard Model

Despite its impressive success in describing all existing experimental data at currently available energies, the SM of particle physics suffers from some serious troubles that are the main motivation for physics BSM. Below is a glance on some of them with more emphasis on the last one as part of this thesis work:

### I. Gravity

Obviously, the SM of particle physics, which embraced the electromagnetic, strong and weak forces, disregarded the fourth fundamental force of nature known famously as the gravitational force. It is not a long time ago since the discovery of gravitational waves which may imply in the near future the existence of the logically hypothesized mediator of the gravitational force, a particle which is absent from the SM, the graviton. These gravitational fields are completely classical and it had been always a difficult task for physicists to come up with a theory to quantize them and get them included into the SM of particle physics.

### II. Unification of the weak, strong and electromagnetic forces

Experiments show that the strong and weak forces become weaker and the electromagnetic force becomes stronger as the energy increases. This is a good indication that at incredibly high energies, the strength of the electromagnetic, weak and the strong forces is probably the same. The SM, however, does not provide a unification of these forces at very high energies.

### III. Neutrino oscillation

Neutrino flavor changes, known also as neutrino oscillations, have been observed and verified with numerous experiments involving atmospheric, solar, reactor and accelerator-made neutrinos (Capozzi et al., 2016; Esteban et al., 2017; Patrignani et al., 2016). This phenomenon emphasizes that at least two of the neutrinos in the SM have a nonzero mass, making this the first deviation from the SM as the mass property is not there in the theory of the SM. Therefore, it is a fact that the SM needs to be

revised in order to accommodate for massive and mixed neutrinos, which in turn leads to physics beyond the SM.

### **VI. Number of generations**

In the SM leptons and quarks are grouped into three generations with all the same properties except masses, but there is no explanation or limitation on the number of generations. The lightest and most stable particles make up the first generation, whereas the less stable and heavier particles belong to the second and third generations. All stable matter in the universe is made from particles that belong to the first generation; any heavier particles quickly decay to the next most stable level. However, SM can not explain why the other two generations are needed and whether or not there are more generations.

### **V. The strong CP problem**

The strong CP problem is a severe weakness of the SM. The SM -which imposes non CP conserving hypothetical processes- failed to answer the perplexing question of why strong interactions do not seem to break CP-symmetry as do the weak interactions despite the fact that the laws governing both interactions are very similar in nature.

### **VI. Matter-antimatter asymmetry**

Why we live in a matter-dominated universe? What happened to all the antimatter in the early universe after the Big Bang? And by the fact that matter asymmetry is consistently referred to as baryon asymmetry, how can this be the reason for our existence? All these questions and many others have fiercely attacked the SM and were one of the reasons to start thinking of other theories that could figure out such a mystery.

### **VII. Dark matter and dark energy**

The SM was brilliantly successful in describing the behavior of our visible universe; that is, everything we were able to witness by our experiments and apparatuses from the large scale of galaxies down to the smallest possible scale of atoms. Indeed, this visible universe appeared to be made up of a bunch of protons and neutrons surrounded by electrons and packaged together into atoms constituting all the ordinary (or baryonic)

matters around us. These, however, form less than 5% of the mass of the universe, which is maybe one of the most shocking exploration happened in the 20<sup>th</sup> century. The rest of the universe appears to be made up of a strange, invisible substance called dark matter (25%) and a force that repels gravity known as dark energy (70%). Both are still ambiguous and are not part of the SM, which means that it clearly cannot be the ultimate story of the universe.

### **VIII. The Higgs hierarchy problem**

The discovery of the long-awaited Higgs boson in 2012 at CERN's large hadron collider (LHC) (ATLAS collaboration, 2012; CMS collaboration, 2012) is not just a discovery of a new particle in the SM theory but also an important sign for the existence of new physics BSM, mainly because of the famous "SM Higgs hierarchy problem".

Typically, in physics, it is more likely that a microscopic theory describes some macroscopic behavior naturally without fine-tuning any parameter in the theory. A hierarchy problem -sometimes called a naturalness or a fine-tuning problem- arises when the value of a physical parameter in a theory needs to be carefully fine-tuned in order to meet some experimental constraints.

Indeed, the SM Higgs boson has a "snowball's chance in hell" as it suffers from infinite quantum corrections leaving it with no option but to be much heavier than the experimentally discovered one. These corrections are mainly due to the Higgs interaction with virtual particles of the SM quarks (mostly the *top* quark), gauge bosons ( $W$ ,  $Z$  and  $\gamma$ ) and the Higgs boson itself, as is presented in Figure 3.1. There are, of course, other possible diagrams of the Higgs interaction with gluons and other quarks in addition to higher order diagrams, as is presented in Figure 3.2, but these are of less importance which makes it sufficient to deal with the three lowest-order diagrams presented as they contribute the most to the infinite radiations of the Higgs mass.

These misbehaved diagrams are the core reason of the hierarchy problem. The Higgs particle can have an intermediate state of some virtual particle for a very short period of time. That is to say, a Higgs coming with some momentum  $p$  can absorb

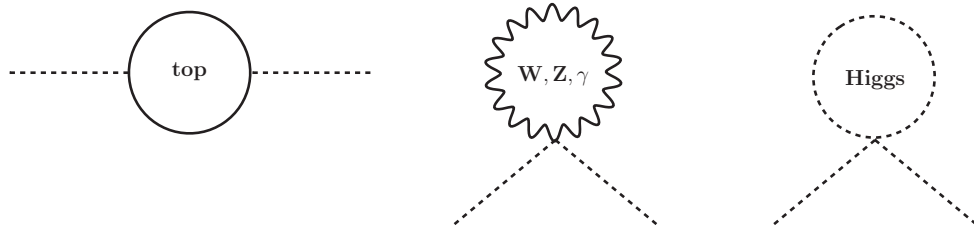


Figure 3.1 Feynman diagrams of the Higgs interaction with the SM top quark (*left*), gauge bosons (*center*) and Higgs boson (*right*)

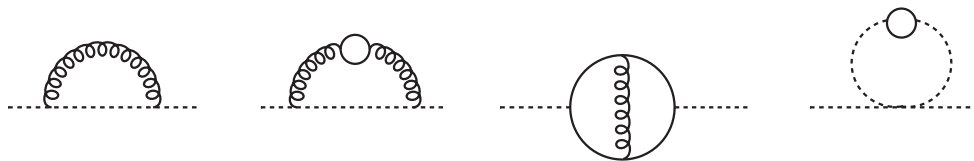


Figure 3.2 Higher order Feynman diagrams of the Higgs interaction with the SM particles

some particle with momentum  $k$  and have a total momentum of  $p + k$  before going back to its original state with momentum  $p$ . Keep in mind that in order to draw Feynman diagrams, momentum should be conserved and so the incoming Higgs and the outgoing Higgs should have the same momentum. The value of the virtual momentum  $k$ , however, is totally arbitrary and one needs to sum over all possible values of  $k$  or equivalently integrate over all possible four-vector  $k$ . Such momentum integrals produce ultraviolet (UV) infinite divergences due to the countless values of possible momenta. Clearly, a particle cannot have an infinite mass and so to obtain a practical finite mass, one needs to regularize (or redefine) these integrals. The method used here is the so-called "cut-off regularization" through which integration of momenta  $k$  is limited to some range  $k < \Lambda$  where  $\Lambda$  is the cut-off scale of the theory. Notwithstanding its disadvantages, this method has an extremely straightforward and simple physical explanation as compared to its nephew method known as "dimensional regularization" through which integration of momenta  $k$  is carried out as a function of space-time dimension  $d$ .

We will mathematically look at this problem by considering three different situations for three different cut-off values  $\Lambda$  (Maarten, 2004):

**Situation 1:**

If we assume that the SM is the fundamental theory of nature and is available even at very high energies, it should break down at the Planck mass-energy equivalent scale  $\Lambda = M_{Planck} = 1.22091 \times 10^{19} \text{ GeV}$ , beyond which the estimation of loop diagrams is out of our current knowledge. This would roughly yield a Higgs of mass  $10^{19} \text{ GeV}$  instead of the experimentally discovered  $125 \text{ GeV}$  Higgs with an unnatural need of about  $10^{17}$  fine-tuning of the SM parameters. More accurately, if the SM breaks down at  $\Lambda = M_{Planck} \approx 10^{19} \text{ GeV}$ , the contributions to the Higgs mass are

$$-\frac{3}{8\pi^2}\lambda_t^2\Lambda^2 \approx -\left(2 \times 10^{15} \text{ TeV}\right)^2 \text{ from the } top \text{ loop,} \quad (3.1)$$

$$\frac{1}{16\pi^2}g^2\Lambda^2 \approx \left(0.7 \times 10^{15} \text{ TeV}\right)^2 \text{ from the } gauge \text{ loop,} \quad (3.2)$$

$$\frac{1}{16\pi^2}\lambda^2\Lambda^2 \approx \left(0.5 \times 10^{15} \text{ TeV}\right)^2 \text{ from the } Higgs \text{ loop.} \quad (3.3)$$

The overall Higgs mass at one-loop order is then

$$m_H^2 = m_{tree}^2 - [(1 - 0.1225 - 0.0625) \times 10^{32}] (200 \text{ GeV})^2. \quad (3.4)$$

If the Higgs mass is to be only a few hundred  $\text{GeV}$ , a fine tuning of order one part in  $10^{32}$  among the tree-level parameters of the SM is required.

**Situation 2:**

Even much earlier, if we assume that the SM breaks down at  $\Lambda = 10 \text{ TeV}$ , the contributions to the Higgs mass are

$$-\frac{3}{8\pi^2}\lambda_t^2\Lambda^2 \approx -(2 \text{ TeV})^2 \text{ from the } top \text{ loop,} \quad (3.5)$$

$$\frac{1}{16\pi^2}g^2\Lambda^2 \approx (0.7 \text{ TeV})^2 \text{ from the } gauge \text{ loop,} \quad (3.6)$$

$$\frac{1}{16\pi^2}\lambda^2\Lambda^2 \approx (0.5 \text{ TeV})^2 \text{ from the } Higgs \text{ loop.} \quad (3.7)$$

The overall Higgs mass at one-loop order is then

$$m_H^2 = m_{tree}^2 - [(1 - 0.1225 - 0.0625) \times 10^2] (200 \text{ GeV})^2. \quad (3.8)$$

And again, if the Higgs mass is to be only a few hundred  $GeV$ , a fine tuning of order one part in 100 among the tree-level parameters of the SM is required.

**Situation 3:**

However, assuming that the SM breaks down at  $\Lambda = 1 TeV$ , the contributions to the Higgs mass are

$$-\frac{3}{8\pi^2}\lambda_t^2\Lambda^2 \approx -(0.2 TeV)^2 \text{ from the } top \text{ loop,} \quad (3.9)$$

$$\frac{1}{16\pi^2}g^2\Lambda^2 \approx (0.07 TeV)^2 \text{ from the } gauge \text{ loop,} \quad (3.10)$$

$$\frac{1}{16\pi^2}\lambda^2\Lambda^2 \approx (0.05 TeV)^2 \text{ from the } Higgs \text{ loop.} \quad (3.11)$$

The overall Higgs mass at one-loop order is then

$$m_H^2 = m_{tree}^2 - [(1 - 0.1225 - 0.0625) \times 10^0] (200 GeV)^2. \quad (3.12)$$

This would give a Higgs mass of a few hundred  $GeV$  as is demanded by the SM without a remarkable need for any fine tuning. Accordingly, the SM can survive naturally and unaided by any new physics BSM up to energy scales of  $1 TeV$ . The reason it should not be shocking when our colliders and accelerators, operating at currently available energies of  $1 TeV$ , do not witness any significant departure from the SM.

As a simple graphical representation of the three situations above, the contributions from the top, gauge and Higgs loops and the fine-tuning required to obtain an acceptable Higgs mass in the SM with cut-offs  $\Lambda \approx 10^{16} TeV$ ,  $\Lambda = 10 TeV$  and  $\Lambda = 1 TeV$  are shown in Figure 3.3.

Clearly, trying to re-normalize our SM theory to a very high scale was not successful in resolving the problem of the infinite quantum corrections to the Higgs mass. Although it succeeded in naturally describing all experimental data at relatively low energies, the SM of particle physics is in a real critical situation when it comes to deal with energies just above the  $1 TeV$  where some serious fine-tuning of its parameters is needed to be in agreement with the experimental data. At this point, the SM is regarded

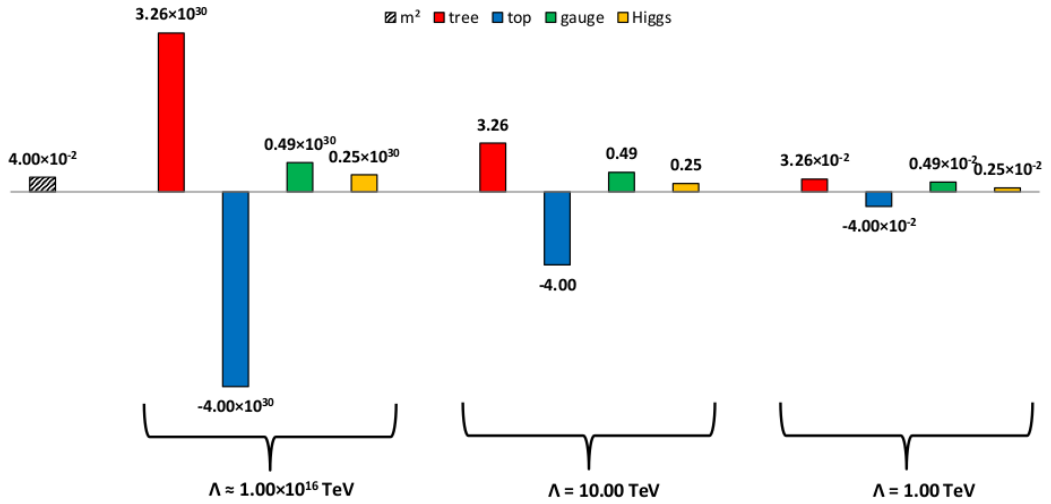


Figure 3.3 The fine-tuning required (*red histogram*) to obtain an acceptable Higgs mass in the SM with cut-offs  $\Lambda \approx 10^{16} \text{ TeV}$ ,  $\Lambda = 10 \text{ TeV}$  and  $\Lambda = 1 \text{ TeV}$

as an effective theory of a more global, fundamental theory expected at high energies.

This what actually urged particle physicists to look for new physics BSM with some new heavy particles in there to hugely fine-tune the Higgs boson mass in such a way to cancel these infinite corrections and leave it relatively light and not too far from  $W$  and  $Z$  gauge bosons masses (around 125 GeV) as is experimentally observed by ATLAS and CMS detectors. The solution we are going to elaborate here -which is the main theme of this work- is known as little Higgs models (LHMs) with an emphasis on one product group model named  $SU(5)$  littlest Higgs model (LTHM) and one simple group model named  $SU(3)$  simple little Higgs model (SLHM).

Note that, at first glance, it seems that all the SM particles have a Planck-scale mass because logically they can also have diagrams with a virtual loop of momentum  $k$  up to  $M_{Planck}$ . It turns out that the hierarchy problem is special to scalar particles and the only scalar particle in the SM theory is the Higgs particle. Fermions and gauge bosons masses are somehow guarded by the mechanism of chirality and gauge invariance, respectively.

### 3.3 Scalar, Pseudoscalar and Tensorial Non-standard Interaction of Neutrinos

In this section, one example of a model-independent BSM researches known as scalar, pseudoscalar and tensorial NSI of neutrinos is going to be carefully investigated both theoretically and analytically via neutrino-electron elastic scattering channel.

By analogy to the experimental fact of quark flavor mixing where not only transitions within the same generations but also cross-generational transitions are allowed by the known non-unitary Kobayashi-Maskawa matrix through (Griffiths, 2008)

$$\begin{pmatrix} d' \\ s' \\ b' \end{pmatrix} = U \begin{pmatrix} d \\ s \\ b \end{pmatrix} = \begin{pmatrix} U_{ud} = 0.974 & U_{us} = 0.227 & U_{ub} = 0.004 \\ U_{cd} = 0.227 & U_{cs} = 0.973 & U_{cb} = 0.042 \\ U_{td} = 0.008 & U_{ts} = 0.042 & U_{tb} = 0.999 \end{pmatrix} \begin{pmatrix} d \\ s \\ b \end{pmatrix}, \quad (3.13)$$

lepton flavors do also mix violating as a result lepton number conservation laws.

As upness-plus-downness, strangeness-plus-charmness and topness-plus-bottomness are violated during cross-generational quark flavor transitions, electron lepton number, muon lepton number and tau lepton number are also violated during lepton flavor mixings. Such process are known as lepton flavor violating process and they are usually split into three categories: charged lepton flavor violating (CLFV) processes where the charged leptons ( $\ell = e^-, \mu^-, \tau^-$ ) undergo flavor transitions as is shown in Fig. 3.4 (a), NSIs of neutrino where the neutral leptons ( $\nu_\ell = \nu_e, \nu_\mu, \nu_\tau$ ) undergo flavor transitions as is shown in Fig. 3.4 (b) and 4-neutrino-NSI which is similar to NSI but with four neutrinos as is shown in Fig. 3.4 (c).

A recent significant achievement in experimental particle physics is the discovery of neutrino flavor transitions described primarily by the mechanism of neutrino oscillations.

NSI of neutrinos is a model-independent framework that can be an effect of the mechanism of neutrino oscillations. NSI of neutrinos is a good channel to look for

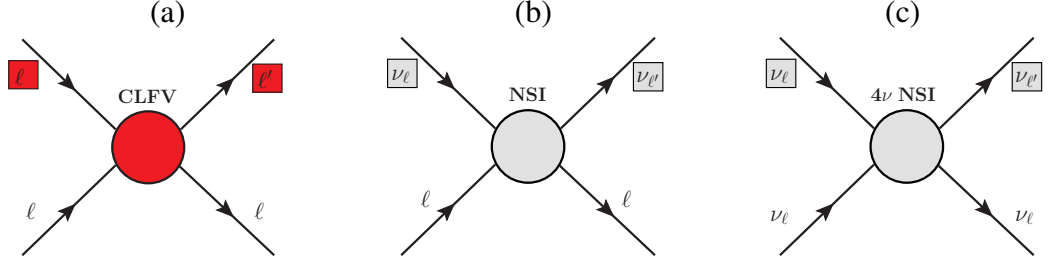


Figure 3.4 Lepton flavor violating processes

physics BSM, because witnessing such interactions experimentally would imply the existence of massive and therefore right-handed neutrinos as opposed by the beliefs of the SM.

Neutrino flavor eigenstates are mixed with mass states by

$$\begin{pmatrix} \nu_e \\ \nu_\mu \\ \nu_\tau \end{pmatrix} = U \begin{pmatrix} \nu_1 \\ \nu_2 \\ \nu_3 \end{pmatrix} = \begin{pmatrix} U_{e1} & U_{e2} & U_{e3} \\ U_{\mu1} & U_{\mu2} & U_{\mu3} \\ U_{\tau1} & U_{\tau2} & U_{\tau3} \end{pmatrix} \begin{pmatrix} \nu_1 \\ \nu_2 \\ \nu_3 \end{pmatrix}, \quad (3.14)$$

where  $U_{e1}$  measures the coupling of  $\nu_e$  to  $\nu_1$ , and so on, and

$$U = \begin{pmatrix} 1 & 0 & 0 \\ 0 & c_{23} & s_{23} \\ 0 & -s_{23} & c_{23} \end{pmatrix} \begin{pmatrix} c_{13} & 0 & s_{13}e^{-i\delta} \\ 0 & 1 & 0 \\ -s_{13}e^{i\delta} & 0 & c_{13} \end{pmatrix} \begin{pmatrix} c_{12} & s_{12} & 0 \\ -s_{12} & c_{12} & 0 \\ 0 & 0 & 1 \end{pmatrix} \times \begin{pmatrix} e^{i\rho} & 0 & 0 \\ 0 & e^{i\sigma} & 0 \\ 0 & 0 & 1 \end{pmatrix}, \quad (3.15)$$

where  $c_{ij} \equiv \cos(\theta_{ij})$  and  $s_{ij} \equiv \sin(\theta_{ij})$ ,  $\theta_{ij}$  are the leptonic mixing parameters,  $\delta$  is the Dirac CP-violating phase,  $\rho$  and  $\sigma$  are the Majorana CP-violating phases.

In the framework of NSI, neutrinos couple to the charged leptons ( $e^-$ ,  $\mu^-$  and  $\tau^-$ ) in the scalar, pseudoscalar and tensorial form in addition to the standard vector-axial vector coupling form offered by the SM.

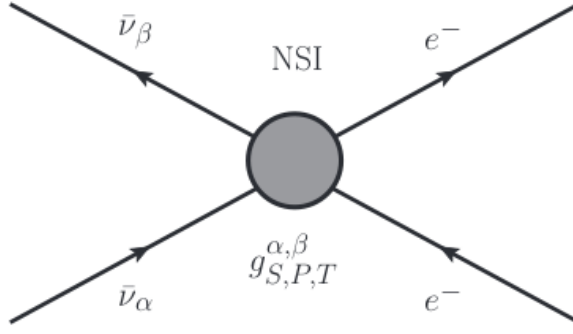


Figure 3.5 NSIs of neutrinos described as four-Fermi interaction with new couplings

In general, NSI of neutrinos can be described as a four-Fermi (a so called point-like or zero-distance) interaction with new modified chiral coupling constants  $g_{L,R}$ . The corresponding Feynman diagram of the various forms of NSI for neutrino-electron scattering is shown in Fig. 3.5.

The effective Lagrangian density for scalar/pseudoscalar interaction among leptons and charged Higgs bosons can be written as

$$\mathcal{L}_{S,P} = \sum_{\alpha} \sum_{\beta} \bar{l}_{\alpha} (\mathcal{O}_{S,P}) \nu_{\beta}, \quad (3.16)$$

where  $\mathcal{O}_{S,P}$  is a general operator with scalar/pseudoscalar interactions and  $\alpha, \beta = e, \mu, \tau$ . For the case of the operator  $\mathcal{O}$ , it is possible to find the general transformation (Galtán et al., 2013)

$$\begin{aligned} & 2 \left[ \bar{l}_{\alpha} (a + b\gamma^5) \nu_{\beta} \right] \left[ \bar{\nu}_{\beta} (c + d\gamma^5) l_{\alpha} \right] \\ &= (a+b)(c+d) \left( \bar{l}_{\alpha} \mathcal{P}_R l_{\alpha} \bar{\nu}_{\beta} \mathcal{P}_R \nu_{\beta} + \frac{1}{4} \bar{l}_{\alpha} \sigma^{\mu\nu} \mathcal{P}_R l_{\alpha} \bar{\nu}_{\beta} \sigma_{\mu\nu} \mathcal{P}_R \nu_{\beta} \right) \\ &+ (a+b)(c-d) \bar{l}_{\alpha} \gamma^{\mu} \mathcal{P}_L l_{\alpha} \bar{\nu}_{\beta} \gamma_{\mu} \mathcal{P}_R \nu_{\beta} \\ &+ (a-b)(c+d) \bar{l}_{\alpha} \gamma^{\mu} \mathcal{P}_R l_{\alpha} \bar{\nu}_{\beta} \gamma_{\mu} \mathcal{P}_L \nu_{\beta} \\ &+ (a-b)(c-d) \left( \bar{l}_{\alpha} \mathcal{P}_L l_{\alpha} \bar{\nu}_{\beta} \mathcal{P}_L \nu_{\beta} + \frac{1}{4} \bar{l}_{\alpha} \sigma^{\mu\nu} \mathcal{P}_L l_{\alpha} \bar{\nu}_{\beta} \sigma_{\mu\nu} \mathcal{P}_L \nu_{\beta} \right). \end{aligned} \quad (3.17)$$

The differential scattering cross section of scalar-pseudoscalar NSI of neutrino for

$\bar{\nu}_e e$  and  $\nu_e e$  can be written respectively as

$$\left[ \frac{d\sigma}{dT}(\bar{\nu}_e e) \right]_{NSI}^{S,P} = \frac{2G_F^2 m_e}{\pi} \left\{ (|g_S^{e,e}| + |g_P^{e,e}|)^2 + g_R \text{Re}(g_S^{e,e} - g_P^{e,e}) - (g_L + 1) \text{Re}(g_S^{e,e} - g_P^{e,e}) \frac{m_e}{2E_\nu^2} \right\}, \quad (3.18)$$

and

$$\left[ \frac{d\sigma}{dT}(\nu_e e) \right]_{NSI}^{S,P} = \frac{2G_F^2 m_e}{\pi} \left\{ \left[ (|g_S^{e,e}| + |g_P^{e,e}|)^2 + g_R \text{Re}(g_S^{e,e} - g_P^{e,e}) \right] \times \left( 1 - \frac{T}{E_\nu} \right)^2 - (g_L + 1) \text{Re}(g_S^{e,e} - g_P^{e,e}) \frac{m_e}{2E_\nu^2} \right\}. \quad (3.19)$$

The effective Lagrangian density for tensorial interaction can be written as (Barraño et al., 2012; Deniz et al., 2017)

$$\mathcal{L}_T = -2\sqrt{2}G_F \varepsilon_{\alpha\beta}^{fT} (\bar{\nu}_\alpha \sigma^{\mu\nu} \nu_\beta) (\bar{f} \sigma_{\mu\nu} f), \quad (3.20)$$

where  $\varepsilon_{\alpha\beta}^{fT}$  is the strength of the tensorial NSI coupling with electrons,  $\sigma^{\mu\nu} = [\gamma^\mu, \gamma^\nu] = \gamma^\mu \gamma^\nu - \gamma^\nu \gamma^\mu$  and  $\alpha, \beta = e, \mu, \tau$ .

The differential scattering cross section of tensorial NSI, however, can be written as

$$\left[ \frac{d\sigma}{dT}(\bar{\nu}_e e) \right]_{NSI}^T = \frac{2G_F^2 m_e}{\pi} \sum_{\beta=e,\mu,\tau} (\varepsilon_{e\beta}^{eT})^2 \left[ 2 \left( 1 - \frac{T}{2E_\nu} \right)^2 - \frac{m_e T}{2E_\nu^2} \right]. \quad (3.21)$$

## CHAPTER FOUR

### LITTLE HIGGS MODELS

In the same way supersymmetric theories try to stabilize the electroweak scale in the ultraviolet (UV) zone by introducing superpartners of the SM particles, technicolor theories do so by introducing new strong dynamics at scales not much above the electroweak scale. Little Higgs models (LHMs) are one concrete example of technicolor theories offered as another solution to the hierarchy problem of the SM. More technically, these models are used to stabilize the SM Higgs boson mass against the large uncontrolled quantum corrections, and thus stabilizing the electroweak scale at  $v = 246 \text{ GeV}$  employing the "collective symmetry breaking" mechanism (Perelstein, 2007; Schmaltz et al., 2005).

LHMs approach the problem by considering the Higgs a pseudo-Goldstone boson (PGB) resulting from symmetry breaking of some global symmetry which in turn allows it to get a relatively light mass free from any one-loop quadratic divergences via symmetry breaking at the electroweak scale.

There are several variations of the LHMs, which differ at least in the assumed structure of the extended higher symmetry electroweak gauge group. They can be generally divided into two classes (Han et al., 2006): Product group models and Simple group models. The  $SU(5)$  littlest Higgs model (LTHM) (Arkani-Hamed et al., 2002; Perelstein, 2007; Schmaltz et al., 2005) and the  $SU(3)$  simple little Higgs model (SLHM) (Kaplan et al., 2003; Perelstein, 2007; Schmaltz et al., 2005) are the basic examples of these two kinds of LHMs, respectively.

#### 4.1 The $SU(5)$ Littlest Higgs Model

$SU(5)$  LTHM is the most economical and the simplest extension of the SM, which is the first model to be explicitly constructed based on the core ideas of little Higgs theories.

From a phenomenological point of view, it consists of a nonlinear  $\sigma$  model with a global  $SU(5)$  symmetry and a locally gauged symmetry  $[SU(2) \times U(1)]^2$ . The global  $SU(5)$  symmetry is broken down to its subgroup  $SO(5)$  at a scale  $f$ , which results in fourteen PGBs. Four of these GBs are eaten by the new heavy bosons ( $Z_H^0$ ,  $A_H^0$  and  $W_H^\pm$ ) predicted by the model as a result of the breaking of  $[SU(2) \times U(1)]^2$  (Arkani-Hamed et al., 2002; Han et al., 2004; Na et al., 2011; Perelstein, 2007; Schmaltz et al., 2005).

In the  $SU(5)$  LTHM, the quadratic divergences cancel between the  $W_L$  and  $W_H$  loops with a partial cancellation between the  $Z_L$  and  $Z_H$  loops. Including the  $A_H$  loop, however, leads to a complete cancellation of the quadratic divergences from the  $Z$  loop.

Compared with the neutrino-electron elastic scattering process in the SM, this process in the  $SU(5)$  LTHM receives additional contributions from the correction terms of the SM  $Z$  and  $W$  couplings and from some new heavy gauge bosons  $Z_H$ ,  $A_H$  and  $W_H$ .

In the framework of the  $SU(5)$  LTHM:

- the vertex factor for the coupling between neutral gauge bosons and leptons can be written in the form

$$-i\frac{g_z}{2}\gamma^\mu \left( g_V^{f'} - g_A^{f'} \gamma^5 \right), \quad (4.1)$$

where the new neutral vector  $g_V^{f'}$  and axial vector  $g_A^{f'}$  coupling constants depend on the mixing parameters  $c$  (or  $s$ ,  $s = \sqrt{1 - c^2}$ ) and  $c'$  (or  $s'$ ,  $s' = \sqrt{1 - c'^2}$ ) and the scale  $f$ . Note that the SM neutral weak coupling constant  $g_z = \frac{g_e}{s_w c_w}$  with  $g_e = 2\sqrt{\pi}e$  is the electromagnetic coupling constant which is known essentially as the charge of the electron.

- the vertex factor for the coupling between charged gauge bosons and leptons can

be written in the form

$$-i \frac{g_w}{2\sqrt{2}} g' \gamma^\mu (1 - \gamma^5), \quad (4.2)$$

where the new charged weak coupling constant  $g'$  depends only on the mixing parameter  $c$  (or  $s$ ) and the scale  $f$ . Note that  $g_w = \frac{g_e}{s_w}$  in the SM.

- the propagator factor can take the form

$$-i \left( \frac{g_{\mu\nu} - \frac{q_\mu q_\nu}{M^2}}{q^2 - M^2} \right) \approx i \frac{g_{\mu\nu}}{M^2} \text{ (strictly in low energy region),} \quad (4.3)$$

where  $q$  and  $M$  refer respectively to the momentum transfer and the mass of the mediator.

- the couplings of the SM  $Z$  and  $W$  intermediate vector gauge bosons and the new heavy  $Z_H$ ,  $A_H$  and  $W_H$  bosons with leptons are given in Table 4.1, where  $x_Z^{W'} = -\frac{1}{2c_w} s c (c^2 - s^2)$ ,  $x_Z^{B'} = -\frac{5}{2s_w} s' c' (c'^2 - s'^2)$  and  $y_e = \frac{3}{5}$  (for anomaly cancellation).

In the scope of neutrino-electron elastic scattering, the  $SU(5)$  LTHM involves both flavor conserving (FC) and flavor violating (FV) processes denoted respectively by  $\nu_e (\bar{\nu}_e) + e \rightarrow \nu_e (\bar{\nu}_e) + e$  and  $\nu_e (\bar{\nu}_e) + e \rightarrow \nu_\alpha (\bar{\nu}_\alpha) + e$  (where  $\alpha \neq e$ ) and mediated by the SM ( $Z$  and  $W$ ) and new heavy ( $Z_H$ ,  $A_H$  and  $W_H$ ) gauge bosons.

Note that both neutral-current (NC) and charged-current (CC) interactions, mediated respectively by the neutral and the charged gauge bosons, along with their interference, take part in the FC processes but only the NC interactions in the FV processes.

Table 4.1 Couplings of the SM  $Z$  and  $W$  gauge bosons and the new heavy  $Z_H$ ,  $A_H$  and  $W_H$  gauge bosons with leptons in the  $SU(5)$  LTHM (Aliev et al., 2008; Han et al., 2004; Poschenrieder et al., 2007)

	SM	$SU(5)$ LTHM
$Z\nu\bar{\nu}$	$g_V^V = \frac{1}{2}$ $g_A^V = \frac{1}{2}$	$g_V^{V'} = \frac{1}{2} - \frac{v^2}{f^2} \left[ c_w x_z^{W'} \frac{c}{2s} + s_w x_z^{B'} \frac{1}{s'c'} (y_e - \frac{4}{5} + \frac{1}{2}c'^2) \right]$ $g_A^{V'} = g_V^{V'}$
$Ze\bar{e}$	$g_V^e = -\frac{1}{2} + 2s_w^2$ $g_A^e = -\frac{1}{2}$	$g_V^{e'} = -\frac{1}{2} + 2s_w^2 - \frac{v^2}{f^2} \left[ -c_w x_z^{W'} \frac{c}{2s} + s_w x_z^{B'} \frac{1}{s'c'} (2y_e - \frac{9}{5} + \frac{3}{2}c'^2) \right]$ $g_A^{e'} = -\frac{1}{2} - \frac{v^2}{f^2} \left[ c_w x_z^{W'} \frac{c}{2s} + s_w x_z^{B'} \frac{1}{s'c'} (-\frac{1}{5} + \frac{1}{2}c'^2) \right]$
$We\bar{\nu}$	$g = 1$	$g' = 1 - \frac{1}{2} \frac{v^2}{f^2} c^2 (c^2 - s^2)$
$Z_H\nu\bar{\nu}$	-	$g_V^{V'} = \frac{1}{2} c_w \frac{c}{s}$ $g_A^{V'} = g_V^{V'}$
$Z_He\bar{e}$	-	$g_V^{e'} = -\frac{1}{2} c_w \frac{c}{s}$ $g_A^{e'} = g_V^{e'}$
$A_H\nu\bar{\nu}$	-	$g_V^{V'} = s_w \frac{1}{s'c'} (y_e - \frac{4}{5} + \frac{1}{2}c'^2)$ $g_A^{V'} = g_V^{V'}$
$A_He\bar{e}$	-	$g_V^{e'} = s_w \frac{1}{s'c'} (2y_e - \frac{9}{5} + \frac{3}{2}c'^2)$ $g_A^{e'} = -s_w \frac{1}{s'c'} (-\frac{1}{5} + \frac{1}{2}c'^2)$
$W_He\bar{\nu}$	-	$g' = -\frac{c}{s} \left[ 1 + \frac{1}{2} \frac{v^2}{f^2} s^2 (c^2 - s^2) \right]$

#### 4.1.1 Antineutrino-Electron Scattering

##### 4.1.1.1 $\bar{\nu}_e + e \rightarrow \bar{\nu}_e + e$ (FC)

Mediated by the SM light gauge bosons, there are two possible tree-level Feynman diagrams for the FC process of  $\bar{\nu}_e e$  elastic scattering.

- One is mediated by  $Z^0$  through a neutral weak process and is manifested by the Feynman diagram in Figure 4.1 (a) with the corresponding amplitude given by

$$\mathcal{M}_Z = \frac{2G_F}{\sqrt{2}} g_V^{V'} \left[ \bar{\nu}(p_1) \gamma^\mu (1 - \gamma^5) \nu(k_1) \right] \left[ \bar{u}(k_2) \gamma_\mu (g_V^{e'} - g_A^{e'} \gamma^5) u(p_2) \right]. \quad (4.4)$$

- The other is mediated by  $W^\pm$  through a charged weak process and is manifested

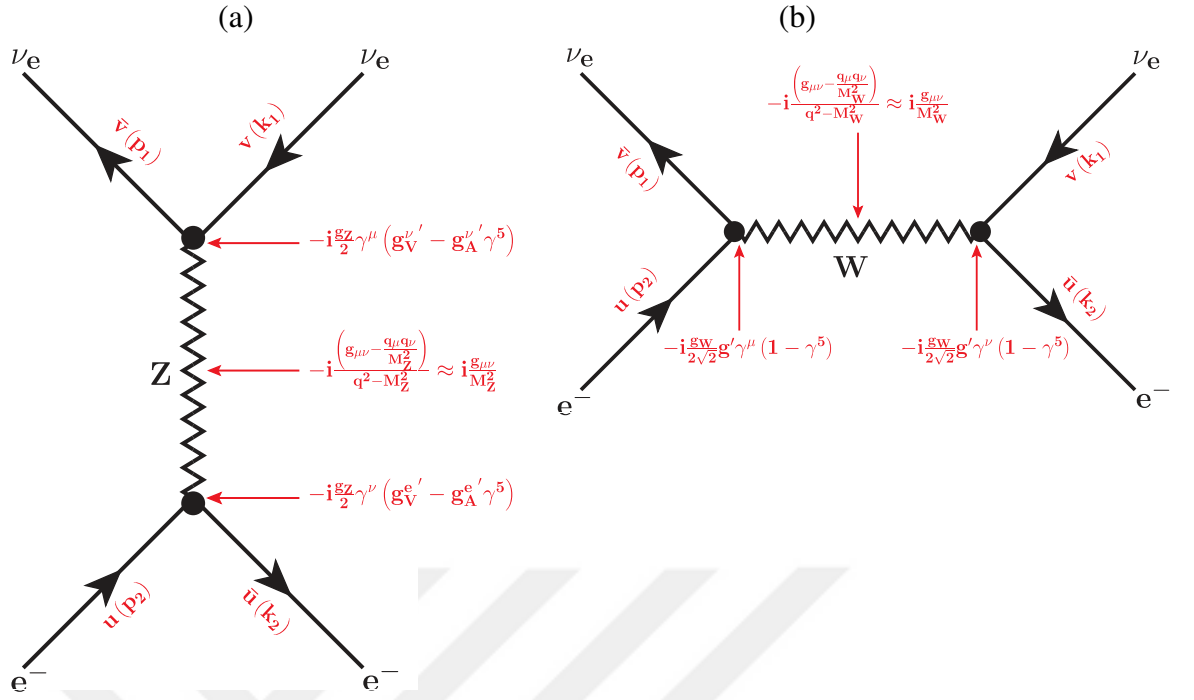


Figure 4.1 Feynman diagrams of (a) Z-mediated and (b) W-mediated antineutrino-electron FC scattering in the  $SU(5)$  LTHM along with the corresponding vertex and propagator factors

by the Feynman diagram in Figure 4.1 (b) with the corresponding amplitude given using Fierz transformation by

$$\mathcal{M}_W = \frac{G_F}{\sqrt{2}}g'^2 [\bar{\nu}(p_1)\gamma^\mu (1 - \gamma^5) \nu(k_1)] [\bar{u}(k_2)\gamma_\mu (1 - \gamma^5) u(p_2)]. \quad (4.5)$$

Then the total amplitude can be simply written as

$$\begin{aligned} \mathcal{M}_t &= \mathcal{M}_Z + \mathcal{M}_W \\ &= \frac{G_F}{\sqrt{2}} [\bar{\nu}(p_1)\gamma^\mu (1 - \gamma^5) \nu(k_1)] \\ &\quad \times [\bar{u}(k_2)\gamma_\mu \{ (2g_V^{\nu'}g_V^{e'} + g'^2) - (2g_V^{\nu'}g_A^{e'} + g'^2)\gamma^5 \} u(p_2)], \end{aligned} \quad (4.6)$$

and together with its hermitian conjugate  $\mathcal{M}_t^\dagger$ , the spin-averaged amplitude square is

$$\begin{aligned}
\langle |\mathcal{M}_t|^2 \rangle &= \frac{1}{2} \sum_{\text{spins}} |\mathcal{M}_t|^2 \\
&= \frac{G_F^2}{4} \sum_{\text{spins}} \left[ \bar{v}(p_1) \gamma^\mu (1 - \gamma^5) v(k_1) \right] \left[ \bar{v}(p_1) \gamma^\nu (1 - \gamma^5) v(k_1) \right]^\dagger \\
&\quad \times \sum_{\text{spins}} \left[ \bar{u}(k_2) \gamma_\mu \left\{ (2g_V^{v'} g_V^{e'} + g'^2) - (2g_V^{v'} g_A^{e'} + g'^2) \gamma^5 \right\} u(p_2) \right] \\
&\quad \times \left[ \bar{u}(k_2) \gamma_\nu \left\{ (2g_V^{v'} g_V^{e'} + g'^2) - (2g_V^{v'} g_A^{e'} + g'^2) \gamma^5 \right\} u(p_2) \right]^\dagger,
\end{aligned} \tag{4.7}$$

where using Casimir's trick (Griffiths, 2008) yields

$$\begin{aligned}
&= \frac{G_F^2}{4} \text{Tr} \left[ \gamma^\mu (1 - \gamma^5) (\not{k}_1 - m_\nu) \gamma^\nu (1 - \gamma^5) (\not{p}_1 - m_\nu) \right] \\
&\quad \times \text{Tr} \left[ \gamma_\mu \left\{ (2g_V^{v'} g_V^{e'} + g'^2) - (2g_V^{v'} g_A^{e'} + g'^2) \gamma^5 \right\} (\not{p}_2 + m_e) \right] \\
&\quad \times \text{Tr} \left[ \gamma_\nu \left\{ (2g_V^{v'} g_V^{e'} + g'^2) - (2g_V^{v'} g_A^{e'} + g'^2) \gamma^5 \right\} (\not{k}_2 + m_e) \right],
\end{aligned} \tag{4.8}$$

and then after evaluating the traces, the previous equation becomes

$$\begin{aligned}
\langle |\mathcal{M}_t|^2 \rangle &= 64G_F^2 \left[ g_V^{v'2} (g_V^{e'} - g_A^{e'})^2 (k_1 \cdot k_2) (p_1 \cdot p_2) \right. \\
&\quad \left. + (g_V^{v'} (g_V^{e'} + g_A^{e'}) + g'^2)^2 (k_1 \cdot p_2) (k_2 \cdot p_1) \right. \\
&\quad \left. - m_e^2 g_V^{v'} (g_V^{e'} - g_A^{e'}) (g_V^{v'} (g_V^{e'} + g_A^{e'}) + g'^2) (k_1 \cdot p_1) \right].
\end{aligned} \tag{4.9}$$

Note that in all what follows, our manual calculations of traces have been also checked out by "FeynCalc" (Mertig et al., 1991; Shtabovenko et al., 2016).

It is advantageous at this stage to pose and simplify the coupling constants of the light  $SU(5)$  LTHM given in Table 4.1 before going on and plugging them into their

places. So by the fact that

$$\begin{aligned}
x_Z^{W'} &= -\frac{1}{2c_W}sc(c^2 - s^2), \\
x_Z^{B'} &= -\frac{5}{2s_W}s'c'(c'^2 - s'^2), \\
y_e &= \frac{3}{5},
\end{aligned} \tag{4.10}$$

it follows that

$$\begin{aligned}
g_V^{v'} &= \frac{1}{2} - \frac{v^2}{f^2} \left[ c_w x_z^{W'} \frac{c}{2s} + s_w x_z^{B'} \frac{1}{s'c'} \left( y_e - \frac{4}{5} + \frac{1}{2}c'^2 \right) \right] \\
&= \frac{1}{2} + \frac{v^2}{f^2} \underbrace{\left[ \frac{1}{4}c^2(c^2 - s^2) + \frac{5}{2}(c'^2 - s'^2) \left( -\frac{1}{5} + \frac{1}{2}c'^2 \right) \right]}_{\equiv \frac{B}{2}} \\
\implies g_V^{v'} &= \frac{1}{2}(1 + B),
\end{aligned} \tag{4.11}$$

where  $B = 2\frac{v^2}{f^2} \left[ \frac{1}{4}c^2(c^2 - s^2) + \frac{5}{2}(c'^2 - s'^2) \left( -\frac{1}{5} + \frac{1}{2}c'^2 \right) \right]$ .

$$\begin{aligned}
g_V^{e'} &= -\frac{1}{2} + 2s_w^2 - \frac{v^2}{f^2} \left[ -c_w x_z^{W'} \frac{c}{2s} + s_w x_z^{B'} \frac{1}{s'c'} \left( 2y_e - \frac{9}{5} + \frac{3}{2}c'^2 \right) \right] \\
&= -\frac{1}{2} + 2s_w^2 - \frac{v^2}{f^2} \underbrace{\left[ \frac{1}{4}c^2(c^2 - s^2) - \frac{5}{2}(c'^2 - s'^2) 3 \left( -\frac{1}{5} + \frac{1}{2}c'^2 \right) \right]}_{\equiv \delta g_V^e} \\
\implies g_V^{e'} &= -\frac{1}{2} + 2s_w^2 + \delta g_V^e,
\end{aligned} \tag{4.12}$$

where  $\delta g_V^e = -\frac{v^2}{f^2} \left[ \frac{1}{4}c^2(c^2 - s^2) - \frac{5}{2}(c'^2 - s'^2) 3 \left( -\frac{1}{5} + \frac{1}{2}c'^2 \right) \right]$ .

$$\begin{aligned}
g_A^{e'} &= -\frac{1}{2} + \frac{v^2}{f^2} \left[ c_w x_z^{W'} \frac{c}{2s} + s_w x_z^{B'} \frac{1}{s'c'} \left( -\frac{1}{5} + \frac{1}{2}c'^2 \right) \right] \\
&= -\frac{1}{2} - \frac{v^2}{f^2} \underbrace{\left[ \frac{1}{4}c^2(c^2 - s^2) + \frac{5}{2}(c'^2 - s'^2) \left( -\frac{1}{5} + \frac{1}{2}c'^2 \right) \right]}_{\equiv \delta g_A^e} \\
\implies g_A^{e'} &= -\frac{1}{2} + \delta g_A^e,
\end{aligned} \tag{4.13}$$

where  $\delta g_A^e = -\frac{v^2}{f^2} \left[ \frac{1}{4}c^2 (c^2 - s^2) + \frac{5}{2} (c'^2 - s'^2) \left( -\frac{1}{5} + \frac{1}{2}c'^2 \right) \right]$ .

$$\begin{aligned} g' &= 1 - \underbrace{\frac{1}{2} \frac{v^2}{f^2} c^2 (c^2 - s^2)}_{\equiv \delta g_l'} \\ \implies g' &= 1 + \delta g_l', \end{aligned} \quad (4.14)$$

where  $\delta g_l' = -\frac{1}{2} \frac{v^2}{f^2} c^2 (c^2 - s^2)$ .

Or, equivalently, expressing the vector and axial-vector coupling constants of the electron in terms of the left-handed and right-handed chiral coupling constants yields

$$\begin{aligned} g_L' &= \frac{1}{2} (g_V^{e'} + g_A^{e'}) \\ &= \frac{1}{2} \left( -\frac{1}{2} + 2s_W^2 + \delta g_V^e - \frac{1}{2} + \delta g_A^e \right) \\ &= -\frac{1}{2} + s_W^2 + \underbrace{\frac{1}{2} (\delta g_V^e + \delta g_A^e)}_{\delta g_L} \\ \implies g_L' &= -\frac{1}{2} + s_W^2 + \delta g_L, \end{aligned} \quad (4.15)$$

where  $\delta g_L = -\frac{v^2}{f^2} \left[ \frac{1}{4}c^2 (c^2 - s^2) - \frac{5}{2} (c'^2 - s'^2) \left( -\frac{1}{5} + \frac{1}{2}c'^2 \right) \right]$ .

$$\begin{aligned} g_R' &= \frac{1}{2} (g_V^{e'} - g_A^{e'}) \\ &= \frac{1}{2} \left( -\frac{1}{2} + 2s_W^2 + \delta g_V^e + \frac{1}{2} - \delta g_A^e \right) \\ &= s_W^2 + \underbrace{\frac{1}{2} (\delta g_V^e - \delta g_A^e)}_{\delta g_R} \\ \implies g_R' &= s_W^2 + \delta g_R, \end{aligned} \quad (4.16)$$

where  $\delta g_R = 5 \frac{v^2}{f^2} (c'^2 - s'^2) \left( -\frac{1}{5} + \frac{1}{2}c'^2 \right)$ .

In terms of  $B$ ,  $\delta g_L$ ,  $\delta g_R$ , and  $\delta g'_L$  given respectively by Equations 4.11, 4.15, 4.16 and 4.14, the spin-averaged amplitude in Equation 4.9 can be written as

$$\begin{aligned} \langle |\mathcal{M}_t|^2 \rangle = & 64G_F^2 m_e^2 \left[ (1+B)^2 (g_R + \delta g_R)^2 E_\nu^2 \right. \\ & + \left. \left\{ (1+B)(g_L + \delta g_L) + (1 + \delta g'_L)^2 \right\}^2 (E_\nu - T)^2 \right. \\ & \left. - (1+B)(g_R + \delta g_R) \left\{ (1+B)(g_L + \delta g_L) + (1 + \delta g'_L)^2 \right\} m_e T \right], \end{aligned} \quad (4.17)$$

where the corresponding kinematic terms found in Appendix B have been also plugged.

Finally, inserting  $\langle |\mathcal{M}_t|^2 \rangle$  into  $\frac{d\sigma}{dT}$  found in Appendix A as

$$\frac{d\sigma}{dT} = \frac{\langle |\mathcal{M}|^2 \rangle}{32\pi m_2 |\vec{p}_1|^2},$$

where  $m_2 \equiv m_e$  and  $|\vec{p}_1|^2 \equiv |\vec{p}_\nu|^2 = E_\nu^2 - m_\nu^2 = E_\nu^2$ , gives as a final result

$$\begin{aligned} \left[ \frac{d\sigma}{dT}(\bar{\nu}_e e) \right]_{Light\ LTHM}^{FC} = & \frac{2G_F^2 m_e}{\pi} \left[ (1+B)^2 (g_R + \delta g_R)^2 \right. \\ & + \left. \left\{ (1+B)(g_L + \delta g_L) + (1 + \delta g'_L)^2 \right\}^2 \left( 1 - \frac{T}{E_\nu} \right)^2 \right. \\ & - (1+B)(g_R + \delta g_R) \left\{ (1+B)(g_L + \delta g_L) \right. \\ & \left. \left. + (1 + \delta g'_L)^2 \right\} \frac{m_e T}{E_\nu^2} \right]. \end{aligned} \quad (4.18)$$

On the other hand, mediated by the  $SU(5)$  LTHM new predicted heavy gauge bosons, there are three possible tree-level Feynman diagrams for the FC process of  $\bar{\nu}_e e$  elastic scattering.

- One is mediated by  $Z_H^0$  through a neutral weak process and is manifested by the

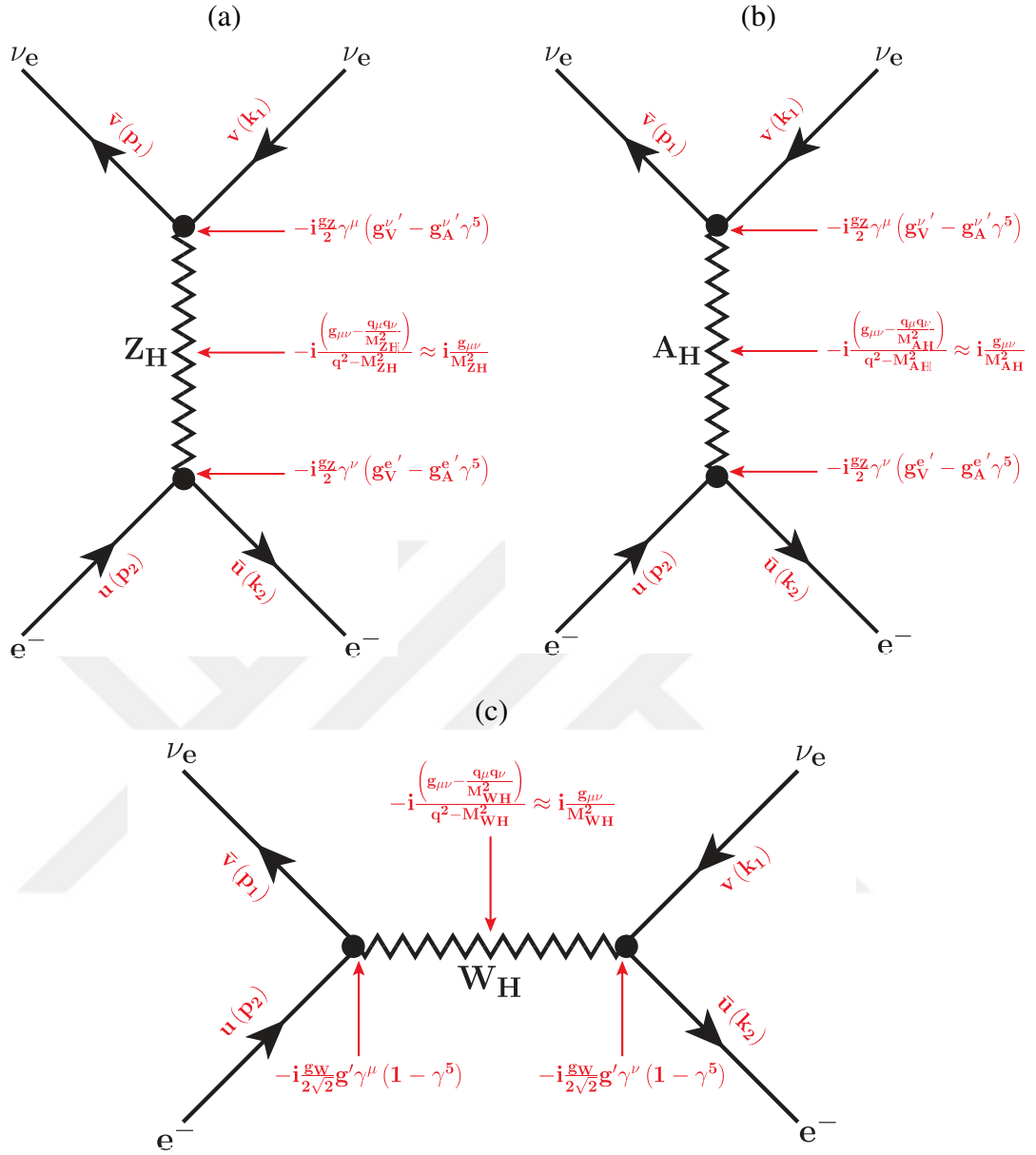


Figure 4.2 Feynman diagrams of (a)  $Z_H$ -mediated, (b)  $A_H$ -mediated and (c)  $W_H$ -mediated antineutrino-electron FC scattering in the  $SU(5)$  LTHM together with the convenient vertex and propagator factors

Feynman diagram in Figure 4.2 (a) with the corresponding amplitude given by

$$\mathcal{M}_{Z_H} = \frac{g_w^2}{4c_W^2 M_{Z_H}^2} g_V^{\nu'} g_V^{e'} \left[ \bar{\nu}(p_1) \gamma^\mu (1 - \gamma^5) \nu(k_1) \right] \left[ \bar{u}(k_2) \gamma_\mu (1 - \gamma^5) u(p_2) \right]. \quad (4.19)$$

- Another one is mediated by  $A_H^0$  through a neutral weak process and is manifested by the Feynman diagram in Figure 4.2 (b) with the corresponding amplitude

given by

$$\mathcal{M}_{AH} = \frac{g_w^2}{4c_W^2 M_{AH}^2} g_V^{v'} \left[ \bar{v}(p_1) \gamma^\mu (1 - \gamma^5) v(k_1) \right] \left[ \bar{u}(k_2) \gamma_\mu (g_V^{e'} - g_A^{e'} \gamma^5) u(p_2) \right]. \quad (4.20)$$

- A last one is mediated by  $W_H^\pm$  through a charged weak process and is manifested by the Feynman diagram in Figure 4.2 (c) with the corresponding amplitude given after Fierz transformation by

$$\mathcal{M}_{WH} = \frac{g_w^2}{8M_{WH}^2} g'^2 \left[ \bar{v}(p_1) \gamma^\mu (1 - \gamma^5) v(k_1) \right] \left[ \bar{u}(k_2) \gamma_\mu (1 - \gamma^5) u(p_2) \right]. \quad (4.21)$$

Then the total amplitude can be simply written as

$$\begin{aligned} \mathcal{M}_t &= \mathcal{M}_{ZH} + \mathcal{M}_{AH} + \mathcal{M}_{WH} \\ &= \frac{g_w^2}{8} \left[ \bar{v}(p_1) \gamma^\mu (1 - \gamma^5) v(k_1) \right] \left[ \bar{u}(k_2) \gamma_\mu \left( \left( \frac{2(g_V^{v'})_{ZH} (g_V^{e'})_{ZH}}{c_W^2 M_{ZH}^2} \right. \right. \right. \\ &\quad \left. \left. \left. + \frac{2(g_V^{v'})_{AH} (g_V^{e'})_{AH}}{c_W^2 M_{AH}^2} + \frac{g'^2}{M_{WH}^2} \right) - \left( \frac{2(g_V^{v'})_{ZH} (g_V^{e'})_{ZH}}{c_W^2 M_{ZH}^2} \right. \right. \right. \\ &\quad \left. \left. \left. + \frac{2(g_V^{v'})_{AH} (g_A^{e'})_{AH}}{c_W^2 M_{AH}^2} + \frac{g'^2}{M_{WH}^2} \right) \gamma^5 \right) u(p_2) \right], \end{aligned} \quad (4.22)$$

where, to avoid any mingling among the couplings of the different mediators, the corresponding couplings of  $Z_H$  and  $A_H$  have been separated.

Together with its hermitian conjugate  $\mathcal{M}_t^\dagger$ , the spin-averaged amplitude square is

$$\begin{aligned}
\langle |\mathcal{M}_t|^2 \rangle &= \frac{1}{2} \sum_{\text{spins}} |\mathcal{M}_t|^2 \\
&= \frac{g_w^4}{128} \sum_{\text{spins}} \left[ \bar{v}(p_1) \gamma^\mu (1 - \gamma^5) v(k_1) \right] \left[ \bar{v}(p_1) \gamma^\nu (1 - \gamma^5) v(k_1) \right]^\dagger \\
&\quad \times \sum_{\text{spins}} \left[ \bar{u}(k_2) \gamma_\mu \left( \left( \frac{2(g_V^{v'})_{Z_H} (g_V^{e'})_{Z_H}}{c_W^2 M_{Z_H}^2} + \frac{2(g_V^{v'})_{A_H} (g_V^{e'})_{A_H}}{c_W^2 M_{A_H}^2} + \frac{g'^2}{M_{W_H}^2} \right) \right. \right. \\
&\quad \left. \left. - \left( \frac{2(g_V^{v'})_{Z_H} (g_V^{e'})_{Z_H}}{c_W^2 M_{Z_H}^2} + \frac{2(g_V^{v'})_{A_H} (g_V^{e'})_{A_H}}{c_W^2 M_{A_H}^2} + \frac{g'^2}{M_{W_H}^2} \right) \gamma^5 \right) u(p_2) \right] \\
&\quad \times \left[ \bar{u}(k_2) \gamma_\nu \left( \left( \frac{2(g_V^{v'})_{Z_H} (g_V^{e'})_{Z_H}}{c_W^2 M_{Z_H}^2} + \frac{2(g_V^{v'})_{A_H} (g_V^{e'})_{A_H}}{c_W^2 M_{A_H}^2} + \frac{g'^2}{M_{W_H}^2} \right) \right. \right. \\
&\quad \left. \left. - \left( \frac{2(g_V^{v'})_{Z_H} (g_V^{e'})_{Z_H}}{c_W^2 M_{Z_H}^2} + \frac{2(g_V^{v'})_{A_H} (g_V^{e'})_{A_H}}{c_W^2 M_{A_H}^2} + \frac{g'^2}{M_{W_H}^2} \right) \gamma^5 \right) u(p_2) \right]^\dagger, \tag{4.23}
\end{aligned}$$

where using Casimir's trick yields

$$\begin{aligned}
&= \frac{g_w^4}{128} Tr \left[ \gamma^\mu (1 - \gamma^5) (\not{k}_1 - m_\nu) \gamma^\nu (1 - \gamma^5) (\not{p}_1 - m_\nu) \right] \\
&\quad \times Tr \left[ \gamma_\mu \left( \left( \frac{2(g_V^{v'})_{Z_H} (g_V^{e'})_{Z_H}}{c_W^2 M_{Z_H}^2} + \frac{2(g_V^{v'})_{A_H} (g_V^{e'})_{A_H}}{c_W^2 M_{A_H}^2} + \frac{g'^2}{M_{W_H}^2} \right) \right. \right. \\
&\quad \left. \left. - \left( \frac{2(g_V^{v'})_{Z_H} (g_V^{e'})_{Z_H}}{c_W^2 M_{Z_H}^2} + \frac{2(g_V^{v'})_{A_H} (g_V^{e'})_{A_H}}{c_W^2 M_{A_H}^2} + \frac{g'^2}{M_{W_H}^2} \right) \gamma^5 \right) (\not{p}_2 + m_e) \right] \\
&\quad \times Tr \left[ \gamma_\nu \left( \left( \frac{2(g_V^{v'})_{Z_H} (g_V^{e'})_{Z_H}}{c_W^2 M_{Z_H}^2} + \frac{2(g_V^{v'})_{A_H} (g_V^{e'})_{A_H}}{c_W^2 M_{A_H}^2} + \frac{g'^2}{M_{W_H}^2} \right) \right. \right. \\
&\quad \left. \left. - \left( \frac{2(g_V^{v'})_{Z_H} (g_V^{e'})_{Z_H}}{c_W^2 M_{Z_H}^2} + \frac{2(g_V^{v'})_{A_H} (g_V^{e'})_{A_H}}{c_W^2 M_{A_H}^2} + \frac{g'^2}{M_{W_H}^2} \right) \gamma^5 \right) (\not{k}_2 + m_e) \right], \tag{4.24}
\end{aligned}$$

and then evaluating the traces and plugging the necessary kinematic terms yield

$$\begin{aligned}
\langle |\mathcal{M}_t|^2 \rangle = & 2g_W^4 m_e^2 \left[ \left\{ \frac{\left( (g_V^{v'2})_{AH} \left( (g_V^{e'})_{AH} - (g_A^{e'})_{AH} \right)^2 \right)}{c_W^4 M_{AH}^4} \right\} E_\nu^2 \right. \\
& + \left\{ \frac{2 (g_V^{v'})_{ZH} (g_V^{e'})_{ZH}}{c_W^2 M_{ZH}^2} + \frac{(g_V^{v'})_{AH} \left( (g_V^{e'})_{AH} + (g_A^{e'})_{AH} \right)}{c_W^2 M_{AH}^2} \right. \\
& \left. \left. + \frac{g'^2}{M_{WH}^2} \right\} (E_\nu - T)^2 \right. \\
& - \left\{ \frac{2 (g_V^{v'})_{ZH} (g_V^{e'})_{ZH} (g_V^{v'})_{AH} \left( (g_V^{e'})_{AH} - (g_A^{e'})_{AH} \right)}{c_W^4 M_{ZH}^2 M_{AH}^2} \right. \\
& + \frac{\left( (g_V^{v'2})_{AH} \left( (g_V^{e'2})_{AH} - (g_A^{e'2})_{AH} \right)}{c_W^4 M_{AH}^4} \right. \\
& \left. \left. + \frac{g'^2 (g_V^{v'})_{AH} \left( (g_V^{e'})_{AH} - (g_A^{e'})_{AH} \right)}{c_W^2 M_{AH}^2 M_{WH}^2} \right\} m_e T \right]. \tag{4.25}
\end{aligned}$$

By plugging the corresponding values of the new coupling constants given in Table 4.1, taking into account the condition for anomaly cancellation, three new terms defined as

$$C_1 = -\frac{1}{2} \frac{c^2}{s^2} \left( \frac{M_W}{M_{ZH}} \right)^2, \tag{4.26}$$

$$C_2 = t_W^2 \frac{\left( -\frac{1}{5} + \frac{1}{2} c'^2 \right) \left( -\frac{2}{5} + c'^2 \right)}{(s' c')^2} \left( \frac{M_W}{M_{AH}} \right)^2, \tag{4.27}$$

$$C_3 = \frac{c^2}{s^2} \left( 1 + \frac{1}{2} \frac{v^2}{f^2} s^2 (c^2 - s^2) \right)^2 \left( \frac{M_W}{M_{WH}} \right)^2 \approx \frac{c^2}{s^2} \left( \frac{M_W}{M_{WH}} \right)^2, \tag{4.28}$$

pop out respectively from  $Z_H$ ,  $A_H$  and  $W_H$  in terms of which the spin-averaged amplitude in Equation 4.25 can be written as

$$\langle |\mathcal{M}_i|^2 \rangle = \frac{2g_W^4 m_e^2}{M_W^4} \left[ (2C_2)^2 E_\nu^2 + (C_1 + C_2 + C_3)^2 (E_\nu - T)^2 - 2C_2 (C_1 + C_2 + C_3) m_e T \right]. \quad (4.29)$$

Finally, inserting Equation 4.29 into the general form of the differential cross section found in Appendix A yields

$$\left[ \frac{d\sigma}{dT}(\bar{\nu}_e e) \right]_{Heavy\ LTHM}^{FC} = \frac{2G_F^2 m_e}{\pi} \left[ (2C_2)^2 + (C_1 + C_2 + C_3)^2 \left( 1 - \frac{T}{E_\nu} \right)^2 - 2C_2 (C_1 + C_2 + C_3) \frac{m_e T}{E_\nu^2} \right]. \quad (4.30)$$

#### 4.1.1.2 $\bar{\nu}_e + e \rightarrow \bar{\nu}_{\alpha \neq e} + e$ (FV)

Mediated by the SM light gauge bosons, there is only one possible tree-level Feynman diagram which contributes to the FV process of  $\bar{\nu}_e e$  elastic scattering.

It is mediated by  $Z^0$  through a neutral weak process and is manifested by the Feynman diagram in Figure 4.3 with the corresponding amplitude given by

$$\mathcal{M}_i = \frac{2G_F}{\sqrt{2}} g_V^{V'} \left[ \bar{\nu}(p_1) \gamma^\mu (1 - \gamma^5) \nu(k_1) \right] \left[ \bar{u}(k_2) \gamma_\mu (g_V^{e'} - g_A^{e'} \gamma^5) u(p_2) \right], \quad (4.31)$$

and then together with its hermitian conjugate  $\mathcal{M}_i^\dagger$ , the spin-averaged amplitude square

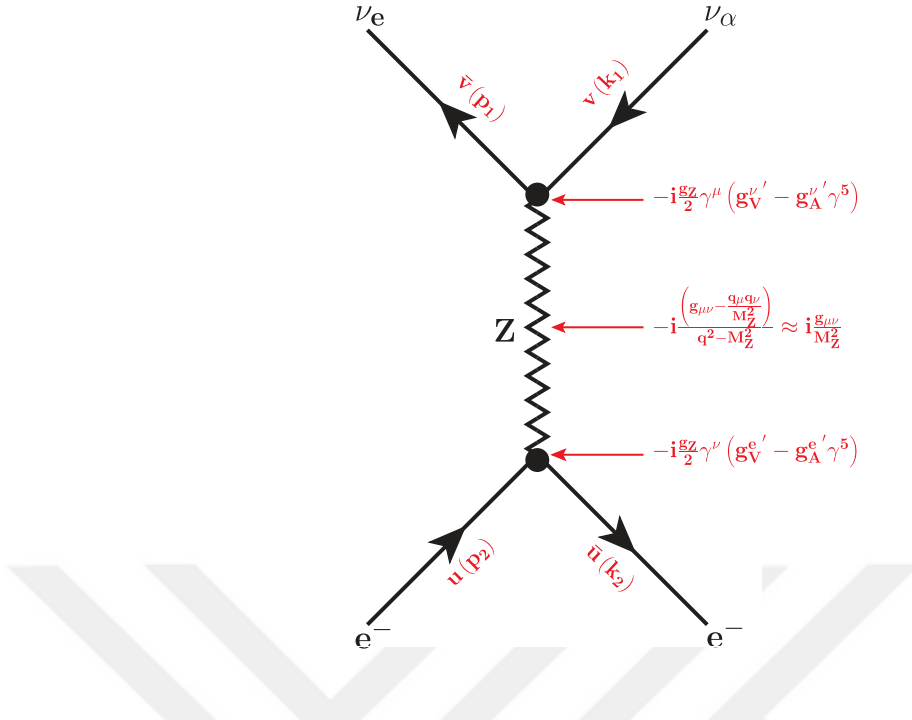


Figure 4.3 Feynman diagram of antineutrino-electron FV scattering via the exchange of a Z boson (NC) in the  $SU(5)$  LTHM with the relevant vertex and propagator factors are also shown

is

$$\begin{aligned}
\langle |\mathcal{M}_t|^2 \rangle &= \frac{1}{2} \sum_{\text{spins}} |\mathcal{M}_t|^2 \\
&= G_F^2 g_V^{\nu^2} \sum_{\text{spins}} \left[ \bar{\nu}(p_1) \gamma^\mu (1 - \gamma^5) \nu(k_1) \right] \left[ \bar{\nu}(p_1) \gamma^\nu (1 - \gamma^5) \nu(k_1) \right]^\dagger \\
&\quad \times \sum_{\text{spins}} \left[ \bar{u}(k_2) \gamma_\mu (g_V^e - g_A^e \gamma^5) u(p_2) \right] \left[ \bar{u}(k_2) \gamma_\nu (g_V^e - g_A^e \gamma^5) u(p_2) \right]^\dagger,
\end{aligned} \tag{4.32}$$

where using Casimir's trick yields

$$\begin{aligned}
&= G_F^2 g_V^{\nu^2} \text{Tr} \left[ \gamma^\mu (1 - \gamma^5) (\not{k}_1 - m_\nu) \gamma^\nu (1 - \gamma^5) (\not{p}_1 - m_\nu) \right] \\
&\quad \times \text{Tr} \left[ \gamma_\mu (g_V^e - g_A^e \gamma^5) (\not{p}_2 + m_e) \gamma_\nu (g_V^e - g_A^e \gamma^5) (\not{k}_2 + m_e) \right],
\end{aligned} \tag{4.33}$$

and then evaluating the traces and plugging the corresponding kinematic terms therein

yield

$$\begin{aligned} \langle |\mathcal{M}_t|^2 \rangle &= 64G_F^2 g_V^{e'2} m_e^2 \left[ (g_V^{e'} - g_A^{e'})^2 E_V^2 + (g_V^{e'} + g_A^{e'})^2 (E_V - T)^2 \right. \\ &\quad \left. - (g_V^{e'} - g_A^{e'}) m_e T \right]. \end{aligned} \quad (4.34)$$

In terms of  $B$ ,  $\delta g_L$ , and  $\delta g_R$ , the spin-averaged amplitude in Equation 4.34 can be written as

$$\begin{aligned} \langle |\mathcal{M}_t|^2 \rangle &= 64G_F^2 m_e^2 \left[ (1+B)^2 (g_R + \delta g_R)^2 E_V^2 + (1+B)^2 (g_L + \delta g_L)^2 (E_V - T)^2 \right. \\ &\quad \left. - (1+B)^2 (g_R + \delta g_R) (g_L + \delta g_L) m_e T \right]. \end{aligned} \quad (4.35)$$

The differential scattering cross section can be finally found as

$$\begin{aligned} \left[ \frac{d\sigma}{dT}(\bar{\nu}_e e) \right]_{Light\ LTHM}^{FV} &= \frac{2G_F^2 m_e}{\pi} \left[ (1+B)^2 (g_R + \delta g_R)^2 \right. \\ &\quad \left. + (1+B)^2 (g_L + \delta g_L)^2 \left( 1 - \frac{T}{E_V} \right)^2 \right. \\ &\quad \left. - (1+B)^2 (g_R + \delta g_R) (g_L + \delta g_L) \frac{m_e T}{E_V^2} \right]. \end{aligned} \quad (4.36)$$

Mediated by the  $SU(5)$  LTHM new predicted heavy gauge bosons, however, there are two possible tree-level Feynman diagrams for the FV process of  $\bar{\nu}_e e$  elastic scattering.

- One is mediated by  $Z_H^0$  through a neutral weak process and is manifested by the Feynman diagram in Figure 4.4 (a) with the corresponding amplitude given by

$$\mathcal{M}_{ZH} = \frac{g_w^2}{4c_W^2 M_{Z_H}^2} g_V^{e'} g_V^{e'} \left[ \bar{\nu}(p_1) \gamma^\mu (1 - \gamma^5) \nu(k_1) \right] \left[ \bar{u}(k_2) \gamma_\mu (1 - \gamma^5) u(p_2) \right]. \quad (4.37)$$

- The other is mediated by  $A_H^0$  through a neutral weak process and is manifested by

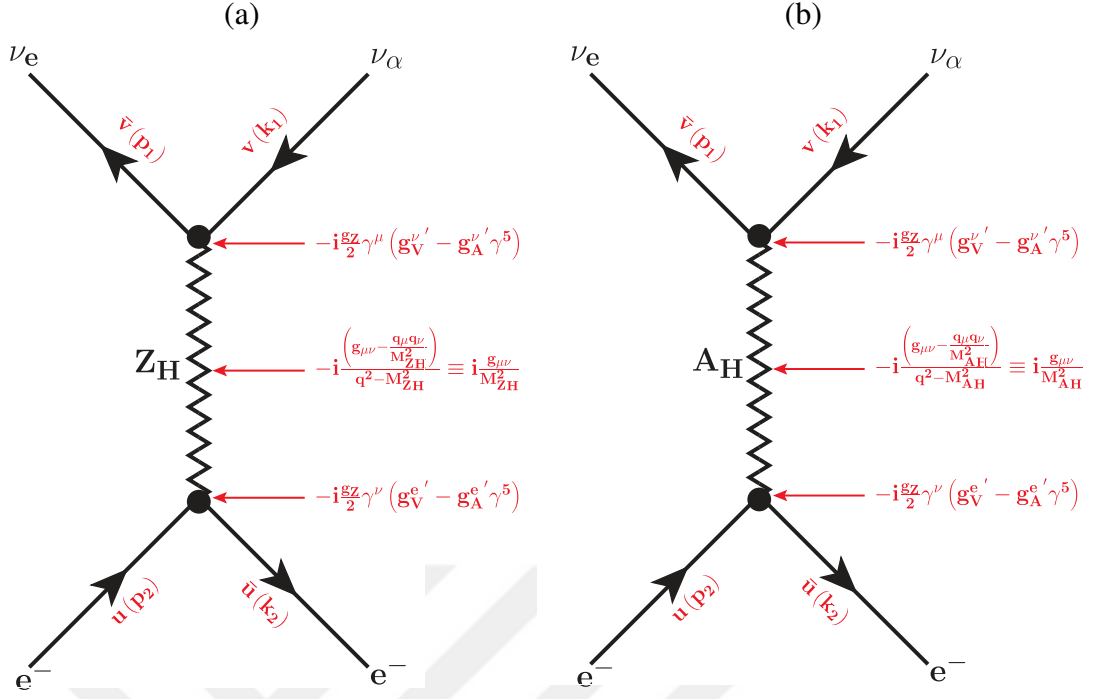


Figure 4.4 Feynman diagrams of antineutrino-electron FV scattering via the exchange of (a)  $Z_H$  and (b)  $A_H$  bosons in the  $SU(5)$  LTHM where the necessary vertex and propagator factors have been also given

the Feynman diagram in Figure 4.4 (b) with the corresponding amplitude given by

$$\mathcal{M}_{A_H} = \frac{g_w^2}{4c_W^2 M_{A_H}^2} g_V^{\nu'} \left[ \bar{\nu}(p_1) \gamma^\mu (1 - \gamma^5) \nu(k_1) \right] \left[ \bar{u}(k_2) \gamma_\mu (g_V^{e'} - g_A^{e'} \gamma^5) u(p_2) \right]. \quad (4.38)$$

Summing both amplitudes, the total amplitude simply becomes

$$\mathcal{M}_t = \frac{g_w^2}{8} \left[ \bar{\nu}(p_1) \gamma^\mu (1 - \gamma^5) \nu(k_1) \right] \left[ \bar{u}(k_2) \gamma_\mu \left( \left( \frac{2(g_V^{\nu'})_{Z_H} (g_V^{e'})_{Z_H}}{c_W^2 M_{Z_H}^2} + \frac{2(g_V^{\nu'})_{A_H} (g_V^{e'})_{A_H}}{c_W^2 M_{A_H}^2} \right) - \left( \frac{2(g_V^{\nu'})_{Z_H} (g_V^{e'})_{Z_H}}{c_W^2 M_{Z_H}^2} + \frac{2(g_V^{\nu'})_{A_H} (g_A^{e'})_{A_H}}{c_W^2 M_{A_H}^2} \right) \gamma^5 \right) u(p_2) \right], \quad (4.39)$$

and then together with its hermitian conjugate  $\mathcal{M}_t^\dagger$ , the spin-averaged amplitude square is

$$\begin{aligned}
\langle |\mathcal{M}_t|^2 \rangle &= \frac{1}{2} \sum_{\text{spins}} |\mathcal{M}_t|^2 \\
&= \frac{g_w^4}{128} \sum_{\text{spins}} \left[ \bar{v}(p_1) \gamma^\mu (1 - \gamma^5) v(k_1) \right] \left[ \bar{v}(p_1) \gamma^\nu (1 - \gamma^5) v(k_1) \right]^\dagger \\
&\quad \times \sum_{\text{spins}} \left[ \bar{u}(k_2) \gamma_\mu \left( \left( \frac{2(g_V^{v'})_{Z_H} (g_V^{e'})_{Z_H}}{c_W^2 M_{Z_H}^2} + \frac{2(g_V^{v'})_{A_H} (g_V^{e'})_{A_H}}{c_W^2 M_{A_H}^2} \right) \right. \right. \\
&\quad \left. \left. - \left( \frac{2(g_V^{v'})_{Z_H} (g_V^{e'})_{Z_H}}{c_W^2 M_{Z_H}^2} + \frac{2(g_V^{v'})_{A_H} (g_V^{e'})_{A_H}}{c_W^2 M_{A_H}^2} \right) \gamma^5 \right) u(p_2) \right] \\
&\quad \times \left[ \bar{u}(k_2) \gamma_\nu \left( \left( \frac{2(g_V^{v'})_{Z_H} (g_V^{e'})_{Z_H}}{c_W^2 M_{Z_H}^2} + \frac{2(g_V^{v'})_{A_H} (g_V^{e'})_{A_H}}{c_W^2 M_{A_H}^2} \right) \right. \right. \\
&\quad \left. \left. - \left( \frac{2(g_V^{v'})_{Z_H} (g_V^{e'})_{Z_H}}{c_W^2 M_{Z_H}^2} + \frac{2(g_V^{v'})_{A_H} (g_V^{e'})_{A_H}}{c_W^2 M_{A_H}^2} \right) \gamma^5 \right) u(p_2) \right]^\dagger, \tag{4.40}
\end{aligned}$$

where using Casimir's trick yields

$$\begin{aligned}
&= \frac{g_w^4}{128} \text{Tr} \left[ \gamma^\mu (1 - \gamma^5) (k_1 - m_\nu) \gamma^\nu (1 - \gamma^5) (p_1 - m_\nu) \right] \\
&\quad \times \text{Tr} \left[ \gamma_\mu \left( \left( \frac{2(g_V^{v'})_{Z_H} (g_V^{e'})_{Z_H}}{c_W^2 M_{Z_H}^2} + \frac{2(g_V^{v'})_{A_H} (g_V^{e'})_{A_H}}{c_W^2 M_{A_H}^2} \right) \right. \right. \\
&\quad \left. \left. - \left( \frac{2(g_V^{v'})_{Z_H} (g_V^{e'})_{Z_H}}{c_W^2 M_{Z_H}^2} + \frac{2(g_V^{v'})_{A_H} (g_V^{e'})_{A_H}}{c_W^2 M_{A_H}^2} \right) \gamma^5 \right) (p_2 + m_e) \right] \\
&\quad \times \gamma_\nu \left( \left( \frac{2(g_V^{v'})_{Z_H} (g_V^{e'})_{Z_H}}{c_W^2 M_{Z_H}^2} + \frac{2(g_V^{v'})_{A_H} (g_V^{e'})_{A_H}}{c_W^2 M_{A_H}^2} \right) \right. \\
&\quad \left. - \left( \frac{2(g_V^{v'})_{Z_H} (g_V^{e'})_{Z_H}}{c_W^2 M_{Z_H}^2} + \frac{2(g_V^{v'})_{A_H} (g_V^{e'})_{A_H}}{c_W^2 M_{A_H}^2} \right) \gamma^5 \right) (k_2 + m_e) \right], \tag{4.41}
\end{aligned}$$

and then evaluating the traces and plugging the kinematic terms yield

$$\begin{aligned}
\langle |\mathcal{M}_t|^2 \rangle = & 2g_W^4 m_e^2 \left[ \left\{ \frac{\left( g_V^{v'2} \right)_{AH} \left( \left( g_V^{e'} \right)_{AH} - \left( g_A^{e'} \right)_{AH} \right)^2}{c_W^4 M_{AH}^4} \right\} E_\nu^2 \right. \\
& + \left. \left\{ \frac{2 \left( g_V^{v'} \right)_{ZH} \left( g_V^{e'} \right)_{ZH} + \left( g_V^{v'} \right)_{AH} \left( \left( g_V^{e'} \right)_{AH} + \left( g_A^{e'} \right)_{AH} \right)}{c_W^2 M_{ZH}^2} + \frac{\left( g_V^{v'} \right)_{AH} \left( \left( g_V^{e'} \right)_{AH} + \left( g_A^{e'} \right)_{AH} \right)}{c_W^2 M_{AH}^2} \right\}^2 \right. \\
& \times (E_\nu - T)^2 - \left. \left\{ \frac{2 \left( g_V^{v'} \right)_{ZH} \left( g_V^{e'} \right)_{ZH} \left( g_V^{v'} \right)_{AH} \left( \left( g_V^{e'} \right)_{AH} - \left( g_A^{e'} \right)_{AH} \right)}{c_W^4 M_{ZH}^2 M_{AH}^2} \right. \right. \\
& \left. \left. + \frac{\left( g_V^{v'2} \right)_{AH} \left( \left( g_V^{e'2} \right)_{AH} - \left( g_A^{e'2} \right)_{AH} \right)}{c_W^4 M_{AH}^4} \right\} m_e T \right], \tag{4.42}
\end{aligned}$$

or in terms of  $C_1$ ,  $C_2$  and  $C_3$

$$\begin{aligned}
\langle |\mathcal{M}_t|^2 \rangle = & \frac{2g_W^4 m_e^2}{M_W^4} \left[ (2C_2)^2 E_\nu^2 + (C_1 + C_2)^2 (E_\nu - T)^2 \right. \\
& \left. - 2C_2 (C_1 + C_2) m_e T \right]. \tag{4.43}
\end{aligned}$$

Substituting the above equation into the differential cross section found in Appendix A gives

$$\begin{aligned}
\left[ \frac{d\sigma}{dT}(\bar{\nu}_e e) \right]_{Heavy\ LTHM}^{FV} = & \frac{2G_F^2 m_e}{\pi} \left[ (2C_2)^2 + (C_1 + C_2)^2 \left( 1 - \frac{T}{E_\nu} \right)^2 \right. \\
& \left. - 2C_2 (C_1 + C_2) \frac{m_e T}{E_\nu} \right]. \tag{4.44}
\end{aligned}$$

## 4.1.2 Neutrino-Electron Scattering

### 4.1.2.1 $\nu_e + e \rightarrow \nu_e + e$ (FC)

Mediated by the SM light gauge bosons, there are two possible tree-level Feynman diagrams that contribute to the FC process of  $\nu_e e$  elastic scattering.

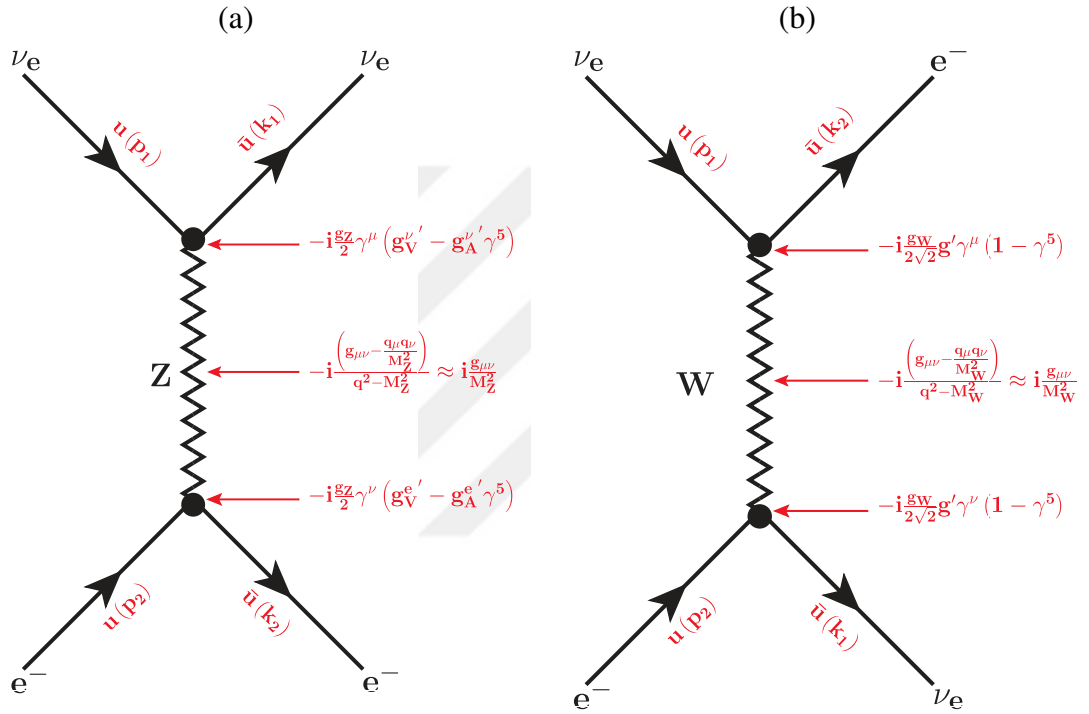


Figure 4.5 Feynman diagrams of (a) Z-mediated and (b) W-mediated FC scattering of neutrino with electron in the  $SU(5)$  LTHM with the appropriate vertex and propagator factors are also shown

- One is mediated by  $Z^0$  through a neutral weak process and is manifested by the Feynman diagram in Figure 4.5 (a) with the corresponding amplitude given by

$$\mathcal{M}_Z = \frac{2G_F}{\sqrt{2}}g_V^{\nu'} \left[ \bar{u}(k_1)\gamma^\mu (1 - \gamma^5) u(p_1) \right] \left[ \bar{u}(k_2)\gamma_\mu (g_V^{e'} - g_A^{e'}\gamma^5) u(p_2) \right]. \quad (4.45)$$

- Another is mediated by  $W^\pm$  through a charged weak process and is manifested by the Feynman diagram in Figure 4.5 (b) with the corresponding amplitude

given using Fierz transformation by

$$\mathcal{M}_W = \frac{G_F}{\sqrt{2}} g'^2 \left[ \bar{u}(k_1) \gamma^\mu (1 - \gamma^5) u(p_1) \right] \left[ \bar{u}(k_2) \gamma_\mu (1 - \gamma^5) u(p_2) \right]. \quad (4.46)$$

Then the total amplitude can be simply written as

$$\begin{aligned} \mathcal{M}_t &= \mathcal{M}_Z + \mathcal{M}_W \\ &= \frac{G_F}{\sqrt{2}} \left[ \bar{u}(k_1) \gamma^\mu (1 - \gamma^5) u(p_1) \right] \\ &\quad \times \left[ \bar{u}(k_2) \gamma_\mu \left\{ \left( 2g_V^{v'} g_V^{e'} + g'^2 \right) - \left( 2g_V^{v'} g_A^{e'} + g'^2 \right) \gamma^5 \right\} u(p_2) \right], \end{aligned} \quad (4.47)$$

and together with its hermitian conjugate  $\mathcal{M}_t^\dagger$ , the spin-averaged amplitude square is

$$\begin{aligned} \langle |\mathcal{M}_t|^2 \rangle &= \frac{1}{2} \sum_{\text{spins}} |\mathcal{M}_t|^2 \\ &= \frac{G_F^2}{4} \sum_{\text{spins}} \left[ \bar{u}(k_1) \gamma^\mu (1 - \gamma^5) u(p_1) \right] \left[ \bar{u}(k_1) \gamma^\nu (1 - \gamma^5) u(p_1) \right]^\dagger \\ &\quad \times \sum_{\text{spins}} \left[ \bar{u}(k_2) \gamma_\mu \left\{ \left( 2g_V^{v'} g_V^{e'} + g'^2 \right) - \left( 2g_V^{v'} g_A^{e'} + g'^2 \right) \gamma^5 \right\} u(p_2) \right] \\ &\quad \times \left[ \bar{u}(k_2) \gamma_\nu \left\{ \left( 2g_V^{v'} g_V^{e'} + g'^2 \right) - \left( 2g_V^{v'} g_A^{e'} + g'^2 \right) \gamma^5 \right\} u(p_2) \right]^\dagger, \end{aligned} \quad (4.48)$$

where using Casimir's trick yields

$$\begin{aligned} &= \frac{G_F^2}{4} Tr \left[ \gamma^\mu (1 - \gamma^5) (\not{p}_1 + m_\nu) \gamma^\nu (1 - \gamma^5) (\not{k}_1 + m_\nu) \right] \\ &\quad \times Tr \left[ \gamma_\mu \left\{ \left( 2g_V^{v'} g_V^{e'} + g'^2 \right) - \left( 2g_V^{v'} g_A^{e'} + g'^2 \right) \gamma^5 \right\} (\not{p}_2 + m_e) \right] \\ &\quad \times Tr \left[ \gamma_\nu \left\{ \left( 2g_V^{v'} g_V^{e'} + g'^2 \right) - \left( 2g_V^{v'} g_A^{e'} + g'^2 \right) \gamma^5 \right\} (\not{k}_2 + m_e) \right]. \end{aligned} \quad (4.49)$$

By evaluating the corresponding traces and plugging their results back, the previous equation becomes

$$\begin{aligned} \langle |\mathcal{M}_t|^2 \rangle = & 64G_F^2 m_e^2 \left[ \left( g_V^{v'} \left( g_V^{e'} + g_A^{e'} \right) + g'^2 \right)^2 E_v^2 + g_V^{v'2} \left( g_V^{e'} - g_A^{e'} \right)^2 (E_v - T)^2 \right. \\ & \left. - g_V^{v'} \left( g_V^{e'} - g_A^{e'} \right) \left( g_V^{v'} \left( g_V^{e'} + g_A^{e'} \right) + g'^2 \right) m_e T \right], \end{aligned} \quad (4.50)$$

with the corresponding kinematic terms directly plugged.

In terms of  $B$ ,  $\delta g_L$ ,  $\delta g_R$ , and  $\delta g'_L$ , the spin-averaged amplitude above can be expressed as

$$\begin{aligned} \langle |\mathcal{M}_t|^2 \rangle = & 64G_F^2 m_e^2 \left[ \left\{ (1+B)(g_L + \delta g_L) + (1 + \delta g'_L)^2 \right\}^2 E_v^2 \right. \\ & + (1+B)^2 (g_R + \delta g_R)^2 (E_v - T)^2 \\ & \left. - (1+B)(g_R + \delta g_R) \left\{ (1+B)(g_L + \delta g_L) + (1 + \delta g'_L)^2 \right\} m_e T \right], \end{aligned} \quad (4.51)$$

and finally substituting this into the differential cross section found in Appendix A gives

$$\begin{aligned} \left[ \frac{d\sigma}{dT}(\nu_e e) \right]_{Light\ LTHM}^{FC} = & \frac{2G_F^2 m_e}{\pi} \left[ \left\{ (1+B)(g_L + \delta g_L) + (1 + \delta g'_L)^2 \right\}^2 \right. \\ & + (1+B)^2 (g_R + \delta g_R)^2 \left( 1 - \frac{T}{E_v} \right)^2 \\ & - (1+B)(g_R + \delta g_R) \left\{ (1+B)(g_L + \delta g_L) \right. \\ & \left. \left. + (1 + \delta g'_L)^2 \right\} \frac{m_e T}{E_v^2} \right]. \end{aligned} \quad (4.52)$$

Additionally, there are three possible tree-level Feynman diagrams for the FC process of  $\nu_e e$  elastic scattering mediated by the  $SU(5)$  LTHM new predicted heavy gauge bosons.

- One is mediated by  $Z_H^0$  through a neutral weak process and is manifested by the

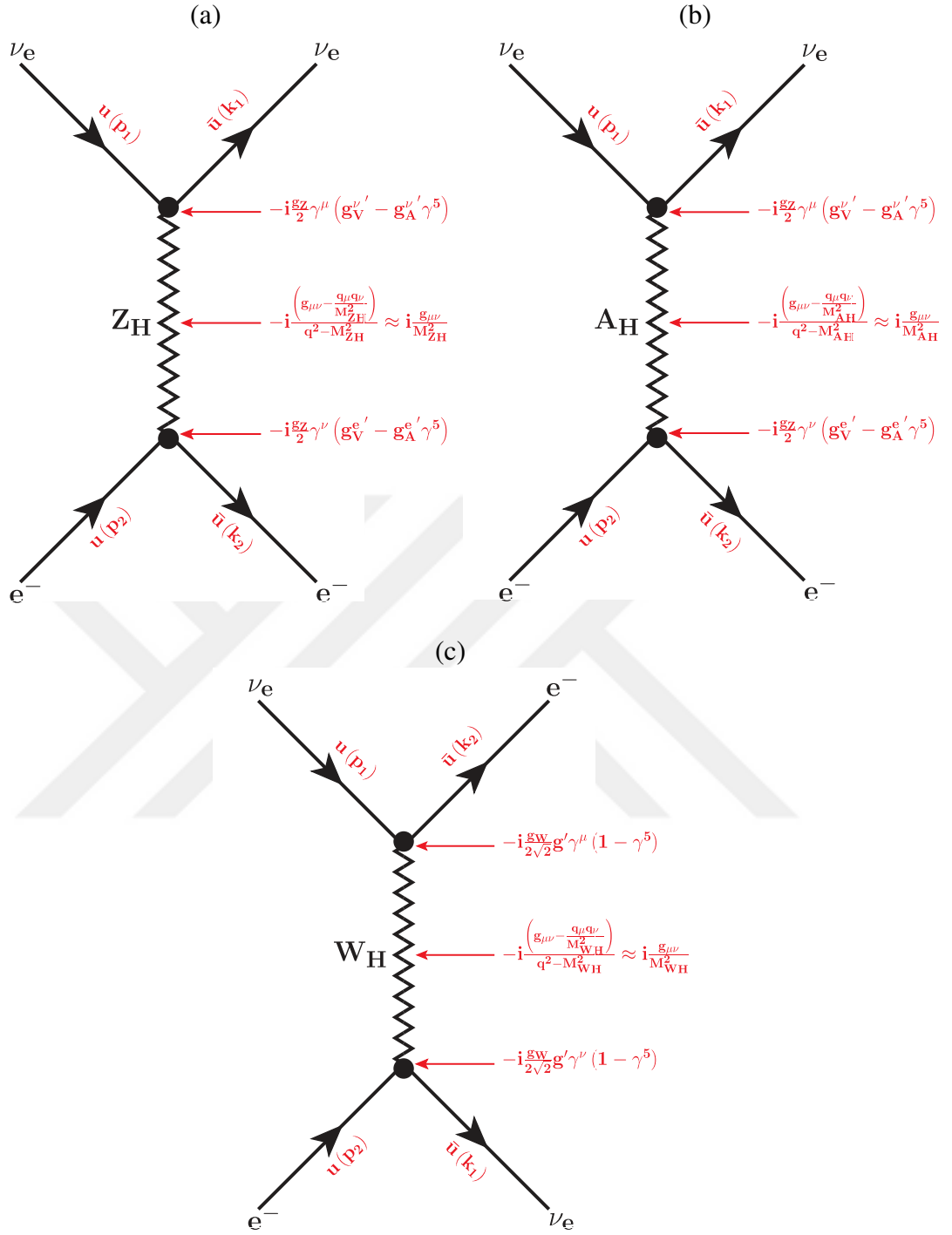


Figure 4.6 Feynman diagrams of the FC neutrino-electron scattering process transmitted by (a)  $Z_H$ , (b)  $A_H$  and (c)  $W_H$  bosons of the  $SU(5)$  LTHM in addition to the suitable vertex and propagator factors

Feynman diagram in Figure 4.6 (a) with the corresponding amplitude given by

$$\mathcal{M}_{ZH} = \frac{g_w^2}{4c_w^2 M_{ZH}^2} g_V^{\nu'} g_V^{e'} \left[ \bar{u}(k_1) \gamma^\mu (1 - \gamma^5) u(p_1) \right] \left[ \bar{u}(k_2) \gamma_\mu (1 - \gamma^5) u(p_2) \right]. \quad (4.53)$$

- Another is mediated by  $A_H^0$  through a neutral weak process and is manifested by the Feynman diagram in Figure 4.6 (b) with the corresponding amplitude given by

$$\mathcal{M}_{AH} = \frac{g_w^2}{4c_W^2 M_{AH}^2} g_V^{v'} \left[ \bar{u}(k_1) \gamma^\mu (1 - \gamma^5) u(p_1) \right] \left[ \bar{u}(k_2) \gamma_\mu (g_V^{e'} - g_A^{e'} \gamma^5) u(p_2) \right]. \quad (4.54)$$

- One another is mediated by  $W_H^\pm$  through a charged weak process and is manifested by the Feynman diagram in Figure 4.6 (c) with the corresponding amplitude given after Fierz reordering by

$$\mathcal{M}_{WH} = \frac{g_w^2}{8M_{WH}^2} g'^2 \left[ \bar{u}(k_1) \gamma^\mu (1 - \gamma^5) u(p_1) \right] \left[ \bar{u}(k_2) \gamma_\mu (1 - \gamma^5) u(p_2) \right]. \quad (4.55)$$

Then the total amplitude can be simply written as

$$\begin{aligned} \mathcal{M}_t &= \mathcal{M}_{ZH} + \mathcal{M}_{AH} + \mathcal{M}_{WH} \\ &= \frac{g_w^2}{8} \left[ \bar{u}(k_1) \gamma^\mu (1 - \gamma^5) u(p_1) \right] \left[ \bar{u}(k_2) \gamma_\mu \left( \left( \frac{2(g_V^{v'})_{ZH} (g_V^{e'})_{ZH}}{c_W^2 M_{ZH}^2} \right. \right. \right. \\ &\quad \left. \left. \left. + \frac{2(g_V^{v'})_{AH} (g_V^{e'})_{AH}}{c_W^2 M_{AH}^2} + \frac{g'^2}{M_{WH}^2} \right) - \left( \frac{2(g_V^{v'})_{ZH} (g_V^{e'})_{ZH}}{c_W^2 M_{ZH}^2} \right. \right. \right. \\ &\quad \left. \left. \left. + \frac{2(g_V^{v'})_{AH} (g_A^{e'})_{AH}}{c_W^2 M_{AH}^2} + \frac{g'^2}{M_{WH}^2} \right) \gamma^5 \right) u(p_2) \right], \end{aligned} \quad (4.56)$$

and together with its hermitian conjugate  $\mathcal{M}_t^\dagger$ , the spin-averaged amplitude square is

$$\begin{aligned}
\langle |\mathcal{M}_t|^2 \rangle &= \frac{1}{2} \sum_{\text{spins}} |\mathcal{M}_t|^2 \\
&= \frac{g_w^4}{128} \sum_{\text{spins}} \left[ \bar{u}(k_1) \gamma^\mu (1 - \gamma^5) u(p_1) \right] \left[ \bar{u}(k_1) \gamma^\nu (1 - \gamma^5) u(p_1) \right]^\dagger \\
&\quad \times \sum_{\text{spins}} \left[ \bar{u}(k_2) \gamma_\mu \left( \left( \frac{2(g_V^{v'})_{Z_H} (g_V^{e'})_{Z_H}}{c_W^2 M_{Z_H}^2} + \frac{2(g_V^{v'})_{A_H} (g_V^{e'})_{A_H}}{c_W^2 M_{A_H}^2} + \frac{g'^2}{M_{W_H}^2} \right) \right. \right. \\
&\quad \left. \left. - \left( \frac{2(g_V^{v'})_{Z_H} (g_V^{e'})_{Z_H}}{c_W^2 M_{Z_H}^2} + \frac{2(g_V^{v'})_{A_H} (g_A^{e'})_{A_H}}{c_W^2 M_{A_H}^2} + \frac{g'^2}{M_{W_H}^2} \right) \gamma^5 \right) u(p_2) \right] \\
&\quad \times \left[ \bar{u}(k_2) \gamma_\nu \left( \left( \frac{2(g_V^{v'})_{Z_H} (g_V^{e'})_{Z_H}}{c_W^2 M_{Z_H}^2} + \frac{2(g_V^{v'})_{A_H} (g_V^{e'})_{A_H}}{c_W^2 M_{A_H}^2} + \frac{g'^2}{M_{W_H}^2} \right) \right. \right. \\
&\quad \left. \left. - \left( \frac{2(g_V^{v'})_{Z_H} (g_V^{e'})_{Z_H}}{c_W^2 M_{Z_H}^2} + \frac{2(g_V^{v'})_{A_H} (g_A^{e'})_{A_H}}{c_W^2 M_{A_H}^2} + \frac{g'^2}{M_{W_H}^2} \right) \gamma^5 \right) u(p_2) \right]^\dagger, \tag{4.57}
\end{aligned}$$

where using Casimir's trick yields

$$\begin{aligned}
&= \frac{g_w^4}{128} \text{Tr} \left[ \gamma^\mu (1 - \gamma^5) (\not{p}_1 + m_\nu) \gamma^\nu (1 - \gamma^5) (\not{k}_1 + m_\nu) \right] \\
&\quad \times \text{Tr} \left[ \gamma_\mu \left( \left( \frac{2(g_V^{v'})_{Z_H} (g_V^{e'})_{Z_H}}{c_W^2 M_{Z_H}^2} + \frac{2(g_V^{v'})_{A_H} (g_V^{e'})_{A_H}}{c_W^2 M_{A_H}^2} + \frac{g'^2}{M_{W_H}^2} \right) \right. \right. \\
&\quad \left. \left. - \left( \frac{2(g_V^{v'})_{Z_H} (g_V^{e'})_{Z_H}}{c_W^2 M_{Z_H}^2} + \frac{2(g_V^{v'})_{A_H} (g_A^{e'})_{A_H}}{c_W^2 M_{A_H}^2} + \frac{g'^2}{M_{W_H}^2} \right) \gamma^5 \right) (\not{p}_2 + m_e) \right] \\
&\quad \times \gamma_\nu \left( \left( \frac{2(g_V^{v'})_{Z_H} (g_V^{e'})_{Z_H}}{c_W^2 M_{Z_H}^2} + \frac{2(g_V^{v'})_{A_H} (g_V^{e'})_{A_H}}{c_W^2 M_{A_H}^2} + \frac{g'^2}{M_{W_H}^2} \right) \right. \\
&\quad \left. - \left( \frac{2(g_V^{v'})_{Z_H} (g_V^{e'})_{Z_H}}{c_W^2 M_{Z_H}^2} + \frac{2(g_V^{v'})_{A_H} (g_A^{e'})_{A_H}}{c_W^2 M_{A_H}^2} + \frac{g'^2}{M_{W_H}^2} \right) \gamma^5 \right) (\not{k}_2 + m_e) \Big] \tag{4.58}
\end{aligned}$$

$$\begin{aligned}
&= 2g_W^4 m_e^2 \left[ \left\{ \frac{\left( g_V^{v'2} \right)_{A_H} \left( \left( g_V^{e'} \right)_{A_H} - \left( g_A^{e'} \right)_{A_H} \right)^2}{c_W^4 M_{A_H}^4} \right\} (E_\nu - T)^2 \right. \\
&\quad + \left\{ \frac{2 \left( g_V^{v'} \right)_{Z_H} \left( g_V^{e'} \right)_{Z_H} + \left( g_V^{v'} \right)_{A_H} \left( \left( g_V^{e'} \right)_{A_H} + \left( g_A^{e'} \right)_{A_H} \right)}{c_W^2 M_{Z_H}^2} + \frac{g'^2}{M_{W_H}^2} \right\} E_\nu^2 \\
&\quad - \left\{ \frac{2 \left( g_V^{v'} \right)_{Z_H} \left( g_V^{e'} \right)_{Z_H} \left( g_V^{v'} \right)_{A_H} \left( \left( g_V^{e'} \right)_{A_H} - \left( g_A^{e'} \right)_{A_H} \right)}{c_W^4 M_{Z_H}^2 M_{A_H}^2} \right. \\
&\quad + \frac{\left( g_V^{v'2} \right)_{A_H} \left( \left( g_V^{e'2} \right)_{A_H} - \left( g_A^{e'2} \right)_{A_H} \right)}{c_W^4 M_{A_H}^4} \\
&\quad \left. + \frac{g'^2 \left( g_V^{v'} \right)_{A_H} \left( \left( g_V^{e'} \right)_{A_H} - \left( g_A^{e'} \right)_{A_H} \right)}{c_W^2 M_{A_H}^2 M_{W_H}^2} \right\} m_e T \Big], \tag{4.59}
\end{aligned}$$

where in the last step the corresponding traces with the necessary kinematics have been plugged.

Again by substituting the values of the new coupling constants given in Table 4.1, the spin-averaged amplitude in Equation 4.59 can be written in terms of  $C_1$ ,  $C_2$  and  $C_3$  as

$$\begin{aligned}
\langle |\mathcal{M}_t|^2 \rangle &= \frac{2g_W^4 m_e^2}{M_W^4} \left[ (C_1 + C_2 + C_3)^2 E_\nu^2 + (2C_2)^2 (E_\nu - T)^2 \right. \\
&\quad \left. - 2C_2 (C_1 + C_2 + C_3) m_e T \right]. \tag{4.60}
\end{aligned}$$

With this amplitude, the differential scattering cross section is

$$\begin{aligned}
\left[ \frac{d\sigma}{dT} (v_e e) \right]_{Heavy\ LTHM}^{FC} &= \frac{2G_F^2 m_e}{\pi} \left[ (C_1 + C_2 + C_3)^2 + (2C_2)^2 \left( 1 - \frac{T}{E_\nu} \right)^2 \right. \\
&\quad \left. - 2C_2 (C_1 + C_2 + C_3) \frac{m_e T}{E_\nu^2} \right]. \tag{4.61}
\end{aligned}$$

#### 4.1.2.2 $\nu_e + e \rightarrow \nu_{\alpha \neq e} + e$ (FV)

Mediated by the SM light gauge bosons, there is only one possible tree-level Feynman diagram for the FV process of  $\nu_e e$  elastic scattering.

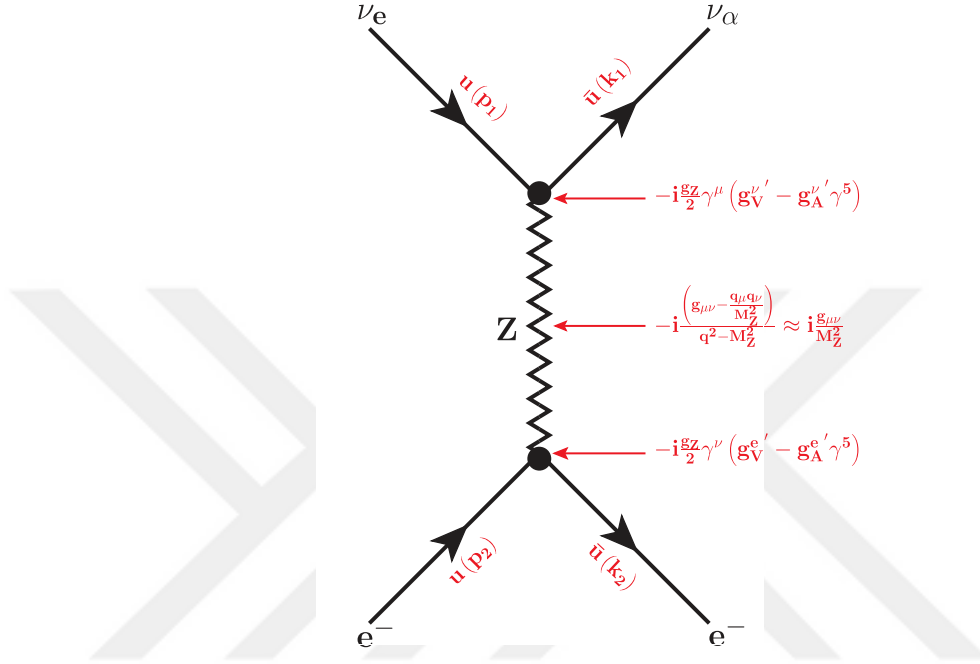


Figure 4.7 Feynman diagram of  $Z$ -mediated neutrino-electron FV scattering in the  $SU(5)$  LTHM

It is mediated by  $Z^0$  through a neutral weak process and is manifested by the Feynman diagram in Figure 4.7 with the corresponding amplitude given by

$$\mathcal{M}_i = \frac{2G_F}{\sqrt{2}} g_V^{\nu'} \left[ \bar{u}(k_1) \gamma^\mu (1 - \gamma^5) u(p_1) \right] \left[ \bar{u}(k_2) \gamma_\mu (g_V^{e'} - g_A^{e'} \gamma^5) u(p_2) \right], \quad (4.62)$$

and together with its hermitian conjugate  $\mathcal{M}_i^\dagger$ , the spin-averaged amplitude square is

$$\begin{aligned} \langle |\mathcal{M}_i|^2 \rangle &= \frac{1}{2} \sum_{\text{spins}} |\mathcal{M}_i|^2 \\ &= G_F^2 g_V^{\nu'^2} \sum_{\text{spins}} \left[ \bar{u}(k_1) \gamma^\mu (1 - \gamma^5) u(p_1) \right] \left[ \bar{u}(k_1) \gamma^\nu (1 - \gamma^5) u(p_1) \right]^\dagger \\ &\quad \times \sum_{\text{spins}} \left[ \bar{u}(k_2) \gamma_\mu (g_V^{e'} - g_A^{e'} \gamma^5) u(p_2) \right] \left[ \bar{u}(k_2) \gamma_\nu (g_V^{e'} - g_A^{e'} \gamma^5) u(p_2) \right]^\dagger, \end{aligned} \quad (4.63)$$

where using Casimir's trick yields

$$\begin{aligned}
&= G_F^2 g_V^{v'2} \text{Tr} \left[ \gamma^\mu (1 - \gamma^5) (\not{p}_1 + m_\nu) \gamma^\nu (1 - \gamma^5) (\not{k}_1 + m_\nu) \right] \\
&\quad \times \text{Tr} \left[ \gamma_\mu (g_V^{e'} - g_A^{e'} \gamma^5) (\not{p}_2 + m_e) \gamma_\nu (g_V^{e'} - g_A^{e'} \gamma^5) (\not{k}_2 + m_e) \right],
\end{aligned} \tag{4.64}$$

and evaluating the traces yields

$$\begin{aligned}
\langle |\mathcal{M}_t|^2 \rangle &= 64 G_F^2 g_V^{v'2} \left[ (g_V^{e'} + g_A^{e'})^2 (k_1 \cdot k_2) (p_1 \cdot p_2) \right. \\
&\quad + (g_V^{e'} - g_A^{e'})^2 (k_1 \cdot p_2) (k_2 \cdot p_1) \\
&\quad \left. - m_e^2 (g_V^{e'2} - g_A^{e'2}) (k_1 \cdot p_1) \right] \\
&= 64 G_F^2 g_V^{v'2} m_e^2 \left[ (g_V^{e'} + g_A^{e'})^2 E_\nu^2 + (g_V^{e'} - g_A^{e'})^2 (E_\nu - T)^2 \right. \\
&\quad \left. - (g_V^{e'2} - g_A^{e'2}) m_e T \right],
\end{aligned} \tag{4.65}$$

where in the last step the kinematics have been plugged.

In terms of  $B$ ,  $\delta g_L$ , and  $\delta g_R$ , the spin-averaged amplitude in Equation 4.65 can be written as

$$\begin{aligned}
\langle |\mathcal{M}_t|^2 \rangle &= 64 G_F^2 m_e^2 \left[ (1+B)^2 (g_L + \delta g_L)^2 E_\nu^2 + (1+B)^2 (g_R + \delta g_R)^2 (E_\nu - T)^2 \right. \\
&\quad \left. - (1+B)^2 (g_R + \delta g_R) (g_L + \delta g_L) m_e T \right].
\end{aligned} \tag{4.66}$$

Finally, inserting  $\langle |\mathcal{M}_t|^2 \rangle$  into  $\frac{d\sigma}{dT}$  found in Appendix A gives as a final result

$$\begin{aligned}
\left[ \frac{d\sigma}{dT}(v_e e) \right]_{\text{Light LTHM}}^{FV} &= \frac{2 G_F^2 m_e}{\pi} \left[ (1+B)^2 (g_L + \delta g_L)^2 \right. \\
&\quad + (1+B)^2 (g_R + \delta g_R)^2 \left( 1 - \frac{T}{E_\nu} \right)^2 \\
&\quad \left. - (1+B)^2 (g_R + \delta g_R) (g_L + \delta g_L) \frac{m_e T}{E_\nu^2} \right].
\end{aligned} \tag{4.67}$$

Mediated by the LTHM new predicted heavy gauge bosons, there are further two

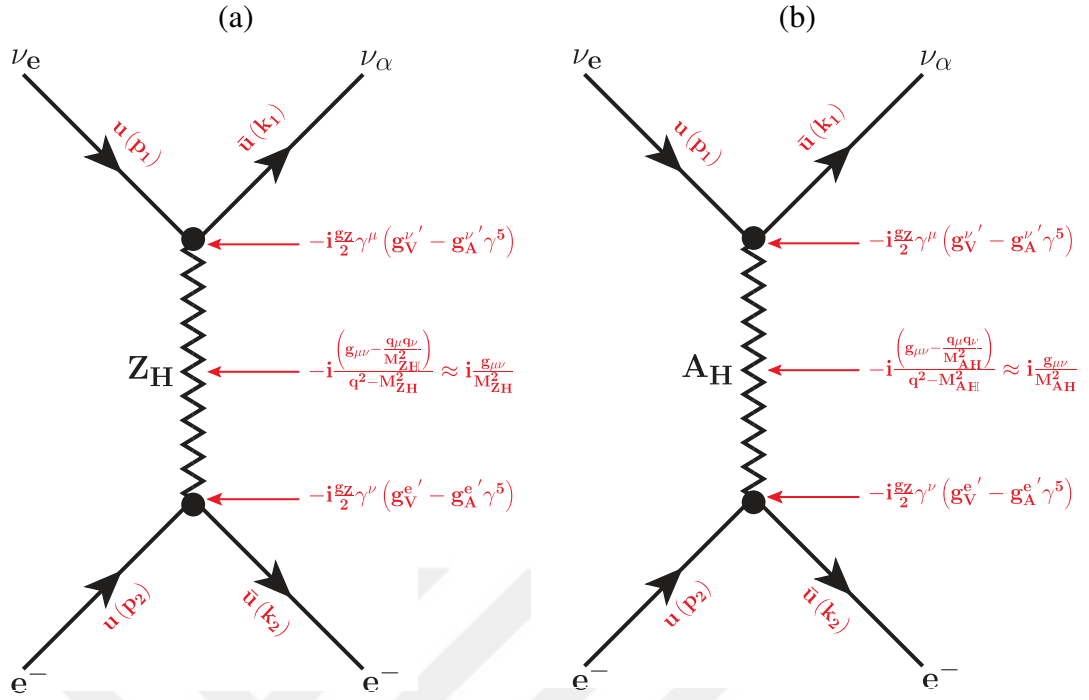


Figure 4.8 Feynman diagrams of (a)  $Z_H$ -mediated and (b)  $A_H$ -mediated neutrino-electron FV scattering in the  $SU(5)$  LTHM where the corresponding vertex and propagator factors are also shown

more possible tree-level Feynman diagrams that contribute to the FV process of  $\nu_e e$  elastic scattering.

- One is mediated by  $Z_H^0$  through a neutral weak process and is manifested by the Feynman diagram in Figure 4.8 (a) with the corresponding amplitude given by

$$\mathcal{M}_{ZH} = \frac{g_w^2}{4c_w^2 M_{Z_H}^2} g_V^{\nu'} g_V^{e'} \left[ \bar{\nu}(p_1) \gamma^\mu (1 - \gamma^5) \nu(k_1) \right] \left[ \bar{u}(k_2) \gamma_\mu (1 - \gamma^5) u(p_2) \right]. \quad (4.68)$$

- The other is mediated by  $A_H^0$  through a neutral weak process and is manifested by the Feynman diagram in Figure 4.8 (b) with the corresponding amplitude given by Equation

$$\mathcal{M}_{AH} = \frac{g_w^2}{4c_w^2 M_{A_H}^2} g_V^{\nu'} \left[ \bar{\nu}(p_1) \gamma^\mu (1 - \gamma^5) \nu(k_1) \right] \left[ \bar{u}(k_2) \gamma_\mu (g_V^{e'} - g_A^{e'} \gamma^5) u(p_2) \right]. \quad (4.69)$$

Then the total amplitude can be simply found as

$$\mathcal{M}_t = \mathcal{M}_{Z_H} + \mathcal{M}_{A_H}, \quad (4.70)$$

where together with its hermitian conjugate

$$\begin{aligned} \mathcal{M}_t^\dagger = & \frac{g_w^2}{8} \left[ \bar{u}(k_1) \gamma^\nu (1 - \gamma^5) u(p_1) \right]^\dagger \left[ \bar{u}(k_2) \gamma_\nu \left( \left( \frac{2 (g_V^{v'})_{Z_H} (g_V^{e'})_{Z_H}}{c_W^2 M_{Z_H}^2} \right. \right. \right. \\ & + \left. \left. \frac{2 (g_V^{v'})_{A_H} (g_V^{e'})_{A_H}}{c_W^2 M_{A_H}^2} \right) - \left( \frac{2 (g_V^{v'})_{Z_H} (g_V^{e'})_{Z_H}}{c_W^2 M_{Z_H}^2} \right. \right. \\ & \left. \left. + \frac{2 (g_V^{v'})_{A_H} (g_A^{e'})_{A_H}}{c_W^2 M_{A_H}^2} \right) \gamma^5 \right] u(p_2) \right]^\dagger, \end{aligned} \quad (4.71)$$

the spin-averaged amplitude square can be written as

$$\begin{aligned} \langle |\mathcal{M}_t|^2 \rangle = & \frac{1}{2} \sum_{\text{spins}} \mathcal{M}_t \mathcal{M}_t^\dagger \\ = & \frac{g_w^4}{128} \sum_{\text{spins}} \left[ \bar{u}(k_1) \gamma^\mu (1 - \gamma^5) u(p_1) \right] \left[ \bar{u}(k_1) \gamma^\nu (1 - \gamma^5) u(p_1) \right]^\dagger \\ & \times \sum_{\text{spins}} \left[ \bar{u}(k_2) \gamma_\mu \left( \left( \frac{2 (g_V^{v'})_{Z_H} (g_V^{e'})_{Z_H}}{c_W^2 M_{Z_H}^2} + \frac{2 (g_V^{v'})_{A_H} (g_V^{e'})_{A_H}}{c_W^2 M_{A_H}^2} \right) \right. \right. \\ & \left. \left. - \left( \frac{2 (g_V^{v'})_{Z_H} (g_V^{e'})_{Z_H}}{c_W^2 M_{Z_H}^2} + \frac{2 (g_V^{v'})_{A_H} (g_A^{e'})_{A_H}}{c_W^2 M_{A_H}^2} \right) \gamma^5 \right) u(p_2) \right] \\ & \times \left[ \bar{u}(k_2) \gamma_\nu \left( \left( \frac{2 (g_V^{v'})_{Z_H} (g_V^{e'})_{Z_H}}{c_W^2 M_{Z_H}^2} + \frac{2 (g_V^{v'})_{A_H} (g_V^{e'})_{A_H}}{c_W^2 M_{A_H}^2} \right) \right. \right. \\ & \left. \left. - \left( \frac{2 (g_V^{v'})_{Z_H} (g_V^{e'})_{Z_H}}{c_W^2 M_{Z_H}^2} + \frac{2 (g_V^{v'})_{A_H} (g_A^{e'})_{A_H}}{c_W^2 M_{A_H}^2} \right) \gamma^5 \right) u(p_2) \right]^\dagger \end{aligned} \quad (4.72)$$

$$\begin{aligned}
&= \frac{g_w^4}{128} Tr \left[ \gamma^\mu (1 - \gamma^5) (\not{p}_1 + m_\nu) \gamma^\nu (1 - \gamma^5) (\not{k}_1 + m_\nu) \right] \\
&\times Tr \left[ \gamma_\mu \left( \left( \frac{2(g_V^{v'})_{Z_H} (g_V^{e'})_{Z_H}}{c_W^2 M_{Z_H}^2} + \frac{2(g_V^{v'})_{A_H} (g_V^{e'})_{A_H}}{c_W^2 M_{A_H}^2} \right) \right. \right. \\
&\quad \left. \left. - \left( \frac{2(g_V^{v'})_{Z_H} (g_V^{e'})_{Z_H}}{c_W^2 M_{Z_H}^2} + \frac{2(g_V^{v'})_{A_H} (g_V^{e'})_{A_H}}{c_W^2 M_{A_H}^2} \right) \gamma^5 \right) (\not{p}_2 + m_e) \right. \\
&\quad \left. \times \gamma_\nu \left( \left( \frac{2(g_V^{v'})_{Z_H} (g_V^{e'})_{Z_H}}{c_W^2 M_{Z_H}^2} + \frac{2(g_V^{v'})_{A_H} (g_V^{e'})_{A_H}}{c_W^2 M_{A_H}^2} \right) \right. \right. \\
&\quad \left. \left. - \left( \frac{2(g_V^{v'})_{Z_H} (g_V^{e'})_{Z_H}}{c_W^2 M_{Z_H}^2} + \frac{2(g_V^{v'})_{A_H} (g_V^{e'})_{A_H}}{c_W^2 M_{A_H}^2} \right) \gamma^5 \right) (\not{k}_2 + m_e) \right] \tag{4.73}
\end{aligned}$$

$$\begin{aligned}
&= 2g_w^4 m_e^2 \left[ \left\{ \frac{\left( (g_V^{v'2})_{A_H} \left( (g_V^{e'})_{A_H} - (g_A^{e'})_{A_H} \right)^2 \right)}{c_W^4 M_{A_H}^4} \right\} (E_\nu - T)^2 \right. \\
&\quad \left. + \left\{ \frac{2(g_V^{v'})_{Z_H} (g_V^{e'})_{Z_H} + (g_V^{v'})_{A_H} \left( (g_V^{e'})_{A_H} + (g_A^{e'})_{A_H} \right)}{c_W^2 M_{Z_H}^2 + c_W^2 M_{A_H}^2} \right\}^2 E_\nu^2 \right. \\
&\quad \left. - \left\{ \frac{2(g_V^{v'})_{Z_H} (g_V^{e'})_{Z_H} (g_V^{v'})_{A_H} \left( (g_V^{e'})_{A_H} - (g_A^{e'})_{A_H} \right)}{c_W^4 M_{Z_H}^2 M_{A_H}^2} \right. \right. \\
&\quad \left. \left. + \frac{\left( (g_V^{v'2})_{A_H} \left( (g_V^{e'2})_{A_H} - (g_A^{e'2})_{A_H} \right) \right)}{c_W^4 M_{A_H}^4} \right\} m_e T \right], \tag{4.74}
\end{aligned}$$

where in the second step Casimir's trick have been applied and in the last step the trace results and the necessary kinematics have been plugged.

In terms of  $C_1$  and  $C_2$  then, the spin-averaged amplitude square is

$$\langle |\mathcal{M}_t|^2 \rangle = \frac{2g_W^4 m_e^2}{M_W^4} \left[ (C_1 + C_2)^2 E_\nu^2 + (2C_2)^2 (E_\nu - T)^2 - 2C_2 (C_1 + C_2) m_e T \right], \quad (4.75)$$

and hence the differential cross section is

$$\left[ \frac{d\sigma}{dT}(\nu_e e) \right]_{Heavy\ LTHM}^{FV} = \frac{2G_F^2 m_e}{\pi} \left[ (C_1 + C_2)^2 + (2C_2)^2 \left( 1 - \frac{T}{E_\nu} \right)^2 - 2C_2 (C_1 + C_2) \frac{m_e T}{E_\nu^2} \right]. \quad (4.76)$$

## 4.2 The $SU(3)$ Simple Little Higgs Model

$SU(3)$  SLHM is constructed by enlarging the SM  $SU(2)_L \times U(1)_Y$  gauge group to  $SU(3) \times U(1)_X$ . The  $SU(3) \times U(1)_X$  gauge symmetry is broken down to the SM electroweak gauge group by two triplet complex scalar fields  $\Phi_{1,2}$  with aligned VEVs  $f_{1,2}$  of order a  $TeV$ , yielding three heavy gauge bosons denoted by  $Z'^0$ ,  $Y^0$  and  $X^\pm$  (or  $W'^\pm$ ) (Kaplan et al., 2003; Perelstein, 2007; Schmaltz et al., 2005).

In the  $SU(3)$  SLHM, the quadratic divergences cancel completely between the  $Z$  and  $Z'$  loops and between the  $W$  and  $X$  loops, with no any contribution from the  $Y$  loop in neutrino-electron scattering due to the uncoupling portability of the  $Y$  gauge boson with the charged leptons, as is seen in Table 4.2.

Similar to the  $SU(5)$  LTHM, the  $SU(3)$  SLHM produces contributions to the neutrino-electron scattering process via some correction terms of the SM  $Ze\bar{e}$ ,  $Z\nu\bar{\nu}$  and  $W\bar{\nu}\nu$  couplings and some additional terms of the new heavy gauge bosons predicted by the model.

The possible tree-level Feynman diagrams for FC and FV processes in the  $SU(3)$  SLHM are similar to those of the  $SU(5)$  LTHM with  $Z$  and  $W$  are again the SM gauge

bosons and  $Z'$ ,  $Y$  and  $X$  (replacing respectively  $Z_H$ ,  $A_H$  and  $W_H$ ) are the new heavy gauge bosons in the model at hand.

Table 4.2 Couplings of the SM  $Z$  and  $W$  gauge bosons and the new heavy  $Z'$ ,  $Y$  and  $X$  gauge bosons with leptons in the  $SU(3)$  SLHM (Aguila et al., 2011)

	SM	$SU(3)$ SLHM
$Z\nu\bar{\nu}$	$g_L^{\nu} = \frac{1}{2}$ $g_R^{\nu} = 0$	$g_L^{\nu'} = \frac{1}{2} (1 - \delta_v^2) + \delta_z \frac{1-2s_w^2}{2c_w\sqrt{3-t_w^2}}$ $g_R^{\nu'} = 0$
$Ze\bar{e}$	$g_L^e = s_w^2 - \frac{1}{2}$ $g_R^e = s_w^2$	$g_L^{e'} = s_w^2 - \frac{1}{2} + \delta_z \frac{1-2s_w^2}{2c_w\sqrt{3-t_w^2}}$ $g_R^{e'} = s_w^2 - \delta_z \frac{s_w^2}{c_w\sqrt{3-t_w^2}}$
$We\bar{\nu}$	$g_L^{e\nu} = \frac{c_w}{\sqrt{2}}$ $g_R^{e\nu} = 0$	$g_L^{e\nu'} = \frac{c_w}{\sqrt{2}} \left(1 - \frac{\delta_v^2}{2}\right)$ $g_R^{e\nu'} = 0$
$Z'\nu\bar{\nu}$	-	$g_L^{\nu'} = \frac{1-2s_w^2}{2c_w\sqrt{3-t_w^2}} \left(1 - \delta_v^2 \frac{c_w^2(3-t_w^2)}{1-2s_w^2}\right) - \frac{1}{2}\delta_z$ $g_R^{\nu'} = 0$
$Z'e\bar{e}$	-	$g_L^{e'} = \frac{1-2s_w^2}{2c_w\sqrt{3-t_w^2}} - \delta_z \left(s_w^2 - \frac{1}{2}\right)$ $g_R^{e'} = -\frac{s_w^2}{c_w\sqrt{3-t_w^2}} - \delta_z s_w^2$
$Y\nu\bar{\nu}$	-	$g_L^{\nu'} = i\delta_v \frac{c_w}{\sqrt{2}}$ $g_R^{\nu'} = 0$
$Ye\bar{e}$	-	$g_L^{e'} = 0$ $g_R^{e'} = 0$
$Xe\bar{\nu}$	-	$g_L^{e\nu'} = -i\delta_v \frac{c_w}{\sqrt{2}}$ $g_R^{e\nu'} = 0$

In the framework of the  $SU(3)$  SLHM:

- the coupling constants of the SM  $Z$  and  $W$  as well as the new heavy  $Z'$ ,  $Y$  and  $X$  bosons with leptons are given in Table 4.2, where  $\delta_z = -\frac{(1-t_w^2)\sqrt{3-t_w^2}}{8c_w} \frac{v^2}{f^2}$  and  $\delta_v = -\frac{1}{\sqrt{2}t_\beta} \frac{v}{f}$ .
- taking into consideration the couplings given in the above table, the vertex factor of both NC and CC processes can be written in equivalence to Equations 4.1 and

4.2 as

$$-ig_z \gamma^\mu \left( g_L^{f'} \mathcal{P}_L + g_R^{f'} \mathcal{P}_R \right), \quad (4.77)$$

where  $g_L^{f'}$  and  $g_R^{f'}$  coupling constants depend on  $t_\beta \equiv \frac{f_2}{f_1}$  and the scale  $f \equiv \sqrt{f_1^2 + f_2^2}$ , with  $f_1$  and  $f_2$  being the VEVs of the two fields responsible of symmetry breaking in the  $SU(3)$  SLHM. Note that  $\mathcal{P}_L = \frac{1-\gamma^5}{2}$  and  $\mathcal{P}_R = \frac{1+\gamma^5}{2}$  are some convenient projection operators for left-handed and right-handed couplings, respectively.

Note that the only places where  $\frac{v^2}{f^2}$  corrections appear are in the definitions of the physical states of the leptons (in  $\delta_\nu^2$ ) and in the  $ZZ'$  mixing (in  $\delta_z$ ) and obviously setting these terms to zero reproduces again the original SM coupling constants.

In the scope of neutrino-electron elastic scattering, the  $SU(3)$  SLHM also involves both FC and FV processes denoted respectively by  $\nu_e(\bar{\nu}_e) + e \rightarrow \nu_e(\bar{\nu}_e) + e$  and  $\nu_e(\bar{\nu}_e) + e \rightarrow \nu_\alpha(\bar{\nu}_\alpha) + e$  (where  $\alpha \neq e$ ) and mediated by the SM ( $Z$  and  $W$ ) and new heavy ( $Z'$ ,  $Y$  and  $X$ ) gauge bosons. Using the appropriate Feynman diagrams, the vertex factor given by Equation 4.77, the proper form of the propagator factor given by Equation 4.3 and the necessary [VFF] couplings given by Table 4.2, it is sufficient to present in details the contributions from the FC neutrino-electron scattering in the  $SU(3)$  SLHM mediated by the light and heavy gauge bosons and then conclude directly by the full formalism of the  $SU(3)$  SLHM as was done for the  $SU(5)$  LTHM.

Mediated by the SM light gauge bosons, the tree-level Feynman diagrams that contribute for the FC process of  $\nu_e e$  elastic scattering are as follows:

- The 1<sup>st</sup> one, mediated by  $Z^0$  through a neutral weak process, has an amplitude

amplitude given by

$$\begin{aligned} \mathcal{M}_Z &= \frac{2G_F}{\sqrt{2}} g_L^{v'} \left[ \bar{u}(k_1) \gamma^\mu (1 - \gamma^5) u(p_1) \right] \\ &\quad \times \left[ \bar{u}(k_2) \gamma_\mu \left\{ g_L^{e'} (1 - \gamma^5) + g_R^{e'} (1 + \gamma^5) \right\} u(p_2) \right]. \end{aligned} \quad (4.78)$$

- The 2<sup>nd</sup> one, mediated by  $W^\pm$  through a charged weak process, has an amplitude given by

$$\mathcal{M}_W = \frac{2G_F}{\sqrt{2}} \frac{1}{c_W^2} g_L^{ev'2} \left[ \bar{u}(k_1) \gamma^\mu (1 - \gamma^5) u(p_1) \right] \left[ \bar{u}(k_2) \gamma_\mu (1 - \gamma^5) u(p_2) \right], \quad (4.79)$$

where Fierz transformation has been applied.

Then the total amplitude can be simply written as

$$\begin{aligned} \mathcal{M}_t &= \mathcal{M}_Z + \mathcal{M}_W \\ &= \frac{2G_F}{\sqrt{2}} \left[ \bar{u}(k_1) \gamma^\mu (1 - \gamma^5) u(p_1) \right] \\ &\quad \times \left[ \bar{u}(k_2) \gamma_\mu \left\{ \left( g_L^{v'} g_L^{e'} + \frac{1}{c_W^2} g_L^{ev'2} \right) (1 - \gamma^5) + g_L^{v'} g_R^{e'} (1 + \gamma^5) \right\} u(p_2) \right], \end{aligned} \quad (4.80)$$

and then together with its hermitian conjugate  $\mathcal{M}_t^\dagger$ , the spin-averaged amplitude square is

$$\begin{aligned} \langle |\mathcal{M}_t|^2 \rangle &= \frac{1}{2} \sum_{\text{spins}} |\mathcal{M}_t|^2 \\ &= G_F^2 \sum_{\text{spins}} \left[ \bar{u}(k_1) \gamma^\mu (1 - \gamma^5) u(p_1) \right] \left[ \bar{u}(k_1) \gamma^\nu (1 - \gamma^5) u(p_1) \right]^\dagger \\ &\quad \times \sum_{\text{spins}} \left[ \bar{u}(k_2) \gamma_\mu \left\{ \left( g_L^{v'} g_L^{e'} + \frac{1}{c_W^2} g_L^{ev'2} \right) (1 - \gamma^5) \right. \right. \\ &\quad \left. \left. + g_L^{v'} g_R^{e'} (1 + \gamma^5) \right\} u(p_2) \right] \\ &\quad \times \left[ \bar{u}(k_2) \gamma_\nu \left\{ \left( g_L^{v'} g_L^{e'} + \frac{1}{c_W^2} g_L^{ev'2} \right) (1 - \gamma^5) \right. \right. \\ &\quad \left. \left. + g_L^{v'} g_R^{e'} (1 + \gamma^5) \right\} u(p_2) \right]^\dagger, \end{aligned} \quad (4.81)$$

where using Casimir's trick yields

$$\begin{aligned}
&= G_F^2 \text{Tr} \left[ \gamma^\mu (1 - \gamma^5) (\not{p}_1 + m_\nu) \gamma^\nu (1 - \gamma^5) (\not{k}_1 + m_\nu) \right] \\
&\times \text{Tr} \left[ \gamma_\mu \left\{ \left( g_L^{v'} g_L^{e'} + \frac{1}{c_W^2} g_L^{e\nu'2} \right) (1 - \gamma^5) + g_L^{v'} g_R^{e'} (1 + \gamma^5) \right\} (\not{p}_2 + m_e) \right. \\
&\left. \times \gamma_\nu \left\{ \left( g_L^{v'} g_L^{e'} + \frac{1}{c_W^2} g_L^{e\nu'2} \right) (1 - \gamma^5) + g_L^{v'} g_R^{e'} (1 + \gamma^5) \right\} (\not{k}_2 + m_e) \right], \quad (4.82)
\end{aligned}$$

and then plugging the values of the traces yields

$$\begin{aligned}
\langle |\mathcal{M}_t|^2 \rangle &= \frac{256 G_F^2}{c_W^4} \left[ \left( g_L^{v'} g_L^{e'} c_W^2 + g_L^{e\nu'2} \right)^2 (k_1 \cdot k_2) (p_1 \cdot p_2) \right. \\
&+ \left( g_L^{v'} g_R^{e'} c_W^2 \right)^2 (k_1 \cdot p_2) (k_2 \cdot p_1) \\
&\left. - m_e^2 \left( g_L^{v'} g_R^{e'} c_W^2 \right) \left( g_L^{v'} g_L^{e'} c_W^2 + g_L^{e\nu'2} \right) (k_1 \cdot p_1) \right], \quad (4.83)
\end{aligned}$$

where our results of traces have been again conformed by "FeynCalc".

It is advantageous again to stop at this stage and simplify the coupling constants of the light  $SU(3)$  SLHM given in Table 4.2 before going on and plugging them into their places. So by the fact that

$$\begin{aligned}
\delta_z &= -\frac{(1 - t_w^2) \sqrt{3 - t_w^2} v^2}{8 c_w} f^2, \\
\delta_v &= -\frac{1}{\sqrt{2} t_\beta} \frac{v}{f}, \quad (4.84)
\end{aligned}$$

the new coupling constants can be written as

$$\begin{aligned}
g_L^{v'} &= \frac{1}{2} (1 - \delta_v^2) + \delta_z \frac{1 - 2s_w^2}{2c_w \sqrt{3 - t_w^2}} \\
&= \frac{1}{2} - \frac{1}{4} \frac{v^2}{f^2} \underbrace{\left[ \frac{1}{t_\beta^2} + \frac{(1 - t_w^2) \left( \frac{1}{2} - s_w^2 \right)}{2c_w^2} \right]}_{\equiv \frac{B}{2}} \\
\implies g_L^{v'} &= \frac{1}{2} (1 + B), \quad (4.85)
\end{aligned}$$

where  $B = -\frac{1}{2} \frac{v^2}{f^2} \left[ \frac{1}{t_\beta^2} + \frac{(1-t_W^2)(\frac{1}{2}-s_W^2)}{2c_W^2} \right]$ .

$$\begin{aligned}
g_L^{e'} &= s_w^2 - \frac{1}{2} + \delta_z \frac{1-2s_w^2}{2c_w \sqrt{3-t_w^2}} \\
&= s_w^2 - \frac{1}{2} - \underbrace{\frac{1}{8} \frac{v^2}{f^2} \frac{(1-t_W^2)(\frac{1}{2}-s_W^2)}{c_W^2}}_{\equiv \delta_{g_L}} \\
\implies g_L^{e'} &= s_w^2 - \frac{1}{2} + \delta_{g_L},
\end{aligned} \tag{4.86}$$

where  $\delta_{g_L} = -\frac{1}{8} \frac{v^2}{f^2} \frac{(1-t_W^2)(\frac{1}{2}-s_W^2)}{c_W^2}$ .

$$\begin{aligned}
g_R^{e'} &= s_w^2 - \delta_z \frac{s_w^2}{c_w \sqrt{3-t_w^2}} \\
&= s_w^2 + \underbrace{\frac{1}{8} \frac{v^2}{f^2} (1-t_W^2) t_W^2}_{\equiv \delta_{g_R}} \\
\implies g_R^{e'} &= s_w^2 + \delta_{g_R},
\end{aligned} \tag{4.87}$$

where  $\delta_{g_R} = +\frac{1}{8} \frac{v^2}{f^2} (1-t_W^2) t_W^2$ .

$$\begin{aligned}
g_L^{e\nu'} &= \frac{c_w}{\sqrt{2}} \left( 1 - \frac{\delta_v^2}{2} \right) \\
&= \frac{c_w}{\sqrt{2}} \left( 1 - \underbrace{\frac{1}{4} \frac{v^2}{f^2} \frac{1}{t_\beta^2}}_{\equiv \delta_{g_L}'} \right) \\
\implies g_L^{e\nu'} &= \frac{c_w}{\sqrt{2}} \left( 1 + \delta_{g_L}' \right),
\end{aligned} \tag{4.88}$$

where  $\delta_{g_L}' = -\frac{1}{4} \frac{v^2}{f^2} \frac{1}{t_\beta^2}$ .

In terms of  $B$ ,  $\delta_{g_L}$ ,  $\delta_{g_R}$  and  $\delta_{g_L}'$  given respectively by Equations 4.85, 4.86, 4.87

and 4.88, the spin-averaged amplitude in Equation 4.83 can be written as

$$\begin{aligned}
\langle |\mathcal{M}_t|^2 \rangle &= 64G_F^2 m_e^2 \left[ \left\{ (1+B)(g_L + \delta g_L) + (1 + \delta g'_L)^2 \right\}^2 E_V^2 \right. \\
&\quad + (1+B)^2 (g_R + \delta g_R)^2 (E_V - T)^2 \\
&\quad \left. - (1+B)(g_R + \delta g_R) \left\{ (1+B)(g_L + \delta g_L) + (1 + \delta g'_L)^2 \right\} m_e T \right], \tag{4.89}
\end{aligned}$$

where the necessary kinematic terms found in Appendix B have been also plugged.

Finally, inserting  $\langle |\mathcal{M}_t|^2 \rangle$  into  $\frac{d\sigma}{dT}$  found in Appendix A

$$\frac{d\sigma}{dT} = \frac{\langle |\mathcal{M}|^2 \rangle}{32\pi m_2 |\vec{p}_1|^2}$$

where  $m_2 \equiv m_e$  and  $|\vec{p}_1|^2 \equiv |\vec{p}_V|^2 = E_V^2 - m_V^2 = E_V^2$  gives as a final result

$$\begin{aligned}
\left[ \frac{d\sigma}{dT}(\nu_e e) \right]_{Light\ SLHM}^{FC} &= \frac{2G_F^2 m_e}{\pi} \left[ \left\{ (1+B)(g_L + \delta g_L) + (1 + \delta g'_L)^2 \right\}^2 \right. \\
&\quad + (1+B)^2 (g_R + \delta g_R)^2 \left( 1 - \frac{T}{E_V} \right)^2 \\
&\quad - (1+B)(g_R + \delta g_R) \left\{ (1+B)(g_L + \delta g_L) \right. \\
&\quad \left. \left. + (1 + \delta g'_L)^2 \right\} \frac{m_e T}{E_V^2} \right]. \tag{4.90}
\end{aligned}$$

Furthermore, mediated by the heavy gauge bosons predicted by the  $SU(3)$  SLHM, there are three possible tree-level Feynman diagrams for the FC process of  $\nu_e e$  elastic scattering given as following:

- The 1<sup>st</sup> one, mediated by  $Z'^0$  through a neutral weak process, has an amplitude

given by

$$\begin{aligned} \mathcal{M}_{Z'} &= \frac{g_W^2}{4c_W^2 M_{Z'}^2} g_L^{v'} \left[ \bar{u}(k_1) \gamma^\mu (1 - \gamma^5) u(p_1) \right] \\ &\times \left[ \bar{u}(k_2) \gamma_\mu \left\{ g_L^{e'} (1 - \gamma^5) + g_R^{e'} (1 + \gamma^5) \right\} u(p_2) \right]. \end{aligned} \quad (4.91)$$

- The 2<sup>nd</sup> one, mediated by  $Y^0$  through a neutral weak process, has an amplitude given by

$$\mathcal{M}_Y = 0. \quad (4.92)$$

- The 3<sup>rd</sup> one, mediated by  $X^\pm$  through a charged weak process, has amplitude given after Fierz transformation by

$$\mathcal{M}_X = \frac{g_W^2}{4c_W^2 M_X^2} g_L^{e\nu'2} \left[ \bar{u}(k_1) \gamma^\mu (1 - \gamma^5) u(p_1) \right] \left[ \bar{u}(k_2) \gamma_\mu (1 - \gamma^5) u(p_2) \right]. \quad (4.93)$$

Then the total amplitude can be simply written as

$$\begin{aligned} \mathcal{M}_t &= \mathcal{M}_{Z'} + \mathcal{M}_X \\ &= \frac{g_W^2}{4c_W^2} \left[ \bar{u}(k_1) \gamma^\mu (1 - \gamma^5) u(p_1) \right] \\ &\times \left[ \bar{u}(k_2) \gamma_\mu \left\{ \left( \frac{g_L^{v'} g_L^{e'}}{M_{Z'}^2} + \frac{g_L^{e\nu'2}}{M_X^2} \right) (1 - \gamma^5) + \frac{g_L^{v'} g_R^{e'}}{M_{Z'}^2} (1 + \gamma^5) \right\} u(p_2) \right], \end{aligned} \quad (4.94)$$

and together with its hermitian conjugate  $\mathcal{M}_i^\dagger$ , the spin-averaged amplitude square is

$$\begin{aligned}
\langle |\mathcal{M}_i|^2 \rangle &= \frac{1}{2} \sum_{\text{spins}} |\mathcal{M}_i|^2 \\
&= \frac{g_w^4}{32c_W^4} \sum_{\text{spins}} \left[ \bar{u}(k_1) \gamma^\mu (1 - \gamma^5) u(p_1) \right] \left[ \bar{u}(k_1) \gamma^\nu (1 - \gamma^5) u(p_1) \right]^\dagger \\
&\quad \times \sum_{\text{spins}} \left[ \bar{u}(k_2) \gamma_\mu \left\{ \left( \frac{g_L^{v'} g_L^{e'}}{M_{Z'}^2} + \frac{g_L^{ev'2}}{M_X^2} \right) (1 - \gamma^5) \right. \right. \\
&\quad \left. \left. + \frac{g_L^{v'} g_R^{e'}}{M_{Z'}^2} (1 + \gamma^5) \right\} u(p_2) \right] \\
&\quad \times \left[ \bar{u}(k_2) \gamma_\nu \left\{ \left( \frac{g_L^{v'} g_L^{e'}}{M_{Z'}^2} + \frac{g_L^{ev'2}}{M_X^2} \right) (1 - \gamma^5) \right. \right. \\
&\quad \left. \left. + \frac{g_L^{v'} g_R^{e'}}{M_{Z'}^2} (1 + \gamma^5) \right\} u(p_2) \right]^\dagger, \tag{4.95}
\end{aligned}$$

where using Casimir's trick yields

$$\begin{aligned}
&= \frac{g_w^4}{32c_W^4} \text{Tr} \left[ \gamma^\mu (1 - \gamma^5) (\not{p}_1 - m_\nu) \gamma^\nu (1 - \gamma^5) (\not{k}_1 - m_\nu) \right] \\
&\quad \times \text{Tr} \left[ \gamma_\mu \left\{ \left( \frac{g_L^{v'} g_L^{e'}}{M_{Z'}^2} + \frac{g_L^{ev'2}}{M_X^2} \right) (1 - \gamma^5) + \frac{g_L^{v'} g_R^{e'}}{M_{Z'}^2} (1 + \gamma^5) \right\} (\not{p}_2 + m_e) \right] \\
&\quad \times \gamma_\nu \left\{ \left( \frac{g_L^{v'} g_L^{e'}}{M_{Z'}^2} + \frac{g_L^{ev'2}}{M_X^2} \right) (1 - \gamma^5) + \frac{g_L^{v'} g_R^{e'}}{M_{Z'}^2} (1 + \gamma^5) \right\} (\not{k}_2 + m_e) \right], \tag{4.96}
\end{aligned}$$

and then plugging our evaluation of the traces and the kinematic terms yield

$$\begin{aligned}
\langle |\mathcal{M}_i|^2 \rangle &= 8 \left( \frac{g_w}{c_W M_{Z'} M_X} \right)^4 m_e^2 \left[ \left( g_L^{v'} g_L^{e'} M_X^2 + g_L^{ev'2} M_{Z'}^2 \right)^2 E_\nu^2 \right. \\
&\quad \left. + \left( g_L^{v'} g_R^{e'} M_X^2 \right)^2 (E_\nu - T)^2 \right. \\
&\quad \left. - \left( g_L^{v'} g_R^{e'} M_X^2 \right) \left( g_L^{v'} g_L^{e'} M_X^2 + g_L^{ev'2} M_{Z'}^2 \right) m_e T \right]. \tag{4.97}
\end{aligned}$$

Now by plugging the values of the new coupling constants given in Table 4.2 and

assuming  $\delta_Z = \delta_V^2 = 0$  at high energies, the new couplings become

$$\begin{aligned}
g_L^{V'} &= \frac{1-2s_w^2}{2c_w\sqrt{3-t_w^2}} \left( 1 - \delta_V^2 \frac{c_w^2(3-t_w^2)}{1-2s_w^2} \right) - \frac{1}{2}\delta_z \approx \frac{\frac{1}{2}-s_W^2}{\sqrt{3-4s_W^2}}, \\
g_L^{e'} &= \frac{1-2s_w^2}{2c_w\sqrt{3-t_w^2}} - \delta_z \left( s_w^2 - \frac{1}{2} \right) \approx \frac{\frac{1}{2}-s_W^2}{\sqrt{3-4s_W^2}}, \\
g_R^{e'} &= -\frac{s_w^2}{c_w\sqrt{3-t_w^2}} - \delta_z s_w^2 \approx -\frac{s_W^2}{\sqrt{3-4s_W^2}}, \\
g_L^{eV'} &= -i\delta_V \frac{c_w}{\sqrt{2}} = i\frac{c_W}{2} \frac{1}{t_\beta} \frac{v}{f},
\end{aligned} \tag{4.98}$$

from which three new terms defined as

$$C_1 = 2 \frac{\left(\frac{1}{2}-s_W^2\right)^2}{c_W^2(3-4s_W^2)} \left(\frac{M_W}{M_{Z'}}\right)^2, \tag{4.99}$$

$$C_2 = -\frac{1}{2} \frac{1}{t_\beta^2} \frac{v^2}{f^2} \left(\frac{M_W}{M_X}\right)^2, \tag{4.100}$$

$$C_3 = 2 \frac{\left(\frac{1}{2}-s_W^2\right)t_W^2}{3-4s_W^2} \left(\frac{M_W}{M_{Z'}}\right)^2, \tag{4.101}$$

pop out from  $Z'$  and  $X$  in terms of which the spin-averaged amplitude in Equation 4.97 can be written as

$$\langle |\mathcal{M}_t|^2 \rangle = \frac{2g_W^4 m_e^2}{M_W^4} \left[ (C_1 + C_2)^2 E_V^2 + C_3^2 (E_V - T)^2 - C_3 (C_1 + C_2) m_e T \right]. \tag{4.102}$$

Thus, the differential scattering cross section following Equation 4.102 can be represented as

$$\begin{aligned}
\left[ \frac{d\sigma}{dT}(\nu_e e) \right]_{Heavy\ SLHM}^{FC} &= \frac{2G_F^2 m_e}{\pi} \left[ (C_1 + C_2)^2 + C_3^2 \left( 1 - \frac{T}{E_V} \right)^2 \right. \\
&\quad \left. - C_3 (C_1 + C_2) \frac{m_e T}{E_V^2} \right].
\end{aligned} \tag{4.103}$$

## CHAPTER FIVE

### ANALYSIS AND DISCUSSION

#### Input Data

Being a purely leptonic process, the neutrino-electron elastic scattering provides a good channel to test the SM theory at low and high energies. Many accelerator and reactor experiments have been built worldwide for this aim. Some of them are shown in Table 5.1 with their corresponding measured values of cross section and Weinberg angle if available.

Table 5.1 A summary of the published measurements of cross section and weak mixing angle by some  $\nu_e e$  and  $\bar{\nu}_e e$  experiments (Deniz et al., 2010)

	Experiment	$\sigma_{exp}$	$\sin^2 \theta_W$
Accelerator $\nu_e$	LAMPF	$[10.0 \pm 1.5 \pm 0.9] \times E_\nu \times 10^{-45} \text{ cm}^2$	$0.249 \pm 0.063$
	LSND	$[10.1 \pm 1.1 \pm 1.0] \times E_\nu \times 10^{-45} \text{ cm}^2$	$0.248 \pm 0.051$
Reactor $\bar{\nu}_e$	Savannah River (original)	$[0.87 \pm 0.25] \times \sigma_{V-A}$ $[1.70 \pm 0.44] \times \sigma_{V-A}$	$0.29 \pm 0.05$
	Savannah River (new analysis)	$[1.35 \pm 0.4] \times \sigma_{SM}$ $[2.0 \pm 0.5] \times \sigma_{SM}$	-
	Krasnoyarsk	$[4.5 \pm 2.4] \times 10^{-46} \text{ cm}^2 / \text{fission}$	$0.22_{-0.8}^{+0.7}$
	Rovno	$[1.26 \pm 0.62] \times 10^{-44} \text{ cm}^2 / \text{fission}$	-
	MUNU	$[1.07 \pm 0.34] \text{ event/day}$	-
	TEXONO	$[1.08 \pm 0.21 \pm 0.16] \times \sigma_{SM}$	$0.251 \pm 0.031 \pm 0.024$

In our analysis of LHM theories, however, only two independent data sets from two different experiments, famously known as TEXONO and LSND experiments and represented respectively by  $\bar{\nu}_e + e \rightarrow \bar{\nu}_e + e$  and  $\nu_e + e \rightarrow \nu_e + e$ , were adopted:

**TEXONO experiment:** Data from this experiment on  $\bar{\nu}_e e$  scatterings was taken at

the Kuo-Sheng Neutrino Laboratory (KSNL) with 29882/7369 *kg day* of reactor ON/OFF exposure of a CsI(Tl) crystal scintillator array detector of effective mass 187 *kg* and 3 – 8  $M_e V_{ee}$  energy range (Deniz et al., 2010) .

**LSND experiment:** Data from this experiment on  $\nu_e e$  scatterings was taken at the Los Alamos Neutron Science Center using liquid scintillator detector exposed to high energy  $\nu_e$ 's produced at the proton beam stop with  $T$  ranges between 18 – 50  $M_e V_{ee}$  (Auerbach et al., 2001) .

After which, the results from both experiments were compared and superimposed to have a more stringent analysis. Furthermore, results from some other experiments, mainly LEP (the large electron-positron collider) and EWPD (electroweak precision data), have been also superimposed where convenient in some of our analysis.

Fitting the experimentally measured event rates of (anti)neutrinos elastically scattered off electrons to the theoretically estimated ones by the simple formula

$$\sigma_{exp} = p_0 \times \sigma_{theo} \quad (5.1)$$

gives as a best fit result

$$p_0 = 1.082 \pm 0.2124 \quad (5.2)$$

by TEXONO experiment as is shown in Figure 5.1 (a) and

$$p_0 = 0.9147 \pm 0.1033 \quad (5.3)$$

by LSND experiment as is shown in Figure 5.1 (b).

By TEXONO experiment,  $\bar{\nu}_e e$  electroweak interaction cross section, neutral vector and axial vector coupling constants ( $g_V$  and  $g_A$ ), weak mixing angle ( $\theta_W$ ), neutrino charge-radius squared and neutrino magnetic moment were measured. And by LSND experiment,  $\nu_e e$  elastic scattering cross section and weak mixing angle were measured.

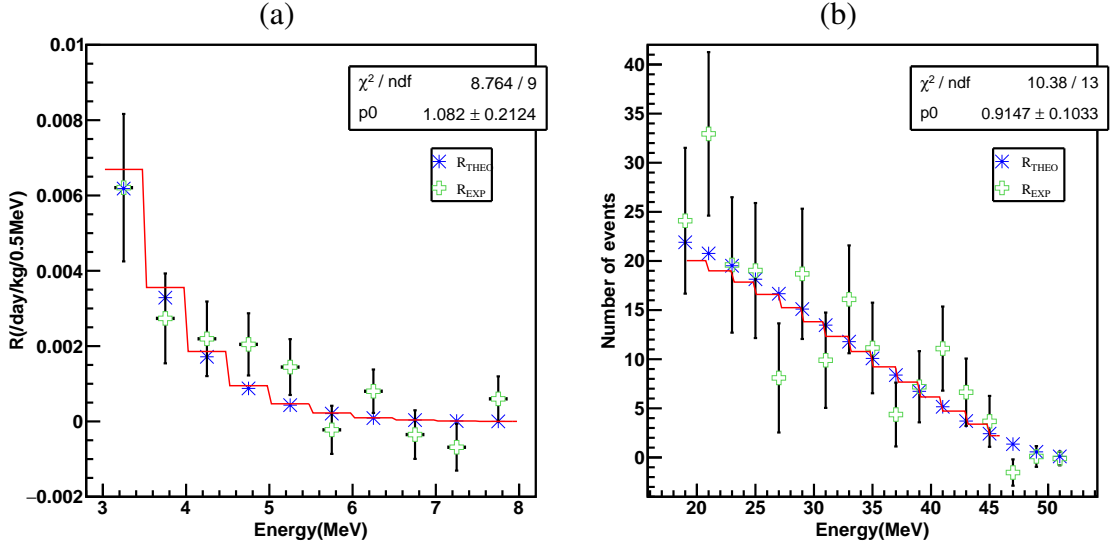


Figure 5.1 The best fit result of (a) TEXONO and (b) LSND experimental measured values to the theoretical ones

One of our previous work using both of these experimental data sets is shown in Figure 5.2, where the limits on  $(g_V, g_A)$  space and  $\sin^2\theta_W$  have been put. For completeness, the corresponding result from Charm-II experiment has been also superimposed as is given in the reference of Tanabashi et al. (2018), hinting that the limits achieved by all these three experiments are in a good agreement with the electroweak precision data.

### Analysis Methods

The expected event rates  $\sigma_X$  can be evaluated for TEXONO experiment via

$$\sigma_X = \rho_e \int_T \int_{E_\nu} \left[ \frac{d\sigma}{dT} \right]'_X \frac{d\phi(\bar{\nu}_e)}{dE_\nu} dE_\nu dT \quad (5.4)$$

and for LSND experiment via

$$\sigma_X = \int_T \int_{E_\nu} \left[ \frac{d\sigma}{dT} \right]_X \left( \frac{1}{\phi} \frac{d\phi(\nu_e)}{dE_\nu} \right) dE_\nu dT, \quad (5.5)$$

where  $\rho_e$  is the electron number density per kg of target mass,  $\frac{d\phi}{dE_\nu}$  is the (anti)neutrino

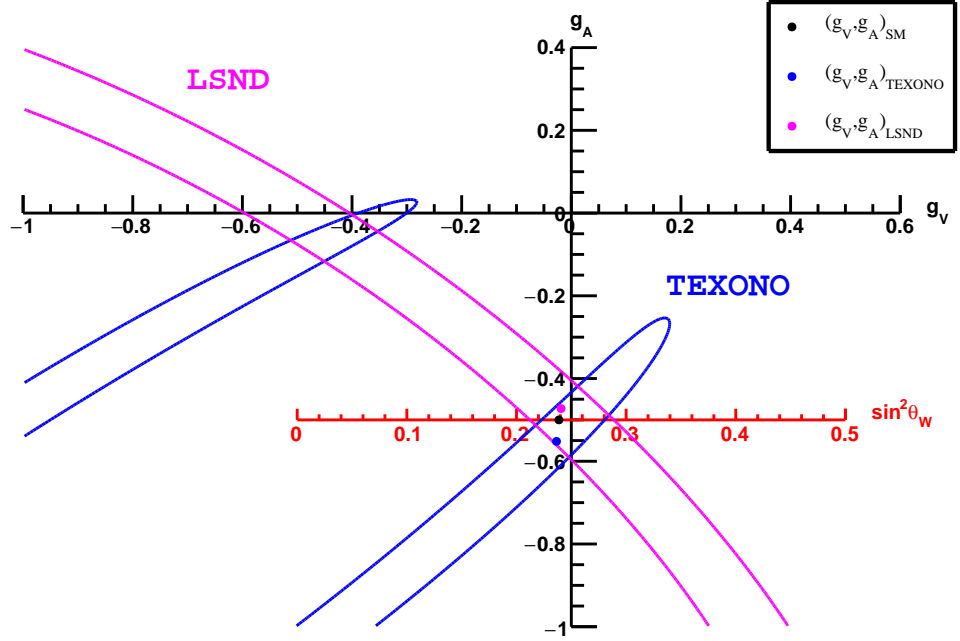


Figure 5.2 The 90% C.L. allowed region put by TEXONO and LSND experiments on the  $(g_V, g_A)$  space and  $\sin^2 \theta_W$

spectrum and  $\phi$  is the total flux of the incident neutrinos. In this work, X represents different theoretical models (SM, NSI of neutrinos,  $SU(5)$  LTHM, and  $SU(3)$  SLHM) via (anti)neutrino-electron scattering channel.

The measurable differential cross section  $[\frac{d\sigma}{dT}]'$  for TEXONO experiment corresponds to convolution of the detector energy resolution to the physical differential cross section  $[\frac{d\sigma}{dT}]$ . In practice, the variations of  $[\frac{d\sigma}{dT}]$  with energy are gradual so that the resolution smearing does not significantly alter the measured spectra in the region of interest. Indeed, the difference  $[\frac{d\sigma}{dT}] - [\frac{d\sigma}{dT}]'$  is less than 0.1%. Accordingly, resolution effects can be neglected in this analysis.

The observed event rates  $\sigma_{exp}$  (expressed in units of  $kg^{-1}MeV^{-1}day^{-1}$ ) of the two data sets used in this analysis were compared to the expected event rates  $\sigma_X$  evaluated for different X channels and constraints were then derived.

A minimum- $\chi^2$  analysis algorithm defined generally by

$$\chi^2 = \sum_{i=1} \left[ \frac{\sigma_{exp}(i) - (\sigma_{SM}(i) + \sigma_X(i))}{\Delta_{stat}(i)} \right]^2 \quad (5.6)$$

was performed in this work, where  $\sigma_{exp}(i)$  are the experimentally observed/measured event rates,  $\sigma_{SM}(i)$  and  $\sigma_X(i)$  are respectively the theoretically expected/calculated event rates on the  $i$ th data bin due to the SM and X (= NSI,  $SU(5)$  LTHM and  $SU(3)$  SLHM) contributions, while  $\Delta_{stat}(i)$  are the corresponding statistical uncertainties of the measurement.

The statistical uncertainties were derived by the minimum- $\chi^2$  method defined above. The systematic uncertainties published by the experiments contribute to shifts of the best fit values of the parameters of interest. The two contributions were added in quadrature to give rise to the combined uncertainties from which the 90% C.L. limits were derived using the prescription in the reference of Feldman et al. (1998).

Table 5.2  $\Delta\chi^2$  as a function of confidence level and number of degrees of freedom (Teukolsky et al., 1992)

C.L.	N.D.F					
	1	2	3	4	5	6
68.3 %	1.00	2.30	3.53	4.72	5.89	7.04
90 %	2.71	4.61	6.25	7.78	9.24	10.6
95.4 %	4.00	6.17	8.02	9.70	11.3	12.8
99 %	6.63	9.21	11.3	13.3	15.1	16.8
99.73 %	9.00	11.8	14.2	16.3	18.2	20.1
99.99 %	15.1	18.4	21.1	23.5	25.7	27.8

The constraints on the parameters in this work are expressed either as "best-fit  $\pm$  statistical  $\pm$  systematic uncertainties" at 1  $\sigma$  level (68.3% confidence level) or as upper and lower limits at 2  $\sigma$  level (90% confidence level). The 1  $\sigma$  level corresponds to

$\chi_{min}^2 + 1$  in a one-dimensional analysis and  $\chi_{min}^2 + 2.3$  in a two-dimensional analysis while the  $2\sigma$  level corresponds to  $\chi_{min}^2 + 2.71$  in a one-dimensional and  $\chi_{min}^2 + 4.61$  in a two-dimensional analysis as is given by Table 5.2.

## 5.1 NSI Analysis Results

The differential scattering cross sections for the scalar, pseudoscalar and tensorial NSI of  $\bar{\nu}_e$  scattered off  $e^-$  using  $CsI(Tl)$  as a target at some specific coupling parameters are shown in Figure 5.3 as a function of the electron recoil kinetic energy. All of which show similar behavior to the SM vector-axialvector coupling of  $\bar{\nu}_e$  to  $e^-$ . This makes it an advantage to work upon NSI of neutrino in the low energy region where the SM effects were measured with good accuracy.

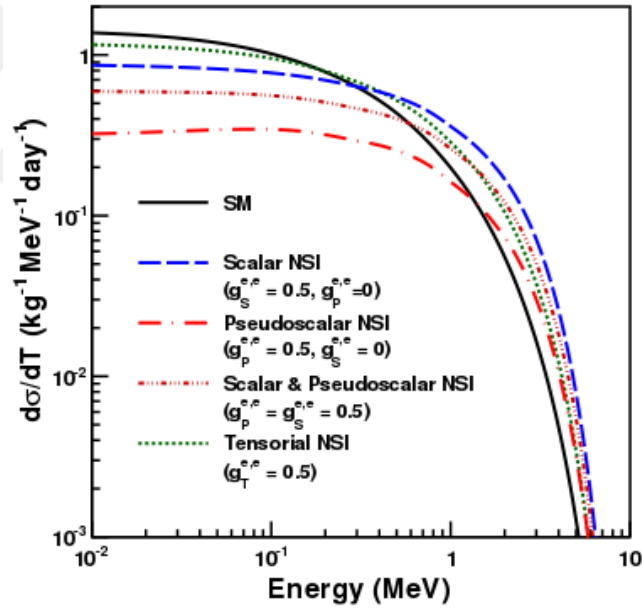


Figure 5.3 Differential cross section as a function of the recoil energy  $T$  with typical reactor  $\bar{\nu}_e$  spectra for scalar, pseudoscalar and tensorial NSIs

And by a two-dimensional analysis of NSI of neutrinos, the 90% C.L. allowed regions in  $g_S^{e,e} - g_P^{e,e}$  and  $\{g_S^{e,e}, g_P^{e,e}\} - (g_T^{e,e})^2$  parameter spaces as well as the upper bounds of  $g_T^{e,e}$  as a function of  $\{g_S^{e,e}, g_P^{e,e}\}$  are displayed respectively in Figure 5.4 (b), (c) and (d), where the TEXONO and LSND contributions are superimposed. Clearly, TEXONO

data sets give more accurate limits on the corresponding NSI parameters compared to those from LSND experiment.

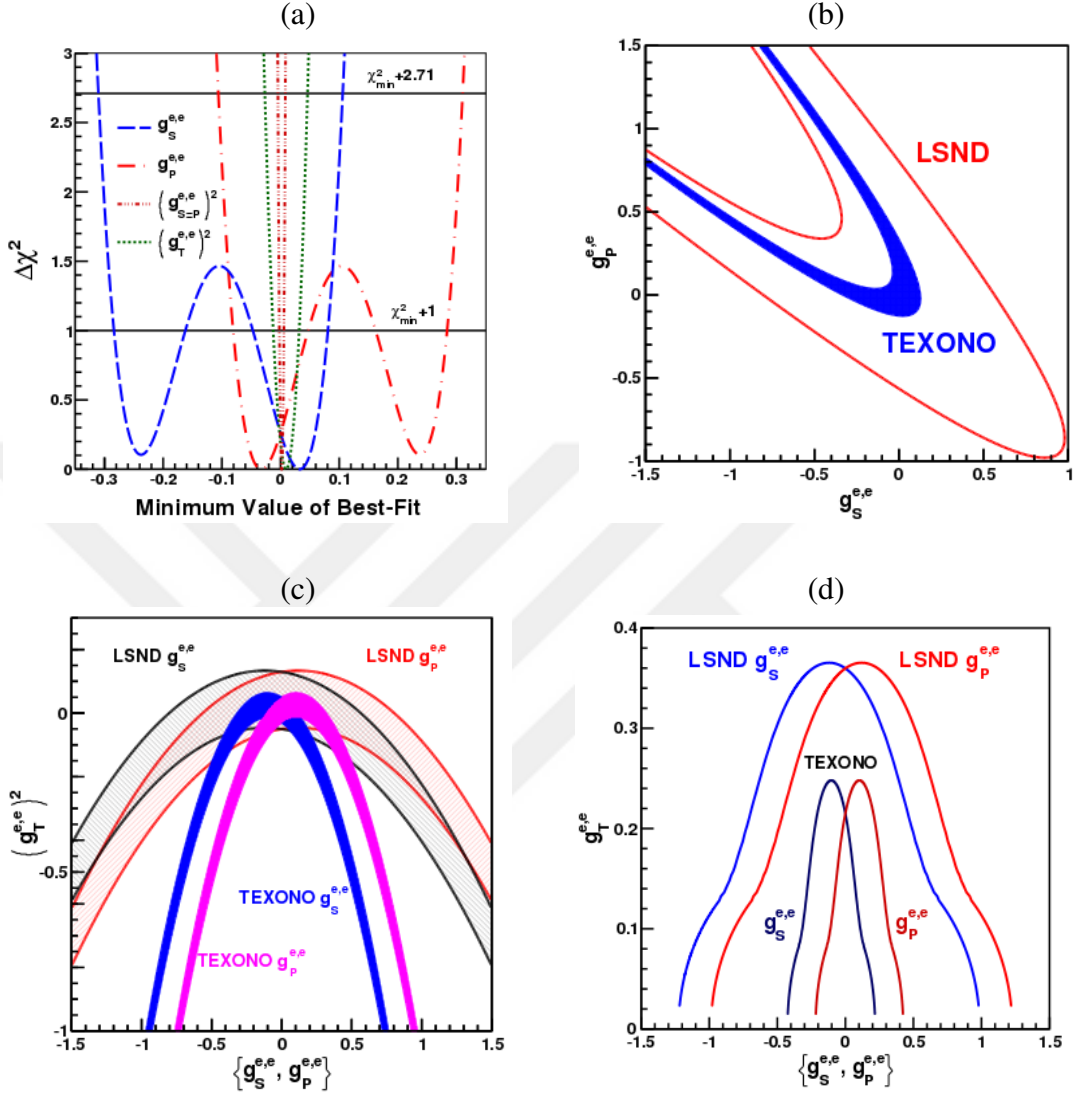


Figure 5.4 (a)  $\Delta\chi^2$  of one-parameter-at-a-time analysis for  $g_{S,P}^{e,e}$ ,  $(g_{S-P}^{e,e})^2$  and  $(g_T^{e,e})^2$ , the 90% C.L. allowed regions from TEXONO and LSND data sets in the parameter spaces of (b)  $g_S^{e,e} - g_P^{e,e}$  and (c)  $g_S^{e,e} (g_P^{e,e}) - (g_T^{e,e})^2$ , and (d) the 90% C.L. upper limits of  $g_T^{e,e}$  as a function of  $g_S^{e,e}$  and  $g_P^{e,e}$

By adopting a parameter-at-a-time analysis, the best fit results and the 90% C.L. bounds of the scalar ( $g_S^{e,e}$ ), pseudoscalar ( $g_P^{e,e}$ ) and tensorial ( $g_T^{e,e}$ ) NSI coupling parameters using TEXONO and LSND data sets are summarized in Table 5.3 with the behavior of  $\Delta\chi^2$  for the different NSI parameters shown in Figure 5.4 (a). As is expected, the bounds put by both experiments on the NSI parameters are in a good agree-

ment with each other, minding that the bound ranges put by TEXONO experiment are more precise compared to those from LSND experiment.

Table 5.3 Bounds on NSI parameters from a one-dimensional analysis using TEXONO and LSND data sets

NSI Parameters	TEXONO			LSND	
	Best Fit Measurements ( $1\sigma$ )	$\chi^2/\text{ndf}$	90% C.L. Limits	Best Fit Measurements ( $1\sigma$ )	90% C.L. Limits
Scalar $g_S^{e,e} (g_P^{e,e} = 0)$	$g_S^{e,e} = [3.27 \pm 6.39 \pm 3.10] \times 10^{-2}$	8.7/9	$-0.317 < g_S^{e,e} < 0.113$	$g_S^{e,e} = 0.27 \pm 0.59 \pm 0.26$	$-0.880 < g_S^{e,e} < 0.642$
Pseudo-scalar $g_P^{e,e} (g_S^{e,e} = 0)$	$g_P^{e,e} = [-3.27 \pm 6.39 \pm 3.10] \times 10^{-2}$	8.7/9	$-0.113 < g_P^{e,e} < 0.317$	$g_P^{e,e} = -0.27 \pm 0.59 \pm 0.26$	$-0.642 < g_P^{e,e} < 0.880$
$g_{S=P}^{e,e} (g_S^{e,e} = g_P^{e,e})$	$(g_{S=P}^{e,e})^2 = [0.19 \pm 0.38 \pm 0.31] \times 10^{-2}$	8.7/9	$ g_{S=P}^{e,e}  < 0.100$	$(g_{S=P}^{e,e})^2 = [3.47 \pm 4.78 \pm 4.36] \times 10^{-2}$	$ g_{S=P}^{e,e}  < 0.375$
Tensorial $g_T^{e,e}$	$(g_T^{e,e})^2 = [0.96 \pm 2.21 \pm 1.82] \times 10^{-2}$	8.7/9	$ g_T^{e,e}  < 0.238$	$(g_T^{e,e})^2 = [3.96 \pm 5.47 \pm 4.97] \times 10^{-2}$	$ g_T^{e,e}  < 0.401$

## 5.2 $SU(5)$ LTHM Analysis Results

The exclusion region for the mixing angle  $c$  of the  $SU(5)$  LTHM in the gauge sector is given in Figure 5.5 by EWPD, where an exclusion limit of  $f \leq 5100 \text{ GeV}$  has been put at 95% C.L. for the LTHM scale  $f$ .

The differential scattering cross sections of the  $SU(5)$  LTHM for the light, heavy and interference terms using  $CsI(Tl)$  as a target at some specific parameters are shown in Figure 5.6 as a function of the electron recoil kinetic energy. All of which show similar behavior to the SM vector-axialvector coupling of  $\bar{\nu}_e$  to  $e^-$ . This makes it an advantage again to work upon LTHM in the low energy region where the SM effects were measured with good accuracy.

By a two-dimensional analysis, the allowed regions given by TEXONO and LSND at 90% C.L. in  $c^2 - c'^2$  parameter space at  $f = 500 \text{ GeV}$  and  $f = 2 \text{ TeV}$  are given by Figure 5.7 (a) and (c), respectively. Hence then by some analytic method, the

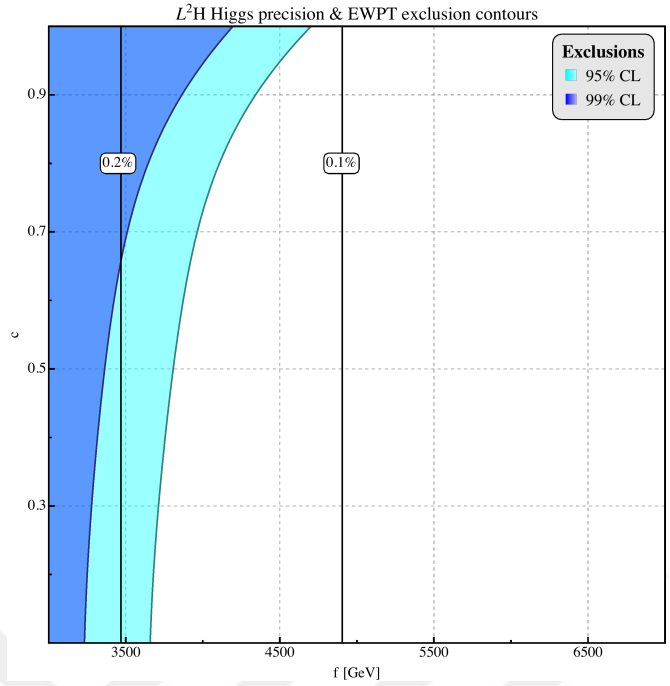


Figure 5.5 Exclusion limits at 95% C.L. (light blue) and 99% C.L. (dark blue) from EWPD and Higgs data combined as a function of the  $SU(5)$  LTHM scale  $f$  with the thick black lines represent contours of required fine-tuning (Reuter et al., 2013)

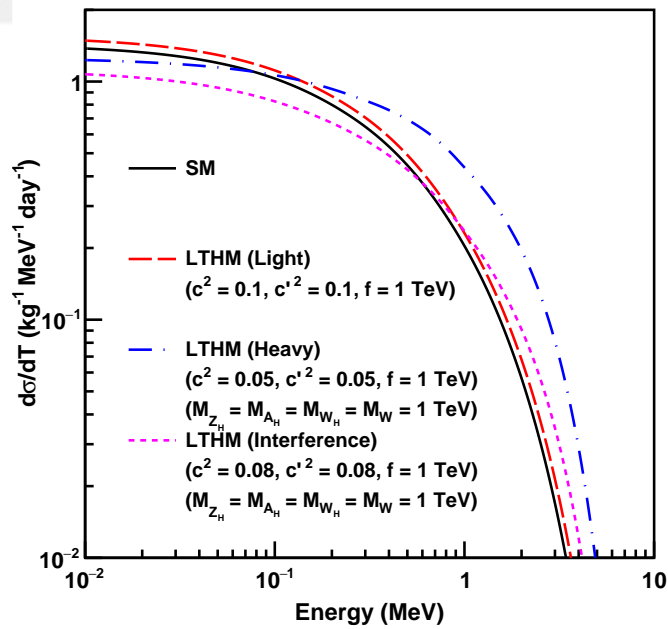


Figure 5.6 Differential cross section as a function of the recoil energy  $T$  with typical reactor  $\bar{\nu}_e$  spectra for  $SU(5)$  LTHM

corresponding upper and lower limits in  $c - c'$  parameter space have been achieved as is shown in Figure 5.7 (b) and (d) for  $f = 500 \text{ GeV}$  and  $f = 2 \text{ TeV}$ , respectively. The contributions from LEP and EWPD experiments have been also superimposed for comparison.

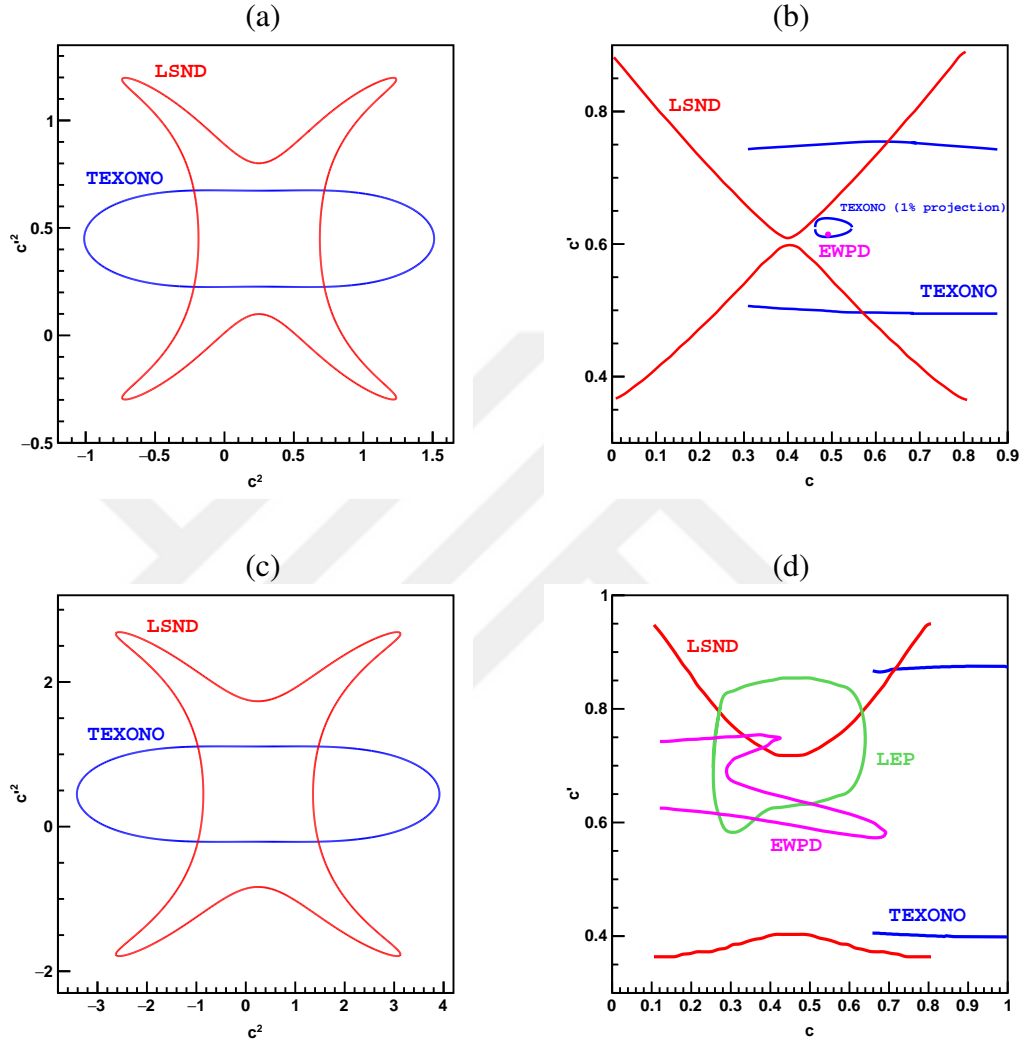


Figure 5.7 The 90% C.L. allowed regions in the  $(c^2, c'^2)$  parameter space for FC  $SU(5)$  LTHM at (a)  $f = 500 \text{ GeV}$  and (c)  $f = 2 \text{ TeV}$  with their corresponding upper and lower bounds in the  $(c, c')$  parameter space given by (b) and (f) respectively from TEXONO and LSND data sets

Clearly from Figure 5.7 (b), the limits put by TEXONO on  $c'$  are roughly constant with about 0.75 as an upper limit and 0.5 as a lower limit. But the limits put on  $c$  vary widely starting about 0.3 as a lower limit reaching 0.88 as an upper limit. On the other hand, the upper and lower limits put by LSND both change significantly

until around  $c = 0.4$  where they give the best limit on  $c'$  roughly as  $0.59 < c' < 0.61$  before continuing to change again. Furthermore, reducing the errors of TEXONO experimental measured values to 1% (which can be and have been actually done by some sort of reducing the background events) shows a good agreement with EWPD result given roughly as  $(0.5, 0.6)$ , a result that takes us back to the SM.

Comparing Figures 5.7 (b) and (d) deduces that as  $f$  increases, both the upper and lower bounds of  $c$  and  $c'$  given by all the experiments deteriorate especially for TEXONO being a low energy experiment.

Moreover, by a one-dimensional analysis, the allowed ranges of  $c$  and  $c'$  by a global analysis from TEXONO and LSND experiments at 90% are listed in Table 5.4. Once again the bounds show a similar behavior with the increase of  $f$  as was seen in the previous two-dimensional analysis.

Table 5.4 Global bounds from TEXONO and LSND experimental data on  $c$  and  $c'$  as a function of  $f$  ranges at 90% C.L. via a one-dimensional statistical analysis

$f$	$c(c' = 0.6)$	$c'(c = 0.5)$
$500 \text{ GeV} \leq f \leq 1 \text{ TeV}$	$0.63 \leq  c  \leq 0.82$	$0.65 \leq  c'  \leq 0.69$
$1 \text{ TeV} \leq f \leq 2 \text{ TeV}$	$0.61 \leq  c  \leq 0.99$	$0.60 \leq  c'  \leq 0.75$
$2 \text{ TeV} \leq f \leq 3 \text{ TeV}$	$0.60 \leq  c  \leq 0.99$	$0.60 \leq  c'  \leq 0.80$
$3 \text{ TeV} \leq f \leq 4 \text{ TeV}$	$0.40 \leq  c  \leq 0.99$	$0.60 \leq  c'  \leq 0.85$
$f \geq 4 \text{ TeV}$	$0.15 \leq  c  \leq 0.99$	$0.40 \leq  c'  \leq 0.90$

### 5.3 SU(3) SLHM Analysis Results

The exclusion region for the mixing angle  $t_\beta$  of the  $SU(3)$  SLHM in the gauge sector is given in Figure 5.8 by EWPD, where an exclusion limit of  $f \leq 3200 \text{ GeV}$  has been put at 95% C.L. for the SLHM scale  $f$ .

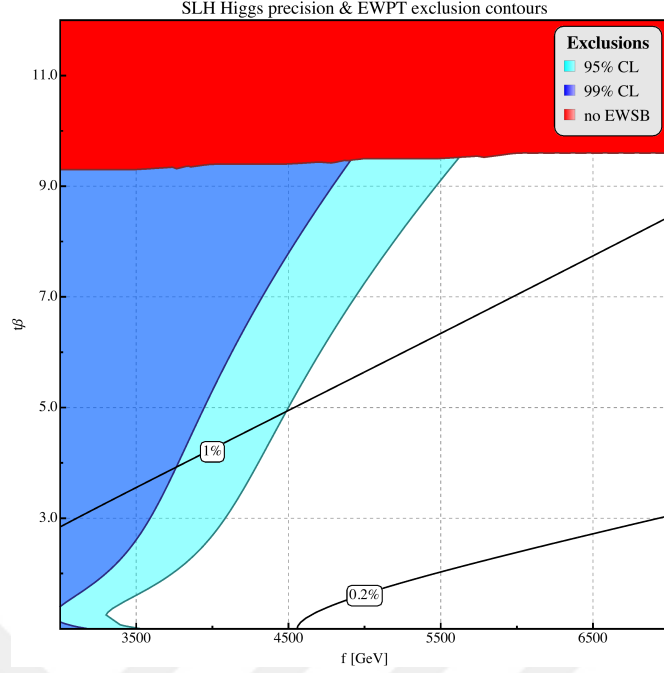


Figure 5.8 Exclusion limits at 95% C.L. (light blue) and 99% C.L. (dark blue) from EWPD and Higgs data combined as a function of the  $SU(3)$  SLHM scale  $f$  with the thick black lines represent contours of required fine-tuning (Reuter et al., 2013)

Through a two-dimensional analysis, the upper and lower limits put respectively by TEXONO and LSND experiments on the mixing angle  $t_\beta$  at 90% C.L. are shown in Figure 5.9 as a function of the energy scale  $f$ . Again as  $f$  increases both limits given by both experiments get worse and worse.

Table 5.5 Global bounds from TEXONO and LSND experimental data on  $t_\beta$  as a function of  $f$  ranges at 90% C.L. via a one-dimensional statistical analysis

$f$	$t_\beta$
$500 \text{ GeV} \leq f \leq 1 \text{ TeV}$	$2.07 \leq t_\beta \leq 4.51$
$1 \text{ TeV} \leq f \leq 2 \text{ TeV}$	$1.26 \leq t_\beta \leq 5.33$
$2 \text{ TeV} \leq f \leq 3 \text{ TeV}$	$0.70 \leq t_\beta \leq 5.72$
$f \geq 3 \text{ TeV}$	$0.40 \leq t_\beta \leq 5.79$

Moreover, by a one-dimensional analysis, the allowed ranges of  $t_\beta$  by a global anal-

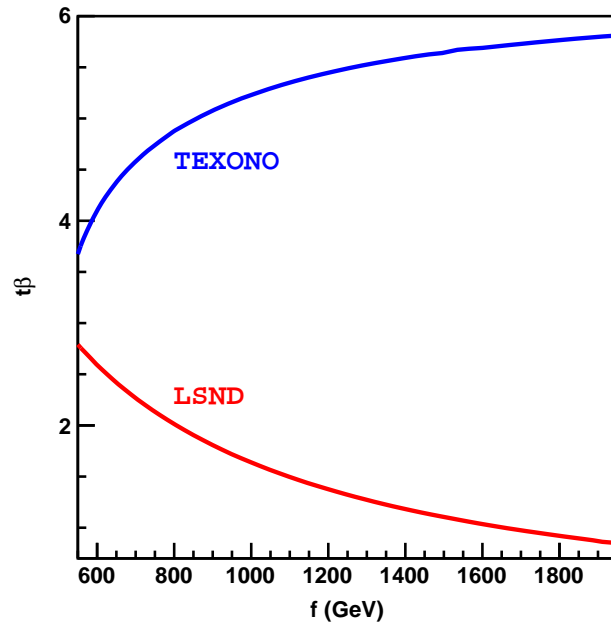


Figure 5.9 The upper and lower limits at 90% C.L. on  $t_\beta$  versus  $f$  from TEXONO and LSND experimental measured values, respectively

ysis from TEXONO and LSND experiments at 90% are listed in Table 5.5. Once again the bounds show a similar behavior with the increase of  $f$  as was seen in the previous two-dimensional analysis.

## CHAPTER SIX

### CONCLUSION AND PROSPECTS

Why we need new physics?, which are the open questions that the SM leave unanswered? and how new theories attempt to answer them? are the main questions that we tackled in this thesis work. More precisely, we have described the unfortunate theoretical limitations of the SM and discussed new phenomena, beyond the normal ones described by the SM, that have been proposed to overcome such limitations using a particular BSM theory as an example. Although there are no hints for new physics BSM in the collider experiments today, the urge to find new physics is always present.

The SM was our starting point in Chapter 2. It describes the world as it is known today with an astonishing precision, introducing matter particles and force carrier particles known as the gauge bosons. All these particles have been observed experimentally with the last one being the Higgs boson, a new piece of nature which was discovered a few years ago. With the Higgs boson, the SM is a weakly coupled elegant theory that fits almost all the data from any experiment ever done on Earth.

Despite its great success, the SM remains only a piece in a bigger puzzle or, in other words, an effective theory in a more fundamental theory. In fact, it leaves many problems unsolved. One of the problems and as a focal point in this work was the hierarchy problem of the SM Higgs boson mass. The SM does not explain why the Higgs boson is measured to be so light while at the same time quantum corrections to its propagator boost its mass to much higher values.

A lot of thought has been given to this and other problems the SM comes with and ways to mitigate them have been attempted by theorists all over the world. Theorists have come up with many theories or models in many variance trying to address one or more problems of the SM at a time. In some of them, they introduce extra space-time dimensions as a way to explain why gravity is a much weaker force than the other fundamental forces. In such theories, hypothetical force carrier particles called

gravitons could be disappearing into extra dimensions after having been created, for example, via the proton-proton collision at the LHC. There are many other theories or models that introduce new particles or interactions. Common in many of these theories is the presence of new heavy bosons similar to the  $W$  and  $Z$  bosons.

A large theoretical framework of BSM physics that has been developed in the last decades is LHMs. It is currently one of the most discussed and studied BSM theories in the literature. Many different variations of LHMs exist; the most fundamental of which are the  $SU(5)$  LTHM and the  $SU(3)$  SLHM which are two concrete examples of a product group symmetry and a simple group symmetry, respectively. All of these models were built on the core idea that the Higgs boson is a PGB that arises from spontaneous symmetry breaking. Hence then, by the mechanism of collective symmetry breaking, the quadratic divergences to the Higgs mass cancel completely or partially between the SM gauge bosons and the new heavy expected bosons leaving the mass of the Higgs as light as it was experimentally observed.

Theoretically, in Chapter 4, we have calculated the contributions from the  $SU(5)$  LTHM and the  $SU(3)$  SLHM to  $\nu_e(\bar{\nu}_e) + e \rightarrow \nu_\alpha(\bar{\nu}_\alpha) + e$  differential scattering cross section, where  $\alpha = e$  and  $\alpha \neq e$  correspond respectively to the FC and FV sectors of the LHM of interest. These contributions come mainly from correction terms of the SM couplings in addition to some slight corrections of new heavy gauge bosons which are negligible and can be safely ignored. In general, both the  $SU(5)$  LTHM and the  $SU(3)$  SLHM differential cross section for FC and FV (anti)neutrino-electron scattering can be expressed in the electron rest frame as

$$\left[ \frac{d\sigma}{dT}(\bar{\nu}_e e) \right] = \frac{2G_F^2 m_e}{\pi} \left[ a_{L(H)}^2 + b_{L(H)}^2 \left( 1 - \frac{T}{E_\nu} \right)^2 - a_{L(H)} b_{L(H)} \frac{m_e T}{E_\nu^2} \right], \quad (6.1)$$

where the coefficients  $a_L$  and  $b_L$  of the  $SU(5)$  LTHM are given in Table 6.1 in terms of the correction terms of the SM  $Z\nu_e\bar{\nu}_e$ ,  $Z e_L \bar{e}_L$ ,  $Z e_R \bar{e}_R$  and  $W e \bar{\nu}_e$  couplings found

Table 6.1 Coefficients in the expression of the FC and FV  $SU(5)$  LTHM differential cross section of  $(\bar{\nu}_e e)$  scattering given by Equation 6.1

	Process	$a_L$	$b_L$	$a_H$	$b_H$
FC	$\bar{\nu}_e + e \rightarrow \bar{\nu}_e + e$	$(1+B)(g_R + \delta g_R)$	$(1+B)(g_L + \delta g_L) + (1 + \delta g'_L)^2$	$2C_2$	$C_1 + C_2 + C_3$
	$\nu_e + e \rightarrow \nu_e + e$	$(1+B)(g_L + \delta g_L) + (1 + \delta g'_L)^2$	$(1+B)(g_R + \delta g_R)$	$C_1 + C_2 + C_3$	$2C_2$
FV ( $\alpha \neq e$ )	$\bar{\nu}_e + e \rightarrow \bar{\nu}_\alpha + e$	$(1+B)(g_R + \delta g_R)$	$(1+B)(g_L + \delta g_L)$	$2C_2$	$C_1 + C_2$
	$\nu_e + e \rightarrow \nu_\alpha + e$	$(1+B)(g_L + \delta g_L)$	$(1+B)(g_R + \delta g_R)$	$C_1 + C_2$	$2C_2$

respectively as

$$\begin{aligned}
 B &= 2 \frac{v^2}{f^2} \left[ \frac{1}{4} c^2 (c^2 - s^2) + \frac{5}{2} (c'^2 - s'^2) \left( -\frac{1}{5} + \frac{c'^2}{2} \right) \right], \\
 \delta g_L &= -\frac{v^2}{f^2} \left[ \frac{1}{4} c^2 (c^2 - s^2) - \frac{5}{2} (c'^2 - s'^2) \left( -\frac{1}{5} + \frac{c'^2}{2} \right) \right], \\
 \delta g_R &= 5 \frac{v^2}{f^2} (c'^2 - s'^2) \left( -\frac{1}{5} + \frac{c'^2}{2} \right), \\
 \delta g'_L &= -\frac{1}{2} \frac{v^2}{f^2} c^2 (c^2 - s^2),
 \end{aligned} \tag{6.2}$$

and the coefficients  $a_H$  and  $b_H$  in terms of some new corrections of  $Z_H$ ,  $A_H$  and  $W_H$  found respectively as

$$\begin{aligned}
 C_1 &= -\frac{1}{2} \frac{c^2}{s^2} \left( \frac{M_W}{M_{Z_H}} \right)^2, \\
 C_2 &= t_W^2 \frac{\left( -\frac{1}{5} + \frac{1}{2} c'^2 \right) \left( -\frac{2}{5} + c'^2 \right)}{(s'c')^2} \left( \frac{M_W}{M_{A_H}} \right)^2, \\
 C_3 &= \frac{c^2}{s^2} \left( 1 + \frac{1}{2} \frac{v^2}{f^2} s^2 (c^2 - s^2) \right)^2 \left( \frac{M_W}{M_{W_H}} \right)^2 \approx \frac{c^2}{s^2} \left( \frac{M_W}{M_{W_H}} \right)^2,
 \end{aligned} \tag{6.3}$$

as well as the coefficients  $a_L$ ,  $b_L$  of the  $SU(3)$  SLHM are given in Table 6.2 in terms of the correction terms of the SM  $Z\nu_e\bar{\nu}_e$ ,  $Z_L\bar{e}_L$ ,  $Z_R\bar{e}_R$  and  $W_e\bar{\nu}_e$  couplings calculated

Table 6.2 Coefficients in the expression of the FC and FV  $SU(3)$  SLHM differential cross section of  $\nu_e (\bar{\nu}_e) e$  scattering given by Equation 6.1

	Process	$a_L$	$b_L$	$a_H$	$b_H$
FC	$\bar{\nu}_e + e \rightarrow \bar{\nu}_e + e$	$(1+B)(g_R + \delta g_R)$	$(1+B)(g_L + \delta g_L) + (1 + \delta g'_L)^2$	$C_1$	$C_3 - C_2$
	$\nu_e + e \rightarrow \nu_e + e$	$(1+B)(g_L + \delta g_L) + (1 + \delta g'_L)^2$	$(1+B)(g_R + \delta g_R)$	$C_3 - C_2$	$C_1$
FV ( $\alpha \neq e$ )	$\bar{\nu}_e + e \rightarrow \bar{\nu}_\alpha + e$	$(1+B)(g_R + \delta g_R)$	$(1+B)(g_L + \delta g_L)$	$C_1$	$-C_2$
	$\nu_e + e \rightarrow \nu_\alpha + e$	$(1+B)(g_L + \delta g_L)$	$(1+B)(g_R + \delta g_R)$	$-C_2$	$C_1$

respectively as

$$\begin{aligned}
 B &= -\frac{1}{2} \frac{v^2}{f^2} \left[ \frac{1}{t_\beta^2} + \frac{(1-t_w^2) \left(\frac{1}{2} - s_w^2\right)}{2c_w^2} \right], \\
 \delta g_L &= -\frac{1}{8} \frac{v^2}{f^2} \frac{(1-t_w^2) \left(\frac{1}{2} - s_w^2\right)}{c_w^2}, \\
 \delta g_R &= \frac{1}{8} \frac{v^2}{f^2} (1-t_w^2) t_w^2, \\
 \delta g'_L &= -\frac{1}{4} \frac{v^2}{f^2} \frac{1}{t_\beta^2},
 \end{aligned} \tag{6.4}$$

and the coefficients  $a_H$  and  $b_H$  expressed in terms of new corrections from  $Z'$  and  $X$  are also calculated as

$$\begin{aligned}
 C_1 &= 2 \frac{\left(\frac{1}{2} - s_w^2\right)^2}{c_w^2 (3 - 4s_w^2)} \left(\frac{M_W}{M_{Z'}}\right)^2, \\
 C_2 &= -\frac{1}{2} \frac{1}{t_\beta^2} \frac{v^2}{f^2} \left(\frac{M_W}{M_X}\right)^2, \\
 C_3 &= 2 \frac{\left(\frac{1}{2} - s_w^2\right) t_w^2}{3 - 4s_w^2} \left(\frac{M_W}{M_{Z'}}\right)^2.
 \end{aligned} \tag{6.5}$$

Then, by comparing our numerical results with the TEXONO and LSND experimental measured values, we have obtained some precise bounds on the free parameters of our models. The related results from LEP and EWPD experiments have been also

superimposed to get a more stringent limits for the free parameters. As was presented in Chapter 5, high energy experiments were able to put more precise limits on the corresponding parameters compared to those from low energy experiments, and this is mainly to achieve a weakly coupled theory from a high energy scale  $f$  of the LHMs.

In the subsequent work, our numerical results from the  $SU(5)$  LTHM and the  $SU(3)$  SLHM are going to be also compared with data from CHARM-II and Borexino experiments to even achieve more precise limits on the relevant free parameters, which might be compatible with those from the EWPD and flavor data. Moreover, three other product gauge group LHMs found in the literature (known as  $SU(5)$  LTHM with T-parity,  $SU(6)$  LHM and  $SU(2)_C$  LTHM) and two other simple gauge group LHMs (known as  $SU(4)$  SLHM and  $SU(9)$  SLHM) are going to be also theoretically and analytically carefully studied via neutrino-electron elastic scattering channel at low energy.

## REFERENCES

- Aguila, F.D., Illana, J.I., & Jenkins, M.D. (2011). Lepton flavor violation in the simplest little Higgs model. *JHEP*, 1103, 080.
- Aliev, T. & Çakır, O. (2008). Probing little Higgs model in  $e^+e^- \rightarrow \nu\bar{\nu}\gamma$  process. *Eur. Phys. J., C* 54, 149-158.
- Arkani-Hamed, N., Cohen, A.G., Katz, E., & Nelson, A.E. (2002). The lightest Higgs. *JHEP*, 0207, 034.
- [ATLAS collaboration] (2012). Observation of a new particle in the search for the standard model Higgs boson with the ATLAS detector at the LHC. *Phys. Lett. B*, 716, 1, 1-29.
- Auerbach, L.B., et al. [LSND collaboration] (2001). Measurement of electron-neutrino electron elastic scattering. *Phys. Rev. D*, 63, 112001.
- Barranco, J., Bolaños, A., Garcés, E.A., Miranda, O.G., & Rashba, T.I. (2012). Tensorial NSI and unparticle physics in neutrino scattering. *Int. J. Mod. Phys., A* 27, 1250147.
- Barranco, J., Bolaños, A., Miranda, O.G., Moura, C.A., & Rashba, T.I. (2009). Unparticle physics and neutrino phenomenology. *Phys. Rev. D*, 79, 073011.
- Barranco, J., Miranda, O.G., Moura, C.A., & Valle, J.W.F. (2006). Constraining non-standard interactions in  $\nu_e e$  or  $\bar{\nu}_e e$  scattering. *Phys. Rev. D*, 73, 113001.
- Barranco, J., Miranda, O.G., Moura, C.A., & Valle, J.W.F. (2008). Constraining non-standard neutrino-electron interactions. *Phys. Rev. D*, 77, 093014.
- Barranco, J., Miranda, O.G., & Rashba, T.I. (2008). *Phys. Lett. B*, 662, 431.
- Bilmiş, S., Deniz, M., Li, H.B., Li, J., Liao, H.Y., Lin, S.T., Singh, V., Wong, H.T.,

- Yıldırım, I.O., Yue, Q., & Zeyrek, M. (2012). Constraints on a noncommutative physics scale with neutrino-electron scattering. *Phys. Rev. D*, 85, 073011.
- Bilmiş, S., Turan, I., Aliev, T.M., Deniz, M., Singh, L., & Wong, H.T. (2015). Constraints on dark photon from neutrino-electron scattering experiments. *Phys. Rev. D*, 92, 033009.
- Capozzi, F., Lisi, E., Marrone, A., Montanino, D., & Palazzo, A. (2016). Neutrino masses and mixings: status of known and unknown 3 $\nu$  parameters. *Nucl. Phys. B*, 908, 218-234.
- Chen, J.W., Chi, H.C., Li, H.B., Liu, C.P., Singh, L., Wong, H.T., Wu, C.L., & Wu, C.P. (2014). Constraints on millicharged neutrinos via analysis of data from atomic ionizations with germanium detectors at sub-keV sensitivities. *Phys. Rev. D*, 90, 011301(R).
- [CMS collaboration] (2012). Observation of a new boson at a mass of 125 GeV with the CMS experiment at the LHC. *Phys. Lett. B*, 716, 1, 30-61.
- Cottingham, W.N. & Greenwood, D.A. (2007). *An introduction to the standard model of particle physics, 2nd edition*. Cambridge University Press, Cambridge.
- Dawson, S. (1999). Introduction to electroweak symmetry breaking. arXiv:hep-ph/9901280v1 [hep-ph].
- Demirci, M. (2015). *Proton-proton çarpışmasında nötralino ve chargino üretimi*. Ph.D. Thesis, Karadeniz Technical University, Turkey.
- Deniz, M., et al. [TEXONO collaboration] (2010). Constraints on nonstandard neutrino interactions and unparticle physics with  $\bar{\nu}_e - e^-$  scattering at the Kuo-Sheng nuclear power reactor. *Phys. Rev. D*, 82, 033004.
- Deniz, M., et al. (2010). Measurement of  $\nu_e - e$  scattering cross-section with a CsI(Tl) scintillating crystal array at the Kuo-Sheng nuclear power reactor. *Phys. Rev. D*, 81, 072001.

- Deniz, M., Sevda, B., Kerman, S., Ajjaq, A., Singh, L., Wong, H.T., & Zeyrek, M. (2017). Constraints on scalar-pseudoscalar and tensorial non-standard interaction and tensorial unparticle couplings from neutrino-electron scattering. *Phys. Rev. D*, 95, 033008.
- Englert, F. & Brout, R. (1964). Broken symmetry and the mass of gauge vector mesons. *Phys. Rev. Lett.*, 13, 9, 321-323.
- Erlar, J. & Langacker, P. (2008). Standard model and related topics. *Phys. Lett. B*, 667, 125, and references therein.
- Esteban, I., Gonzalez-Garcia, M.C., Maltoni, M., Martinez-Soler, I., & Schwetz, T. (2017). Updated fit to three neutrino mixing: exploring the accelerator-reactor complementarity. *JHEP*, 1701, 087.
- Ettefaghi, M.M. & Shakouri, T. (2010). Neutrino-electron scattering in noncommutative space. *JHEP*, 1011, 131.
- Fehling, D. (2008). The standard model of particle physics: a lunchbox's guide. The Johns Hopkins University. *File:StandardModelofElementaryParticles.svg*.
- Feldman, G.J. & Cousins, R.D. (1998). Unified approach to the classical statistical analysis of small signals. *Phys. Rev. D*, 57, 3873.
- Formaggio, J.A. & Zeller, G.P. (2012). From eV to EeV: neutrino cross sections across energy scales. *Rev. Mod. Phys.*, 84, 1307.
- Galtán, R., Garcés, E.A., Miranda, O.G., & Montes de Oca Y, J.H. (2013). Scalar-pseudoscalar interactions in neutrino-electron scattering. *Int. J. Mod. Phys., A* 28, 1350124.
- Glashow, S.L. (1961). Partial-symmetries of weak interactions. *Nucl. Phys.*, 22, 579-588.
- Gouvea, A.D. & Jenkins, J. (2006). What can we learn from neutrino electron scattering? *Phys. Rev. D*, 74, 033004.

- Griffiths, D.J. (2008). *Introduction to elementary particles, 2nd edition*. Weinheim: Wiley-VCH.
- Han, T., Logan, H.E., McElrath, B., & Wang, L.T. (2004). Phenomenology of the little Higgs model. *Phys. Rev. D*, *67*, 095004.
- Han, T., Logan, H.E., & Wang, L.T. (2006). Smoking gun signatures of little Higgs models. *JHEP*, *099*, 01.
- Higgs, P.W. (1964). Broken symmetries, massless particles and gauge fields. *Phys. Rev. Lett.*, *12*, 132-133.
- Hooft, G. (1971). Prediction for neutrino-electron cross-sections in Weinberg's model of weak interactions. *Phys. Lett. B*, *37*, 195.
- Kaplan, D.E. & Schmaltz, M. (2003). The little Higgs from a simple group. *JHEP*, *0310*, 039.
- Kayser, B., Fischbach, E., Rosen, S.P., & Spivack, H. (1979). Charged- and neutral-current interference in  $\nu_e - e$  scattering. *Phys. Rev. D*, *20*, 87.
- Khan, A.N. & Tahir, F. (2011). Absolute values of nonstandard interaction parameters in  $\nu_e e$  and  $\bar{\nu}_e e$ -scatterings. arXiv:1102.1869v2 [hep-ph].
- Khan, A.N. & Tahir, F. (2011). Nonstandard interactions and interference effect in low energy  $\nu_e e$ -scattering process. arXiv:1101.3191v2 [hep-ph].
- Lewis, G.M. (1970). *Neutrinos, 1st edition*. Wykeham, London, p. 30.
- Maarten, B. (2004). The hierarchy problem in the SM and little Higgs theories. *Research Gate*.
- Marciano, W.J. & Parsa, Z. (2003). Neutrino-electron scattering theory. *J. Phys. G*, *29*, 2629-2645.
- Mertig, R., Böhm, M., & Denner, A. (1991). Feyn Calc - Computer-algebraic calcula-

- tion of Feynman amplitudes. *Comput. Phys. Commun.*, 64, 345-359.
- Miranda, O.G. & Nunokawa, H. (2015). Non standard neutrino interactions: current status and future prospects. *New Journal of Physics*, 17(9), 095002.
- Na, L., Chong-Xing, Y., & Xu-Xin, L. (2011). Neutrino-electron scattering and the little Higgs models. *Chin. Phys. Lett.*, 28(10), 107305, and references therein.
- Ohlsson, T. (2013). Status of non-standard neutrino interactions. *Rep. Prog. in Phys.*, 76, 044201.
- Panman, J. & Langacker, P. (1995). Precision tests of the standard electroweak model. *World Scientific* 504-544.
- Patrignani, C., et al. [particle data group] (2016). Review of particle physics. *Chin. Phys. C*, 40, 100001.
- Perelstein, M. (2007). Little Higgs models and their phenomenology. *Prog. Part. Nucl. Phys.*, 58, 247-291.
- Poschenrieder, A. (2007). The littlest Higgs and its phenomenological implications for flavor changing neutral currents and lepton flavor violating processes. *Technische Uni.*, D-85748, Garching.
- Reuter, J., Tonini, M., & De Vries, M. (2013). Little Higgs model limits from LHC. *JHEP*, 1307, 010.
- Salam, A. (1968). Svartholm, N., ed. Elementary particle physics: relativistic groups and analyticity. *8th nobel symposium*, Stockholm: Almquist & Wiksell, 367.
- Schmaltz, M. & Tucker-Smith, D. (2005). Little Higgs review. *Ann. Rev. Nucl. Part. Sci.*, 55, 229-270.
- Shtabovenko, V., Mertig, R., & Orellana, F. (2016). New developments in FeynCalc 9.0. *Phys. Commun.*, 207, 432-444.

Tanabashi, M., et al. [Particle Data Group] (2018). The Review of particle physics. *Phys. Rev. D* 98, 030001.

Teukolsky, S., Press, W.H., Vetterling, W.T., & Flannery, B.P. (1986). *The art of scientific computing, 3rd edition*. Numerical Recipes in C, Cambridge University Press, Cambridge.

Weinberg, S. (1967). A model of leptons. *Phys. Rev. Lett.*, 19, 1264.



## APPENDICES

### Appendix A: Differential Scattering Cross Section

Note that due to its convenience in relativistic quantum field theories,  $\hbar = c = 1$  have been used throughout this thesis work.

In the scope of scattering processes, the physical quantity of interest is usually the **scattering (differential) cross section** which is roughly the likely hood of some particular event to occur. It can be evaluated in either the laboratory frame where the target particle is at rest in a fixed target experiment or the center of mass frame where the colliding particles have equal but opposite momenta in a collider experiment.

The general form of the differential scattering cross section for any scattering process of the form

$$1 + 2 \rightarrow 3 + 4 + \dots + n$$

is given according to the famous Fermi's Golden Rule by the formula (Griffiths, 2008)

$$\begin{aligned} d\sigma &= |\mathcal{M}|^2 \times \text{phase space} \\ &= |\mathcal{M}|^2 \frac{S}{4\sqrt{(p_1 \cdot p_2)^2 - (m_1 m_2)^2}} (2\pi)^4 \delta^4(p_1 + p_2 - p_3 - \dots - p_n) \\ &\quad \times \prod_{j=3}^n 2\pi \delta(p_j^2 - m_j^2) \theta(p_j^0) \frac{d^4 p_j}{(2\pi)^4}, \end{aligned} \quad (\text{A.1})$$

where  $S = \frac{1}{s!}$  is a statistical factor that corrects for  $s$ -counting of identical particles in the final state,  $\mathcal{M}(p_1, p_2, p_3, \dots, p_n)$  is the corresponding amplitude that comprise all the dynamical facts of the process of interest,  $p$  is the four-momentum vector of the different particles and  $m$  is their corresponding mass. Note that the phase space that comprise all the kinematical facts of the process allows to integrate over all outgoing four-momenta subject to three kinematical constraints enforced by the delta and theta functions.

Solving for the constraints implied by the one-dimensional delta function together with the theta step function, we can rewrite the differential cross section of Equation A.1 as

$$d\sigma = |\mathcal{M}|^2 \frac{S}{4\sqrt{(p_1 \cdot p_2)^2 - (m_1 m_2)^2}} (2\pi)^4 \delta^4(p_1 + p_2 - p_3 - \dots - p_n) \times \prod_{j=3}^n \frac{1}{2\sqrt{|\vec{p}_j|^2 + m_j^2}} \frac{d^3 \vec{p}_j}{(2\pi)^3} \quad (\text{A.2})$$

due to the fact that

$$d^4 p = dp^0 d^3 \vec{p} \quad (\text{A.3})$$

and

$$\begin{aligned} & \delta(p^2 - m^2) \\ &= \delta\left[(p^0)^2 - (\vec{p})^2 - m^2\right] \\ &= \delta\left[(p^0)^2 - \left((\vec{p})^2 + m^2\right)\right] \\ &= \frac{1}{2\sqrt{|\vec{p}|^2 + m^2}} \left[ \delta\left(p^0 - \sqrt{|\vec{p}|^2 + m^2}\right) + \delta\left(p^0 + \sqrt{|\vec{p}|^2 + m^2}\right) \right], \end{aligned} \quad (\text{A.4})$$

where the second delta function is neglected by the constraint  $p^0 > 0$  set by the theta function.

Throughout this thesis work, however, we were interested in a two-body scattering process of the form

$$1 + 2 \rightarrow 3 + 4,$$

namely neutrino-electron elastic scattering process

$$\nu + e \rightarrow \nu + e$$

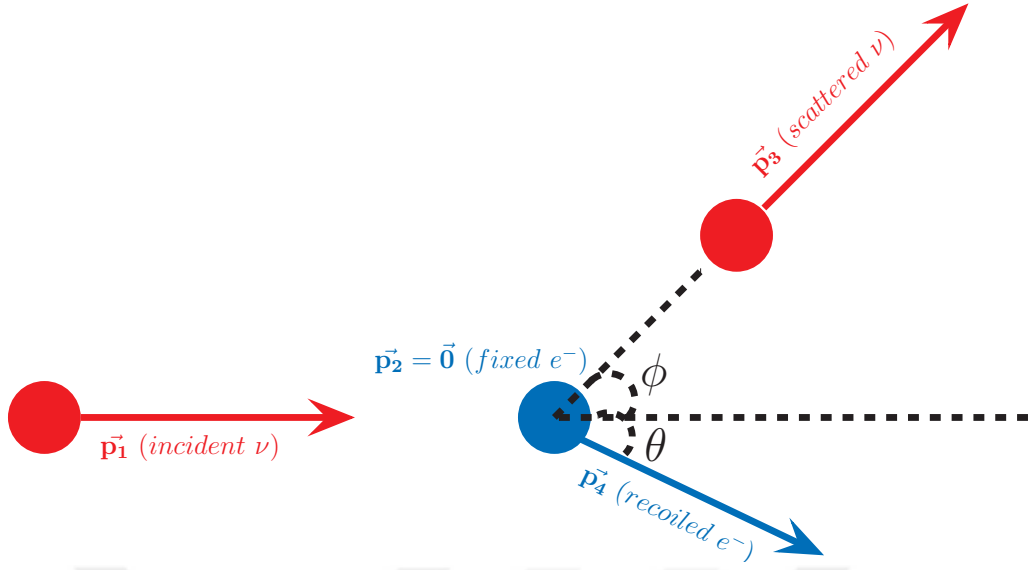


Figure A.1 A schematic diagram of neutrino-electron two-body collision in the lab frame

in the laboratory frame as is shown by Figure A.1.

In this case, the general differential cross section given by Equation A.2 is simply

$$\begin{aligned}
 d\sigma &= |\mathcal{M}|^2 \frac{1}{4\sqrt{(p_1 \cdot p_2)^2 - (m_1 m_2)^2}} (2\pi)^4 \delta^4(p_1 + p_2 - p_3 - p_4) \\
 &\times \left[ \left( \frac{1}{2\sqrt{|\vec{p}_3|^2 + m_1^2}} \frac{d^3 \vec{p}_3}{(2\pi)^3} \right) \left( \frac{1}{2\sqrt{|\vec{p}_4|^2 + m_2^2}} \frac{d^3 \vec{p}_4}{(2\pi)^3} \right) \right] \quad (\text{A.5})
 \end{aligned}$$

by the fact that  $S = 1$ ,  $m_1 = m_3 = m_\nu$  and  $m_2 = m_4 = m_e$ .

The four-vector momenta in terms of temporal and spatial components can be written in the lab frame as

$$\begin{aligned}
 p_1 &= (p_1^0, \vec{p}_1) = (E_1, \vec{p}_1) = \left( \sqrt{|\vec{p}_1|^2 + m_1^2}, \vec{p}_1 \right), \\
 p_2 &= (p_2^0, \vec{p}_2) = (E_2, \vec{p}_2) = \left( m_2, \vec{0} \right), \\
 p_3 &= (p_3^0, \vec{p}_3) = (E_3, \vec{p}_3) = \left( \sqrt{|\vec{p}_3|^2 + m_1^2}, \vec{p}_3 \right), \\
 p_4 &= (p_4^0, \vec{p}_4) = (E_4, \vec{p}_4) = \left( \sqrt{|\vec{p}_4|^2 + m_2^2}, \vec{p}_4 \right). \quad (\text{A.6})
 \end{aligned}$$

It follows that

$$\begin{aligned}
& (p_1 \cdot p_2)^2 - (m_1 m_2)^2 \\
&= (E_1 m_2 - \vec{p}_1 \cdot \vec{0})^2 - (m_1 m_2)^2 \\
&= m_2^2 (E_1^2 - m_1^2) \\
&= m_2^2 |\vec{p}_1|^2
\end{aligned}$$

$$\implies \sqrt{(p_1 \cdot p_2)^2 - (m_1 m_2)^2} = m_2 |\vec{p}_1|, \quad (\text{A.7})$$

and

$$\begin{aligned}
& \delta^4(p_1 + p_2 - p_3 - p_4) \\
&= \delta(p_1^0 + p_2^0 - p_3^0 - p_4^0) \delta^3(\vec{p}_1 + \vec{p}_2 - \vec{p}_3 - \vec{p}_4) \\
&= \delta(E_1 + m_2 - E_3 - E_4) \delta^3(\vec{p}_1 - \vec{p}_3 - \vec{p}_4)
\end{aligned}$$

$$\begin{aligned}
\implies \delta^4(p_1 + p_2 - p_3 - p_4) &= \delta \left( \sqrt{|\vec{p}_1|^2 + m_1^2} + m_2 - \sqrt{|\vec{p}_3|^2 + m_1^2} \right. \\
&\quad \left. - \sqrt{|\vec{p}_4|^2 + m_2^2} \right) \delta^3(\vec{p}_1 - \vec{p}_3 - \vec{p}_4).
\end{aligned} \quad (\text{A.8})$$

Plugging the results of Equations A.7 and A.8 into Equation A.5 yields

$$\begin{aligned}
d\sigma &= \frac{|\mathcal{M}|^2}{64\pi^2 m_2 |\vec{p}_1|} \frac{\delta \left( \sqrt{|\vec{p}_1|^2 + m_1^2} + m_2 - \sqrt{|\vec{p}_3|^2 + m_1^2} - \sqrt{|\vec{p}_4|^2 + m_2^2} \right)}{\sqrt{|\vec{p}_3|^2 + m_1^2} \sqrt{|\vec{p}_4|^2 + m_2^2}} \\
&\quad \times \delta^3(\vec{p}_1 - \vec{p}_3 - \vec{p}_4) d^3 \vec{p}_3 d^3 \vec{p}_4.
\end{aligned} \quad (\text{A.9})$$

To get rid of  $\vec{p}_3$ , for example, integrating over it allows to make the replacement

$\vec{p}_3 \rightarrow \vec{p}_1 - \vec{p}_4$  and consequently gives

$$d\sigma = \frac{|\mathcal{M}|^2}{64\pi^2 m_2 |\vec{p}_1|} \times \frac{\delta\left(\sqrt{|\vec{p}_1|^2 + m_1^2} + m_2 - \sqrt{|\vec{p}_1 - \vec{p}_4|^2 + m_1^2} - \sqrt{|\vec{p}_4|^2 + m_2^2}\right)}{\sqrt{|\vec{p}_1 - \vec{p}_4|^2 + m_1^2} \sqrt{|\vec{p}_4|^2 + m_2^2}} d^3 \vec{p}_4, \quad (\text{A.10})$$

where

$$|\vec{p}_1 - \vec{p}_4|^2 = |\vec{p}_1|^2 + |\vec{p}_4|^2 - 2|\vec{p}_1||\vec{p}_4|\cos\theta. \quad (\text{A.11})$$

Left is the integral over  $\vec{p}_4$  which is convenient to do in spherical coordinates by replacing the volume element  $d^3 \vec{p}_4$  with its equivalent spherical expression

$$d^3 \vec{p}_4 = |\vec{p}_4|^2 \sin\theta d\vec{p}_4 d\theta d\phi. \quad (\text{A.12})$$

In spherical coordinates then, Equation A.10 becomes

$$\begin{aligned} \frac{d\sigma}{d|\vec{p}_4|} &= \frac{|\mathcal{M}|^2}{64\pi^2 m_2 |\vec{p}_1|} \frac{|\vec{p}_4|^2}{\sqrt{|\vec{p}_4|^2 + m_2^2}} \int_0^{2\pi} d\phi \\ &\times \int_0^\pi d\theta \left\{ \frac{\sin\theta}{\sqrt{|\vec{p}_1|^2 + |\vec{p}_4|^2 - 2|\vec{p}_1||\vec{p}_4|\cos\theta + m_1^2}} \right. \\ &\times \delta\left(\sqrt{|\vec{p}_1|^2 + m_1^2} + m_2 - \sqrt{|\vec{p}_4|^2 + m_2^2} \right. \\ &\left. \left. - \sqrt{|\vec{p}_1|^2 + |\vec{p}_4|^2 - 2|\vec{p}_1||\vec{p}_4|\cos\theta + m_1^2}\right) \right\}, \quad (\text{A.13}) \end{aligned}$$

where the  $\phi$  integral is simply

$$\int_0^{2\pi} d\phi = [\phi]_0^{2\pi} = 2\pi, \quad (\text{A.14})$$

and the  $\theta$  integral is

$$\begin{aligned}
& \int_0^\pi d\theta \sin \theta \\
& \times \frac{\delta \left( \sqrt{|\vec{p}_1|^2 + m_1^2} + m_2 - \sqrt{|\vec{p}_4|^2 + m_2^2} - \sqrt{|\vec{p}_1|^2 + |\vec{p}_4|^2 - 2|\vec{p}_1||\vec{p}_4| \cos \theta + m_1^2} \right)}{\sqrt{|\vec{p}_1|^2 + |\vec{p}_4|^2 - 2|\vec{p}_1||\vec{p}_4| \cos \theta + m_1^2}} \quad (\text{A.15}) \\
& = \int_1^{-1} du \frac{\delta \left( \sqrt{|\vec{p}_1|^2 + m_1^2} + m_2 - \sqrt{|\vec{p}_4|^2 + m_2^2} - \sqrt{|\vec{p}_1|^2 + |\vec{p}_4|^2 - 2|\vec{p}_1||\vec{p}_4|u + m_1^2} \right)}{\sqrt{|\vec{p}_1|^2 + |\vec{p}_4|^2 - 2|\vec{p}_1||\vec{p}_4|u + m_1^2}} \\
& = \frac{1}{|\vec{p}_1||\vec{p}_4|}.
\end{aligned}$$

in which the following change of variables

$$\begin{aligned}
u &\equiv \cos \theta \\
du &= -\sin \theta d\theta
\end{aligned} \quad (\text{A.16})$$

have been used in the last step.

Inserting Equations A.14 and A.15 into Equation A.13 produces

$$\begin{aligned}
\frac{d\sigma}{d|\vec{p}_4|} &= \frac{|\mathcal{M}|^2}{64\pi^2 m_2 |\vec{p}_1|} \frac{|\vec{p}_4|^2}{\sqrt{|\vec{p}_4|^2 + m_2^2}} \frac{2\pi}{|\vec{p}_1||\vec{p}_4|} \\
&= \frac{|\mathcal{M}|^2}{32\pi m_2 |\vec{p}_1|^2} \frac{|\vec{p}_4|}{\sqrt{|\vec{p}_4|^2 + m_2^2}} \quad (\text{A.17}) \\
\Rightarrow \frac{d\sigma}{|\vec{p}_4| d|\vec{p}_4|} &= \frac{|\mathcal{M}|^2}{32\pi m_2 |\vec{p}_1|^2} \frac{1}{\sqrt{|\vec{p}_4|^2 + m_2^2}}.
\end{aligned}$$

In an aim to evaluate the differential cross section as a function of the recoil energy of the target electron  $\frac{d\sigma}{dT}$ , it is convenient to define

$$T = E_4 - m_4 \quad (\text{A.18})$$

as the recoil kinetic energy of the target particle.

So it follows from the energy-momentum relativistic relation that

$$\begin{aligned}
E_4^2 - m_4^2 &= |\vec{p}_4|^2 \\
\implies (E_4 - m_4)(E_4 + m_4) &= |\vec{p}_4|^2 \\
\implies T(T + 2m_4) &= |\vec{p}_4|^2 \\
\implies 2(T + m_4) dT &= 2|\vec{p}_4| d|\vec{p}_4|,
\end{aligned} \tag{A.19}$$

where in the last step we have differentiated both sides of the equation.

As a final step, plugging the result of Equation A.19 into Equation A.17 gives rise to

$$\begin{aligned}
\frac{d\sigma}{(T + m_4) dT} &= \frac{|\mathcal{M}|^2}{32\pi m_2 |\vec{p}_1|^2} \frac{1}{\sqrt{|\vec{p}_4|^2 + m_2^2}} \\
\implies \frac{d\sigma}{dT} &= \frac{\langle |\mathcal{M}|^2 \rangle}{32\pi m_2 |\vec{p}_1|^2} \frac{(T + m_4)}{\sqrt{|\vec{p}_4|^2 + m_2^2}} \\
\implies \boxed{\frac{d\sigma}{dT} = \frac{\langle |\mathcal{M}|^2 \rangle}{32\pi m_2 |\vec{p}_1|^2}} & \tag{A.20}
\end{aligned}$$

by the fact that  $\sqrt{|\vec{p}_4|^2 + m_2^2}$  (in Equation A.6) =  $T + m_4$  (in Equation A.18) =  $E_4$ .

## Appendix B: Kinematic Terms

For the neutrino-electron elastic scattering process

$$\nu(p_1) + e(p_2) \rightarrow \nu(k_1) + e(k_2),$$

the different kinematic terms can be found using the law of conservation of momentum

$$p_1 + p_2 = k_1 + k_2, \quad (\text{B.1})$$

where  $p_1$  and  $k_1$  are respectively the incoming and outgoing momenta of neutrino while  $p_2$  and  $k_2$  are those of electron.

In the lab frame, these momenta can be expressed in a four-vector notation as

$$\begin{aligned} p_1 &= (E_\nu, \vec{p}_1), \\ p_2 &= (m_e, \vec{0}), \\ k_1 &= (E'_\nu, \vec{k}_1) \text{ such that } E'_\nu = E_\nu - T, \\ k_2 &= (E_e, \vec{k}_2) \text{ such that } E_e = m_e + T, \end{aligned} \quad (\text{B.2})$$

where  $T$  is the recoil energy of the target electron.

It then follows that

•

$$\begin{aligned} (p_1 + p_2)^2 &= (k_1 + k_2)^2 \\ \implies p_1^2 + p_2^2 + 2p_1 \cdot p_2 &= k_1^2 + k_2^2 + 2k_1 \cdot k_2 \\ \implies m_e^2 + 2p_1 \cdot p_2 &= m_e^2 + 2k_1 \cdot k_2 \\ \implies \boxed{p_1 \cdot p_2 = k_1 \cdot k_2 = m_e E_\nu}, \end{aligned} \quad (\text{B.3})$$

followed from the fact that

$$p_1 \cdot p_2 = E_V m_e - \vec{p}_1 \cdot \vec{0} = m_e E_V.$$

•

$$\begin{aligned} (p_2 - k_1)^2 &= (k_2 - p_1)^2 \\ \implies p_2^2 + k_1^2 - 2p_2 \cdot k_1 &= k_2^2 + p_1^2 - 2k_2 \cdot p_1 \\ \implies m_e^2 - 2p_2 \cdot k_1 &= m_e^2 - 2k_2 \cdot p_1 \\ \implies p_2 \cdot k_1 &= k_2 \cdot p_1 = m_e (E_V - T), \end{aligned} \tag{B.4}$$

followed from the fact that

$$p_2 \cdot k_1 = m_e E_V' - \vec{0} \cdot \vec{k}_1 = m_e (E_V - T).$$

•

$$\begin{aligned} (p_2 - k_2)^2 &= (k_1 - p_1)^2 \\ \implies p_2^2 + k_2^2 - 2p_2 \cdot k_2 &= k_1^2 + p_1^2 - 2k_1 \cdot p_1 \\ \implies m_e^2 + m_e^2 - 2p_2 \cdot k_2 &= -2k_1 \cdot p_1 \\ \implies 2(m_e^2 - p_2 \cdot k_2) &= -2k_1 \cdot p_1 \\ \implies k_1 \cdot p_1 &= m_e T, \end{aligned} \tag{B.5}$$

followed from the fact that

$$p_2 \cdot k_2 = m_e E_e - \vec{0} \cdot \vec{k}_2 = m_e (m_e + T).$$